ON THE DETECTION OF PERIODICITIES IN THE RESPONSE TIMES OF SIMPLE VISUAL TASKS

Thesis for the Degree of M. S.

MICHIGAN STATE UNIVERSITY

DUANE G. LEET

1968

ON THE DETECTION OF PERIODICITIES IN THE RESPONSE TIMES OF SIMPLE VISUAL TASKS

By

Duane G. Leet

A THESIS

Submitted to
Michigan State University
in partial fulfillment of the requirements
for the degree of

MASTER OF SCIENCE

Department of Biophysics

1968

TABLE OF CONTENTS

LIST OF TABLES

LIST OF FIGURES

CHAPTER I

INTRODUCTION

I.10. The Information Sciences and the Brain

The function the Egyptians attributed to the brain is not known, but it could not have been very important. This is obvious from the fact that when the Egyptians embalmed their dead, the brain was retracted through the left nostril and discarded. Today, even a youngster would laugh if you told him that the function of the brain was to cool the blood, as Aristotle had believed. To him the brain is for "thinking." But what does he mean? To answer the question "What is the function of the brain?" satisfactorily requires a language that is less than a quarter of a century old, the language of the information sciences. Using this language, the function of the brain is to collect "sensory information and (correlate) this . . . with stored information to compute the daily course of bodily activity." (8)

The methods of information processing used by the nervous systems of even primitive organisms are just beginning to be understood. A basic philosophy used by scientists to achieve this understanding is to divide the nervous system of the organism being studied into

subsystems. The functions of these subsystems are described and the connections between them are detailed to give the organism as a complete system. The subsystems are then explored to determine the techniques of information processing used by the subsystem.

I.20. The Thesis

In this spirit, this report examines a thesis which has been proposed to explain how humans process information acquired by the visual system. The thesis was inspired by a postulate of Stroud's: If continuous physical time is represented in the experience of man as psychological time T, then T is not a continuous variable. On the basis of experimental evidence, Stroud has concluded that the resolution or moment of T is between 0.05 and 0.2 seconds. The phenomenon that leads most directly to his postulate is flicker fusion (18). If a subject is asked to count the number of flashes of light and the light is flashing at a frequency above a critical frequency called the flicker fusion frequency, then the number of flashes that the subject sees is consistently lower than the actual number. The flicker fusion frequency is usually somewhere between 20 and 70 cps., with 30 cps. being the mean. This type of phenomenon has also been reported with sound and touch inputs (20). If a noncontinuous information system is hypothesized, then the phenomenon is easily explained.

Using Stroud's postulate as a starting point, Augenstein wondered if the information processing technique of humans might be analogous to the technique used by the digital computer, for if Stroud had as evidence experiments performed on a digital computer, he would have arrived at an identical postulate. This is because the operations of a computer are controlled by a discrete clock, called the master clock. In the computer, if the master clock were to die, or even become ill, computations and commands would become hopelessly fouled up; in short, the computer could not function.

After some preliminary experimentation, Augenstein developed the following thesis (1): Information presented to the human visual system is first coded into an internal symbolism in an operation analogous to that performed by the input black box of the basic information processing system. It is then processed for meaning. This "processing black box" operates in a manner similar to that of a synchronous sequential system: it accepts an input or makes a binary decision only at periodic* intervals. Finally, the decision is relayed to the appropriate centers for the execution of the decision (the output black box).

The following chapters discuss the experimentation that led Augenstein to this thesis and also some experiments which have been performed to test further its validity.

---

*The terms "period" and "periodic" are used in the intuitive sense, not in the rigorous mathematical sense.

CHAPTER II

BACKGROUND EXPERIMENTATION

II.10. A Statistical Model for the Function Which Generates Response Times

Consider the simple visual task of deciding whether some aspect of a visual pattern is or is not present. If a naive attempt is made to predict the response time for this task, it might be considered to be the sum of the random variables corresponding to the acquisition and accomodation time, $T_a(\cdot)$, the time to input the pattern, $T_i'(\cdot)$, the time necessary to reach a decision ,$T_p'(\cdot)$ and the time for the output of the corresponding response, $T_o(\cdot)$. The response time is, therefore, the random function*

Eqn II.10.10. $$T(s) = T_a(s) + T_i'(s) + T_p'(s) + T_o(s).$$

---

*The notation used in this thesis follows the current trend (6). A random variable in the implicit form will be written $T_a(\cdot)$. A random function in the implicit form will be written in the same way. A random function written in the explicit form (i.e., as an equation) will have an argument supplied with all the component random variables [e.g., T(s)]. Throughout, the argument commonly used is s, a single trial of an experiment. The notation for an implicit density function will be of the form $f_T(\cdot)$ or $p_T(\cdot)$. The f signifies a continuous function and the p signifies a discrete function. The subscript is the random variable (function) associated with the density function. An argument is supplied when the function is written explicitly.

Now assume that the subsystems of the visual system performing the inputting and decision-making operations have the property that they produce outputs sequentially and that each operates in a synchronous fashion (i.e., has a cycle time). Furthermore, assume that the lengths of the cycle times for the two subsystems are different. Thus, an output from the input subsystems occurs bt_i seconds after the initial input of information, where b is an integer and t_i is the cycle time for input; an output from the decision-making subsystem occurs at at_p seconds after the initial input, where a is an integer and t_p is the processing cycle time. By allowing both variability in the number of cycles required by each subsystem and a slight variability in their cycle time, the total times for the inputting and decision-making operations become

Eqn. II.10.11. $$T_i'(s) = B(s)T_i(s)$$

and

Eqn. II.10.12. $$T_p'(s) = A(s)T_p(s).$$

Finally, assume that the density function of the random variables $T_a(\cdot)$ and $T_o(\cdot)$ are Gaussian. Since the sum of random variables with Gaussian densities is a random function with Gaussian density, $T_a(\cdot)$ and $T_o(\cdot)$ can be combined into the random function

Eqn II.10.13. $T_s(s) = T_a(s) + T_o(s)$.

Combining Eqns. II.10.10.--II.10.13.,

Eqn II.10.14. $T(s) = T_s(s) + B(s)T_i(s) + A(s)T_p(s)$.

Note that the means of $T_i(\cdot)$ and $T_p(\cdot)$, which will be designated by t_i and t_p respectively, are the values of primary importance.

The following pages review experiments Augenstein (1, 2, 3) developed to test the ability of $T(\cdot)$ to describe the response times generated by humans performing simple visual tasks.

II.20. Criteria for a Good Experimental Task Design

The model has several properties that were used to design tasks to emphasize, if possible, the values of the parameters t_p and t_i. The first of these can be seen in an intuitive way by considering the following density functions for each of the random variables of Eqn. II.10.14:

Eqn II.20.10. $p_{T_s}(t_1) = 1, \; t_1 = 400$

$= 0$, otherwise;

Eqn II.20.11. $p_B(b) = 1, \; b = 0$

$= 0$, otherwise;

Eqn II.20.12. $p_A(a) = .2,\ a = 1,2,3,4,5$

$= 0$, otherwise;

Eqn II.20.13. $p_{T_p}(t_2) = 1,\ t_2 = 50$

$= 0$, otherwise.

These density functions are simple enough that the density function $p_T(\cdot)$ can be constructed by inspection (see Fig. II.10). The important property to note is that the value of t_p can be determined directly from the density function. It is the distance between the impulses.

Suppose that now, instead of Eqn II.20.10.,*

Eqn II.20.14. $f_{T_s}(t_1) = N(t_s, \sigma_s)$.

With a little thought Figure II.20 can be shown to be the general shape of $f_T(\cdot)$. Note that if the ratio of σ_s/t_p is "small enough," the value of t_p can again be determined by visual inspection. It would, therefore, be advantageous to have this ratio and, in any more general analysis, the ratios σ_i/t_p and σ_p/t_p as small as possible. In order to optimize this possibility experimentally, the following criteria were established:

---

*This notation will be used for a Gaussian density function of mean t_s and standard deviation σ_s.

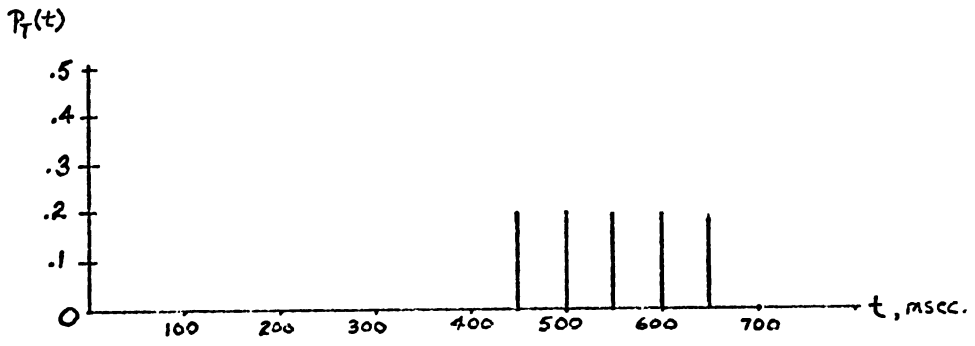

Figure II.10. The density $p_T(.)$, where the component density functions are defined in Eqns. II.20.10-II.20.13.

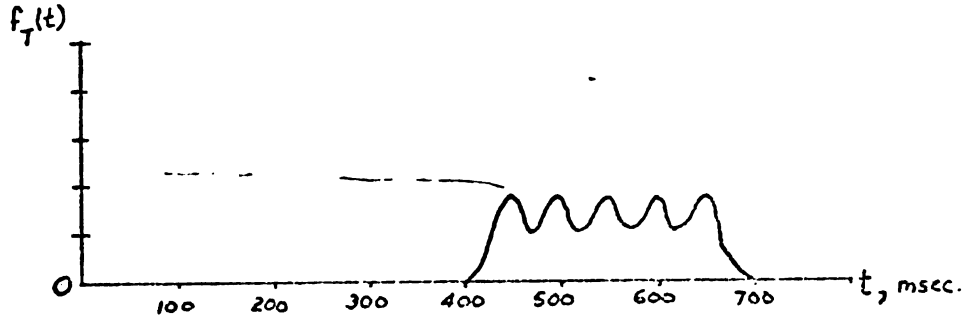

Figure II.20. The density $f_T(.)$, where the component density functions are defined by Eqns. II.20.11-II.20.14.

C1. Either a single response or very simple responses should be required.

C2. The tasks should be self-paced.

Assuming the model is correct, if the cycle time is to be detected by measuring the distance between peaks, then the task should require more than one cycle. On the other hand, if the task requires complex memory references, or the pattern to be acted upon contains unfamiliar symbols or requires an unusual response, then the data may contain elements not postulated by the model. Hence, the following criteria:

C3. The patterns should consist of simple, familiar symbols.

C4. Each response should be formulated by making a sequence of simple unequivocal decisions.

C5. Each response should require many such decisions.

The next criterion was:

C6. Ths displays should be shown in a random order. This was adopted so that the subject could not anticipate the exact composition of the display.

Stroud's prediction of the magnitude of the fundamental quantum (50-200msec) suggests a final criterion:

C7. The data and analysis should allow for the detection of values for t_p and t_i in the 25-300 msec range.

II.30. Some Designs for Experimental Visual Tasks.

The tasks which Augenstein designed using the above criteria are outlined in Table II.1. One task, SHN, is of particular interest and will be described in detail.

A pattern (hereafter called a stimulus) for SHN consisted of a 26 element sequence of letters and numbers. An example of such a sequence is

DSVCYKGMHPSZ2WX5R4K5M7Z38X .

The stimulus variable of interest was the first position from the left to contain a number (2 in this case). The position (13 in this case) which contains this first number will be called the target element.

All positions previous to the target element contained a letter chosen at random from 23 equiprobable letters (Q, O and I were not used because of their similarity to numbers). The digit in the target element was chosen at random from the equiprobable numbers 2 through 9. The positions following the target element contained either a letter or number chosen at random from the 23 letters and 8 numbers, all equiprobable.

There were a total of 251 different sequences typed on white cards. The target element occurred 25 times in each of the positions 3, 8, 13, 18 and 23 of the sequence. The target element occurred a total of six times

TABLE II.1.--Summary of experimental types and designations and descriptions of the tasks designed by Augenstein(1).

Type	Symbols	
1. Scanning	SV	Recognition of first letter in a vertical list of mixed numbers and letters--all positions equiprobable.
	SHE	Recognition of left-most letter in a horizontal list of mixed numbers and letters --all positions equiprobable.
	SHN	Same as SHE except all positions were not equiprobable.
	SO	Recognition of either 10 or 01 in a vertical column of 00 and 11 symbols--all positions equiporbable.
	SA	Addition of vertical columns of numbers.
2. Minimal scanning	WS4	Synthesis of a 4-letter English word from a scrambled tetragram.
	WS3	Synthesis of the 4-letter English word from one of its scrambled permutations.
3. Muscular response	MRS	Skeet shooting.
	MRT	Typing random text.
4. All factors minimized	NN	Null response

in each of the remaining 21 positions. The cards were shuffled at the beginning of each experimental run.

The lighting in the room where the task was performed was described as being comfortable for reading. To begin a trial, the subject was required to focus his eyes on a fixation point on a Gerbrand Tachistoscope screen. When the subject felt that he was ready to begin, he depressed an easy action microswitch. This turned off the light illuminating the spot and turned on the fluorescent light illuminating one of the stimulus cards from the shuffled group of 251. All symbols fell to the right of the fixation point as the subject viewed the stimulus. A timer with an expressed accuracy of ±3msec. was triggered with the lights. The subject had been instructed and trained beforehand on the method he was to use to search for the target element. Specifically, when the stimulus appeared the subject was to move his eyes from the fixation point to the beginning of the sequence. He was to scan the sequence from left to right until he came to the target element. When the subject became aware of the target element, he released the microswitch. This stopped the timer and turned off the illumination on the stimulus. The subject then identified the number in the target element. The experimenter recorded the response time to the nearest ten msec., replaced the stimulus with a new one, reset the timer and signaled the subject that he could begin a new trial.

The response times obtained for each subject were assembled to give a histogram of the number of times a given response time occurs. Note that a histogram can be thought of as an unnormalized estimate of the density function of the response times.

II.40. The Model and Power Spectral Analysis

II.40.10. An Aside on Digital Power Spectral Analysis of Real Periodic Signals in Ergodic Noise.

--A standard technique for detecting signals in noise, and particularly periodic signals, is to calculate the power spectral estimate of the available signal. This paragraph will heuristically develop from basic principles a commonly used method for calculating the power spectral estimate (PSE).

To begin with, define $X(\cdot,\cdot) = X$ to be a real orgodic stochastic process.* A member of the ensemble of time functions will be signified by $X(\cdot,\phi)$ and a random variable can be defined for any particular t by using the notation $X(t,\cdot)$. Weiner (10) has shown that the following are a Fourier transform pair:

Eqn II.40.10. $$R(T)=E\{X(t,\cdot),X(t+T,\cdot)\}=\int_{-\infty}^{\infty}P(w)e^{jwT}dw$$

Eqn II.40.11. $$P(w) = \frac{1}{2\pi}\int_{-\infty}^{\infty}R(T)e^{-jwT}dT$$

---

*For definitions and discussion, see Reference 11, pp. 323-332 and Reference 4, p. 11.

R(T) is called the autocorrelation of $X(t,\cdot)$ and P(w) is called the power spectrum. Since ergodicity has been assumed, an equivalent expression for the autocorrelation is

Eqn II.40.15. $$R(T)=\lim_{T\to\infty}\frac{1}{T}\int_{-T/2}^{T/2}X(t,\phi)X(t+T,\phi)dt$$

Therefore, for the ergodic case, only one member and not the entire ensemble is required in order to calculate R(T).

Several simplifications can be made in the calculation of the expressions for R(T) and P(w). First, assuming that $X(\cdot,\phi)$ is real, R(T) is real and P(w) can be written in the form:

Eqn II.40.20. $$P(w) = \frac{1}{2\pi}\int_{-\infty}^{\infty}R(T)\cos wT dT$$

R(T) and P(w) are even functions (because they are real),

Eqn II.40.22. $$R_1(T)=2\lim_{T\to\infty}\int_{0}^{T}X(t,\phi)X(t+T,\phi)dt \quad \text{for } T\geq 0$$

and

Eqn II.40.23. $$P_1(w)=\frac{1}{\pi}\int_{0}^{\infty}R_1(T)\cos wT dT \quad \text{for } w\geq 0.$$

$R_1(T)$ is called the one-sided autocorrelation (AC) and $P_1(w)$ is called the one-sided power spectrum (PS).

From the statistical point of view, the AC and PS are important invariant properties of the stochastic process X. From a communications point of view, they allow for the design of systems which can take advantage of the frequency properties of the noise in that system. There would be little more to be said at this point if it were not that in practical situations it is impossible to record $X(\cdot,\phi)$ from $t = -\infty$ to $t = +\infty$. Instead, the signal is recorded over the interval [O,T]. An autocorrelation expression for finite signals is*:

Eqn II.40.40. $$\hat{R}_1(T) = \frac{1}{T-T}\int_0^{T-T} X(t,\phi)X(t+T,\phi)dt \qquad O \leq T \leq m < T_{max}$$

where T_{max} is the greatest possible lag. There has been much study concerning the comparison between finite and true autocorrelation values for various types of signals. For instance, the mean square error of $\hat{R}_1(T)$ increases with increasing T and decreases with increasing T. The expression for the finite power spectrum corresponding to $\hat{R}_1(T)$ is

Eqn II.40.45. $$\hat{P}_1(\omega) = \frac{1}{\pi}\int_0^m \hat{R}_1(T)\cos\omega T dT \qquad o \leq \omega \leq \omega.$$

Note that this is an estimate of the true power spectrum and so it is called the power spectral estimate (PSE) of X.

---

*Note that a change of variable, $t' = \frac{T}{2} + t$, allows this expression to conform to the previous arguments concerning evenness.

The effect of $\hat{R}_1(T)$ on the power spectrum has been studied extensively. Several modifications of $\hat{R}_1(T)$ have been proposed as a result of these studies. A modification which helps compensate both for the finite signal length and the decreasing accuracy of $\hat{R}_1(T)$ with increasing T is to multiply $\hat{R}_1(T)$ by a window function, D(T) before taking its transform. A very common window function is the hamming window, which is defined as

Eqn II.40.50. $$D(T) = 0.54 + 0.46 \cos \frac{\pi T}{m} \qquad 0 \leq T \leq m \ .$$

Another modification which is used specifically to correct for error in $R_1(T)$ due to large lag is to use a correlation coefficient expression instead of the standard autocorrelation (13):

Eqn II.40.60. $$R_1(T) \frac{\hat{R}_1(T) - E'\{X(\cdot,\phi)\}E''\{X(\cdot,\phi)\}}{\sqrt{\sigma_x'^2 \ \sigma_x''^2}}$$

where the prime superscript indicates that the value is calculated over the interval $t\varepsilon[o,T-T]$, and the double prime superscript indicates that the value is calculated over the interval $t\varepsilon[T-T, T\}$. Note that $-1 \leq \hat{R}_1(T) \leq 1$.

If the time function is recorded digitally, then digital autocorrelation and PSE expressions can be defined which include the modifications of Eqn II.40.50 and II.40.60:

Eqn II.40.70 $$R_1(K\Delta T)=\frac{\overline{X(i\Delta t)X[(i+K)\Delta t]}-\overline{X(i\Delta t)}\ \overline{X[(i+K)\Delta t]}}{\sqrt{\sigma_i^2(K)\ \sigma_{i+K}^2(K)}}$$

where $0\leq K\leq M$, Δt is the time between samples, assuming equispaced samples, N is the number of samples, ΔT is the fundamental lag time, and m is the maximum lag count. Also,

Eqn. II.40.71. $$\overline{X(i\Delta t)X[(i+K)\Delta t]}=\frac{1}{N-K+1}\sum_{i=0}^{N-K}X(i\Delta t)X[i+K)\Delta t]$$

Eqn II.40.72. $$X(i\Delta t)=\frac{1}{N-K+1}\sum_{i=0}^{N-K}X(i\Delta t)$$

Eqn II.40.73. $$\overline{X[(i+K)\Delta t]}=\frac{1}{N-K+1}\sum_{i=0}^{N-K}X[(i+K)\Delta t]$$

Eqn II.40.74. $$\sigma_i^2(K)=\frac{1}{N-K+1}\sum_{i=0}^{N-K}[X^2(i\Delta t)]-\frac{1}{(N-K+1)}\left[\sum_{i=0}^{N-K}X(i\Delta t)\right]^2$$

Eqn II.40.75. $$\sigma_{i+K}^2(K)=\frac{1}{N-K+1}\sum_{i=0}^{N-K}X[(i+K)\Delta t]-\frac{1}{(N-K+1)^2}\left[\sum_{i=0}^{N-K}[(i+K)\Delta t]\right]^2$$

and

Eqn II.40.80. $$P_o(pf_o)=\frac{\hat{P}(pf_o)}{P_{max}}=\frac{1}{P_{max}}\sum_{K=0}^{m}D(K\Delta T)R_1(K\Delta T)\cos K\Delta T pf_o$$

where $f_o=\frac{1}{2m\Delta t}$, P_{max} is the maximum $P(pf_o)$ values (this means that $P_o(pf_o)\leq 1$) and

Eqn II.50.81. $$D(K\Delta T)=0.54+0.46\cos K\Delta T\pi/m.$$

Note that this PSE has an additional source of error. Because of aliasing, the frequencies above $\frac{1}{2\Delta t}$ are not included in the PS. If there is significant power at a frequency higher than this, it is not detected.

II.40.20. The Reason for Using Power Spectral Analysis on the Histograms.--The density functions which were plotted in Figures II.10 and II.20 are periodic with period equal to the value of t_p on the interval where the density functions are non-zero. It was expected that the histograms would also be periodic, but that the periodicity would be difficult to detect visually because of the noise caused by the small number of data points. Since the power spectral technique has been used successfully to detect periodic signals in noise, Augenstein felt that it would be a useful analytical technique for detecting the values of t_p and t_i in his histograms.

II.50. The Analytical Methods, Results, and Conclusions.

II.50.10. Power Spectral Analysis.--A computer program was written to calculate Eqns. II.50.70 and II.50.80 from the histograms. Figures II.40 and II.50 are PSE's from two subjects under two different experimental conditions. Twenty-one PSE's, including these two, from six subjects under six experimental conditions were averaged and normalized to give the PSE of Figure II.70. The peaks

in the spectrum which are larger than background have been labeled with the period corresponding to the frequency at which the peak occurred.

Augenstein interpreted this PSE with the aid of a computer program which generated data according to the following density functions for the random variables that made up $T(\cdot)$:

Eqn II.50.10. $p_{T_s} = N(400,\sigma s)$

Eqn II.50.11. $p_B(b) = 0$, for all b

Eqn II.50.12. $p_{T_p}(t_3) = N(t_p, \sigma p)$

An attempt was made to match PSE's calculated from data generated by varying σs, t_p, σp and $p_A(a)$. Augenstein found that by using the density functions

Eqn II.50.20. $p_{T_s}(t_1) = N(400,13)$

Eqn II.50.21 $p_{T_p}(t_3) = N(33,0)$

Eqn II.50.22. $p_B(b) = 0$, for all b

Eqn II.50.23. $p_A(a) =$ see Figure II.30.

he could generate data which resulted in the PSE's shown in Figure II.71. Figure II.60 is the renormalized average of these PSE's. Augenstein noted the resemblance of this plot

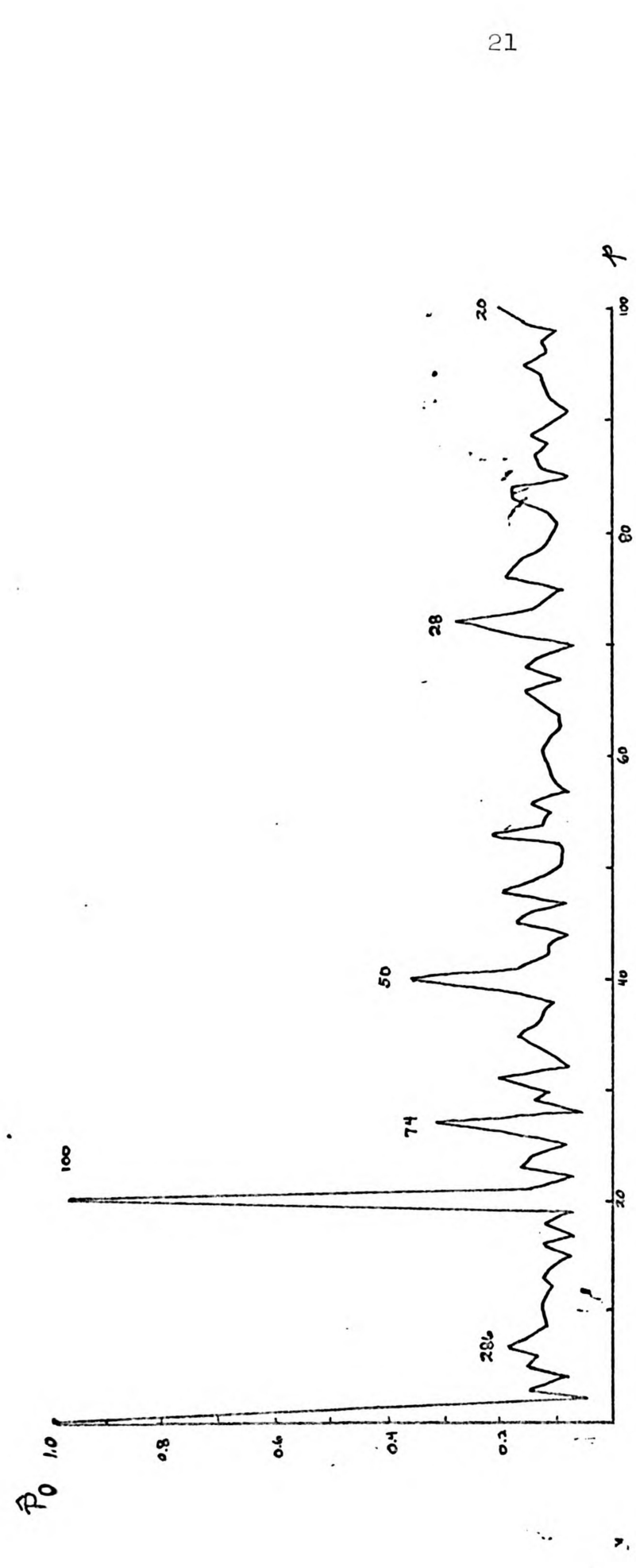

Figure II.40. Power spectral estimate for subject SR in experiment SO. From (1).

Figure II.50. Power spectral estimate for subject BR in experiment SHN. From (1).

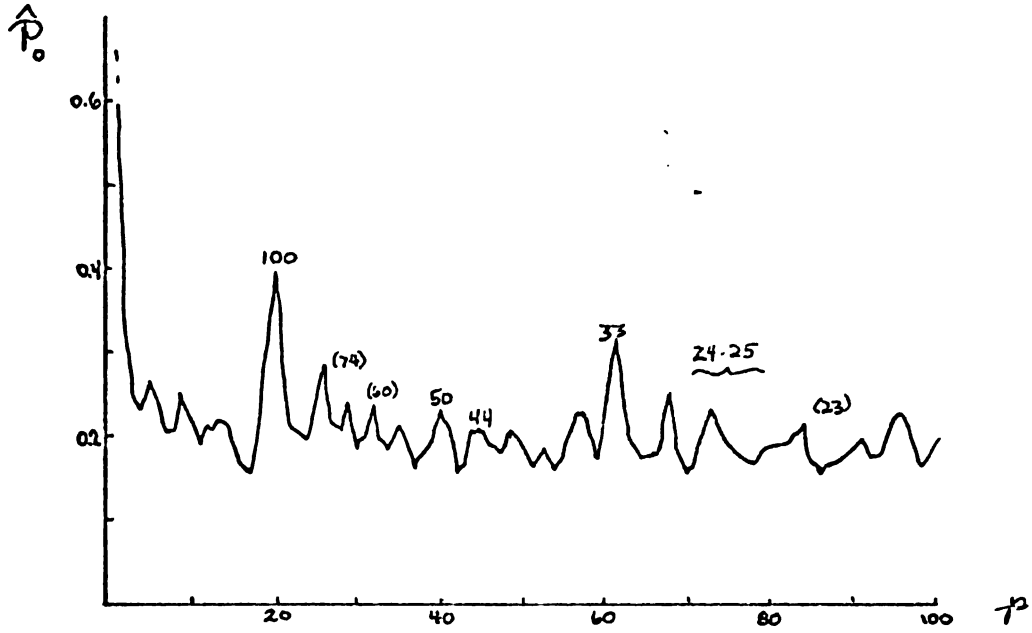

Figure II.60. The power spectral estimate which is the normalized sum of the power spectral estimates of Figure II.71. From (2).

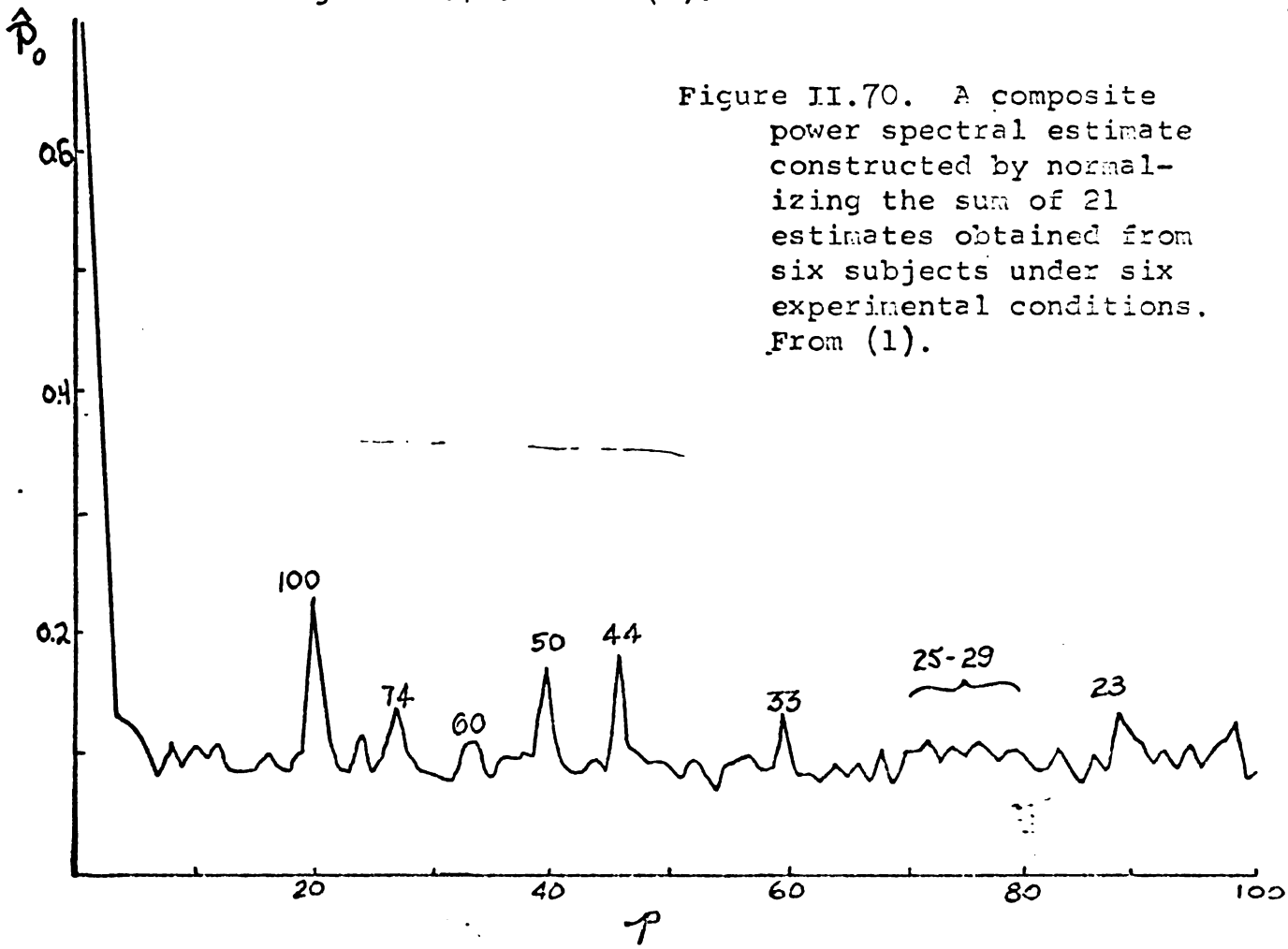

Figure II.70. A composite power spectral estimate constructed by normalizing the sum of 21 estimates obtained from six subjects under six experimental conditions. From (1).

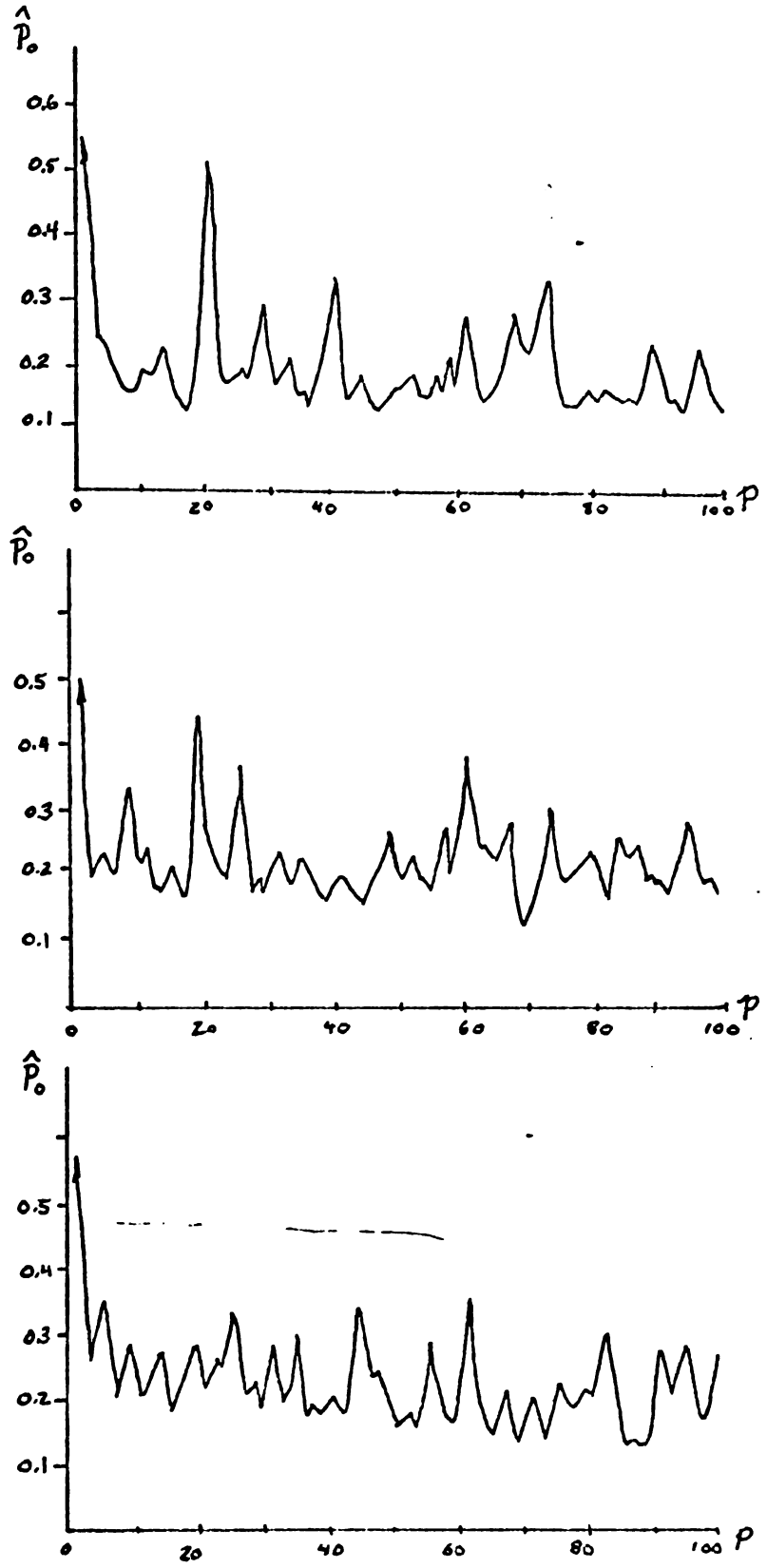

Figure II.71. Power spectral estimates calculated from histograms generated by the density functions defined in Eqns. II.40.20-II.40.23. From (1).

to Figure II.70. Based on this correspondence and on the general shape of the individual experimental PSE's he concluded that (1)

1. there was "strong evidence of a 100 msec. periodicity in most of our subjects";
2. "the fundamental 33 msec. periods probably occur in groups of three";
3. "the 33 msec. value is probably for both t_i and t_p."

It is important to recognize that the statistical model is in the form

Eqn II.50.30 $$T(s) = T_S(s) + A(s)T_P(s).$$

The interpretation of this eqn. resulted in the thesis stated in Chapter I.

II.50.20. Average time per symbol.--Recall that in the SHN experiment the stimuli had many more target elements in the 3rd, 8th, 13th, 18th and 23rd positions than in the other positions. For each subject Augenstein collected the appropriate response times and constructed a histogram for each of these five positions. One such set of histograms is Figure II.80. The dotted line in the figure connects the approximate average response time for each of the positions. Using these averages, average times per symbol of 61-72 msec. were obtained for the three subjects studied.

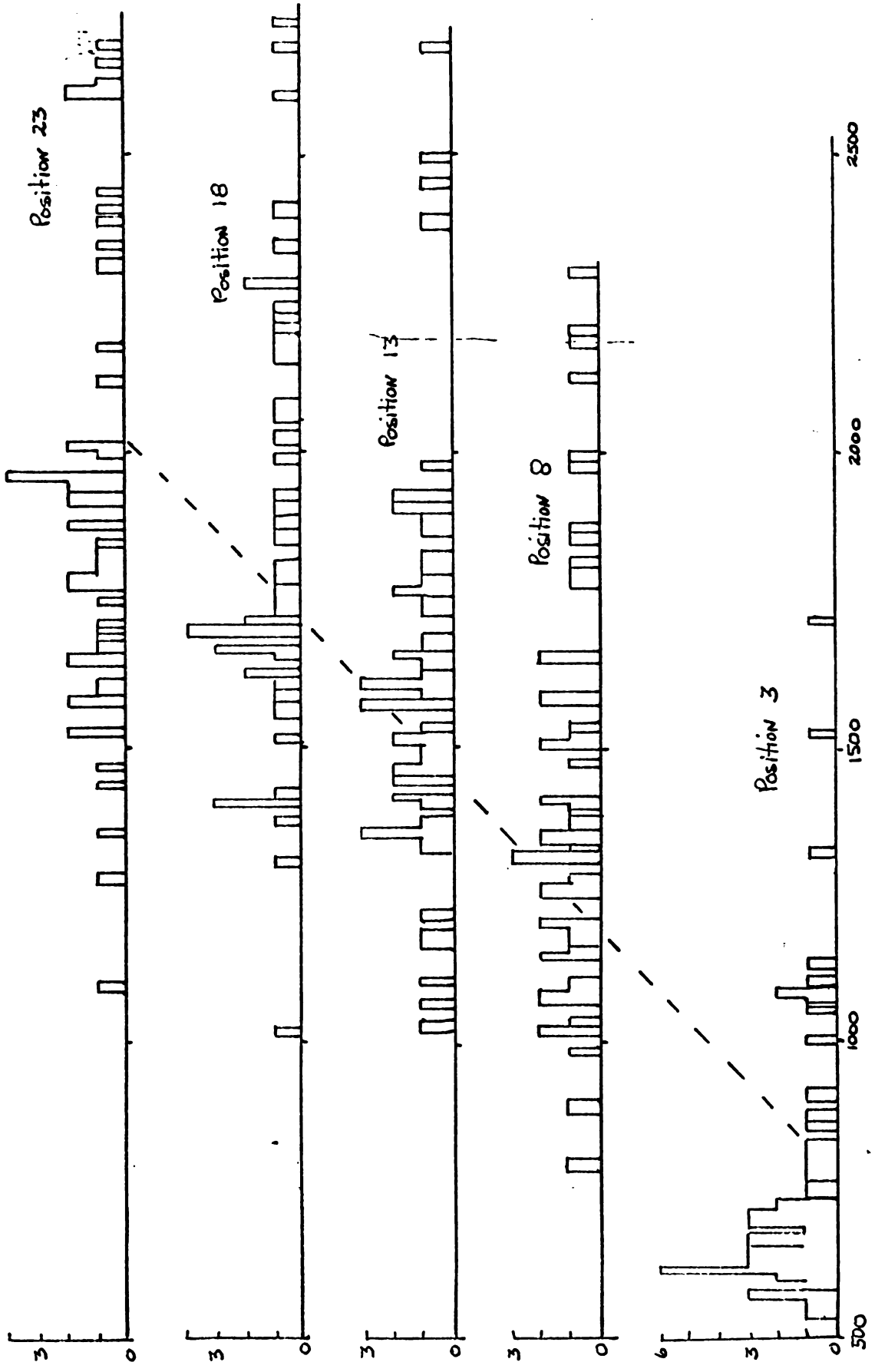

Figure II.80. Histograms by position: Subject Hi in Experiment SHN.

CHAPTER III

DISCUSSION: PART I

III.10. Criticisms of the SHN Experimental Procedure

A critical review of the experimental method and procedures used in SHN suggests two sources of data artifacts.

To understand the first source of error, note that when a continuous function is recorded at discrete intervals (either by sampling or by quantizing the data) it is possible that the values of power density at frequencies above $f_c = 1/2\Delta t$ cps. will not be correct. The analytical procedure that Augenstein used sidestepped this issue by not calculating the power density in the frequencies above f_c. However, the true density function could contain significant power at these frequencies. The source of the second potential error was the fluorescent lighting used in the Gerbrand Tachistoscope. Due to their 60 cps. flicker, fluorescent tubes have been observed to cause a stroboscopic effect. Therefore, there was the possibility that this flicker was introducing a periodic artifact into the response times.

III.20. Criticisms of the Foregoing Model

Recall that Augenstein concluded that a sufficient statistical model for his data was

Eqn III.20.10. $$T(s) = T_s(s) + A(s)T_p(s).$$

This equations says that a response time is the sum of an acquisition and accomodation time plus an integral number of fundamental quanta. "Within each fundamental quantum either data are input or one binary decision can be made" (1). Note, however, that the equation requires that the quantum remain constant for the duration of the performance of the task. Such a requirement is not necessary and indeed is not consistent if it is assumed that (1) the variability in the cycle time is due to random fluctuations in the neural pathways and (2) the variability is relatively independent of the nature of the information being processed. Therefore, the following model is proposed to more completely describe the random function associated with the generation of response times of simple visual tasks:

Eqn III.20.20. $$T(s) = T_s(s) + \sum_{i=1}^{A(s)} T_{P_i}(s)$$

This expression says that a response time is the sum of the times necessary to input the stimulus and make the response $T_s(s)$ plus an integral number of processing cyles

$T_{p_i}(s)$, with the possibility of each individual cycle having a slightly different length. If the same stimulus is presented again under exactly the same conditions, the time $T_s(s)$, the number of cycles required for processing A(s), and, of course, the length of the cycles will be different. Hence the random nature of the expression.

CHAPTER IV

EXPERIMENTATION

IV.10. Introduction

Augenstein's experiments and the criticisms made of them inspired the series of three experiments reported in this chapter and the next. The first series, named B-1, was designed to eliminate from the experimental procedure the lighting and data accuracy as sources of error. The PSE's that were calculated from the data of this experiment were not at all similar to the PSE's calculated in SHN. A review of the differences in the experimental procedures that were previously considered unimportant lead to the design of the second series of experiments, B-2. The third series, B-3, investigated the problem of PSE interpretation.

IV.20. Experiment B-1

IV.20.10. Experimental design and procedure.--

This experiment was designed to duplicate experiment SHN in principle, while at the same time the procedure was modified to increase the resolution of the data and the amount of data that could be collected. In addition, incandescent rather than fluorescent lights were used.

The Stimuli. The stimulus format was the same as in SHN. However, instead of typing the sequences on cards and presenting them to the subject using a tachistoscope, the cards were photographed and made into 2"x2" glass slides. The total number of stimuli was increased from 251 to 1235, with 100 target elements in each of the 3rd, 8th, 13th, 18th and 23rd positions and 35 target elements in each of the other positions.

The Experimental Equipment and the Task. The experiment was automated through the use of a Kodak Carousel Slide Projector (Model 500R) with a shutter arrangement, solid state control circuitry, a digital clock and a paper tape punch output. A description of a trial of the experiment will serve to introduce the task as well as the relationship of the equipment to the task.

The subject was seated in a secretarial chair behind a low table (36"). His head was positioned on a headrest and his right index finger was used to operate a microswitch taped to the table top. A 60 watt incandescent lamp was placed behind the subject to give indirect illumination of the screen. When the subject felt that he was ready to begin a trial he would focus on a 2"x2" "Everglo" night lamp placed about seven degrees of visual angle to the left of the point where the left most element of the sequence was to be flashed. It should be noted that special care was taken in the construction of the slides

and the selection of a projector to insure that the first position would fall at approximately the same point on the screen trial after trial (there was less than a 0.5 degree of visual angle variation measured during a test run). The logic system was brought into play when the subject depressed the microswitch and held it down. Within the next millisecond the timer was triggered and the Synchronome shutter pulsed to reveal a sequence to the subject. The subject was instructed to move his eyes to the beginning of the sequence when he became aware of the display and to scan it from left to right for the first number. Scanning was necessary because only five to six elements were subtended by the fovea at any one time. Upon recognition of the target element, the subject was instructed to release the switch and enunciate the digit. The release of the switch turned off the timer and pulsed the shutter. At the same time the switch was deactivated until the housekeeping duties of the logic system were completed (about 3 sec.). These housekeeping duties consisted of punching the time on paper tape, clearing the timer and changing the slide.

The Experimental Procedure. Four subjects, all college students*, were used in this experiment: The subjects performed at a rate of one 80 slide tray every

---

*Subject DJ was the only female.

5 minutes. About 2 minutes were required to change trays and tend to the paper tape. The subject rested during this time. Each was given a practice session of between 400 and 500 trials to learn the correct procedure. Each subject was required to complete 5600 trials during a series of experimental sessions lasting one and one-half hours each.

At the conclusion of the experiment the data on the paper tapes were transferred to magnetic tapes and edited for errors, such as faulty punching and mistrials.

IV.20.20. Power spectral analysis.--The edited data from each subject were arranged in histograms having 1 msec. intervals. Histograms with 3, 5, 7 and 10 msec. intervals were compiled from the 1 msec. histograms by using a lumping technique. For instance, the first entry in the 10 msec. intervals histogram is obtained by adding the values of the 1 msec. interval histogram between 0 and 9 msec. The 10 msec. interval histograms are shown in Figure IV.20.

Each of the histograms was examined and the portion T[a,b] with no long strips of zeroes was chosen for power spectral analysis. PSE's were calculated as in SHN for several values* of m and m'. Some of the most interesting PSE's are shown in Figure IV.30. The major characteristic

---

*The parameters m=m' were set equal to .5., .3 and .25 of the total number of points in the interval [a,b].

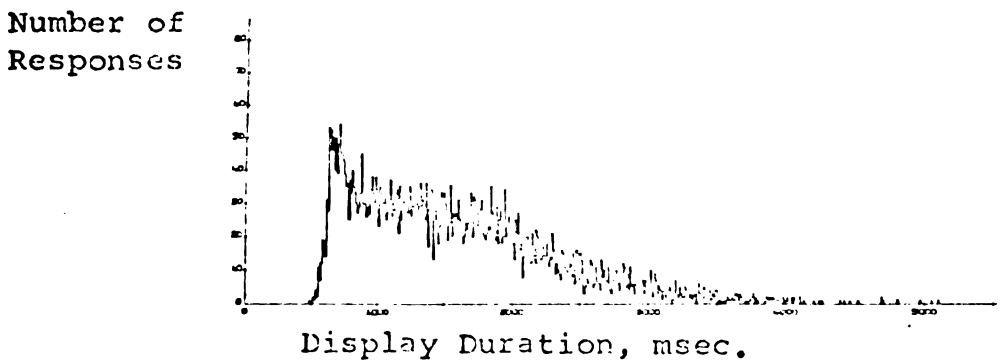

Figure IV.20.1. Histogram with 10 msec. intervals: Subject DJ in Experiment B-1.

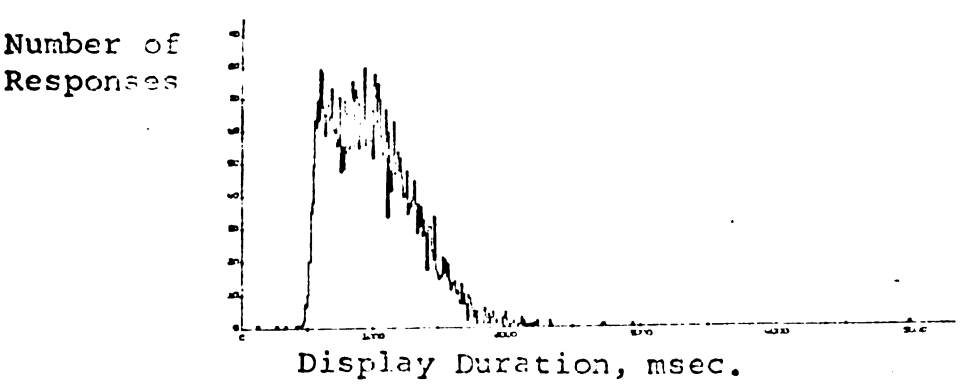

Figure IV.20.2. Histogram with 10 msec. intervals: Subject PA in Experiment B-1.

Figure IV.30. Examples of power spectral estimates and their autocorrelations calculated from histograms of Experiment B-1. The autocorrelation is the upper or leftmost of the two graphs that make up each subfigure. The abscissa for the autocorrelation is the lag number k. The ordinate is $\hat{R}(k\Delta T)$. See Eqn II.40.70. Conversion to time lag ΔT can be made using $\Delta T = K\Delta t$. The abscissa for the power spectrum is p, which is related to frequency by $f = p/2m\Delta t$. The ordinate is $\hat{P}_o(p)$. See Eqn II.40.80. T[a,b] denotes the histogram interval analyzed, Δt is the histogram interval size, $m^* = m \cdot \Delta t/(b-a-1)$, $m'^* = m' \cdot \Delta t/(b-a-1)$, and s^* is the average number of responses/interval in the histogram over T[a,b].

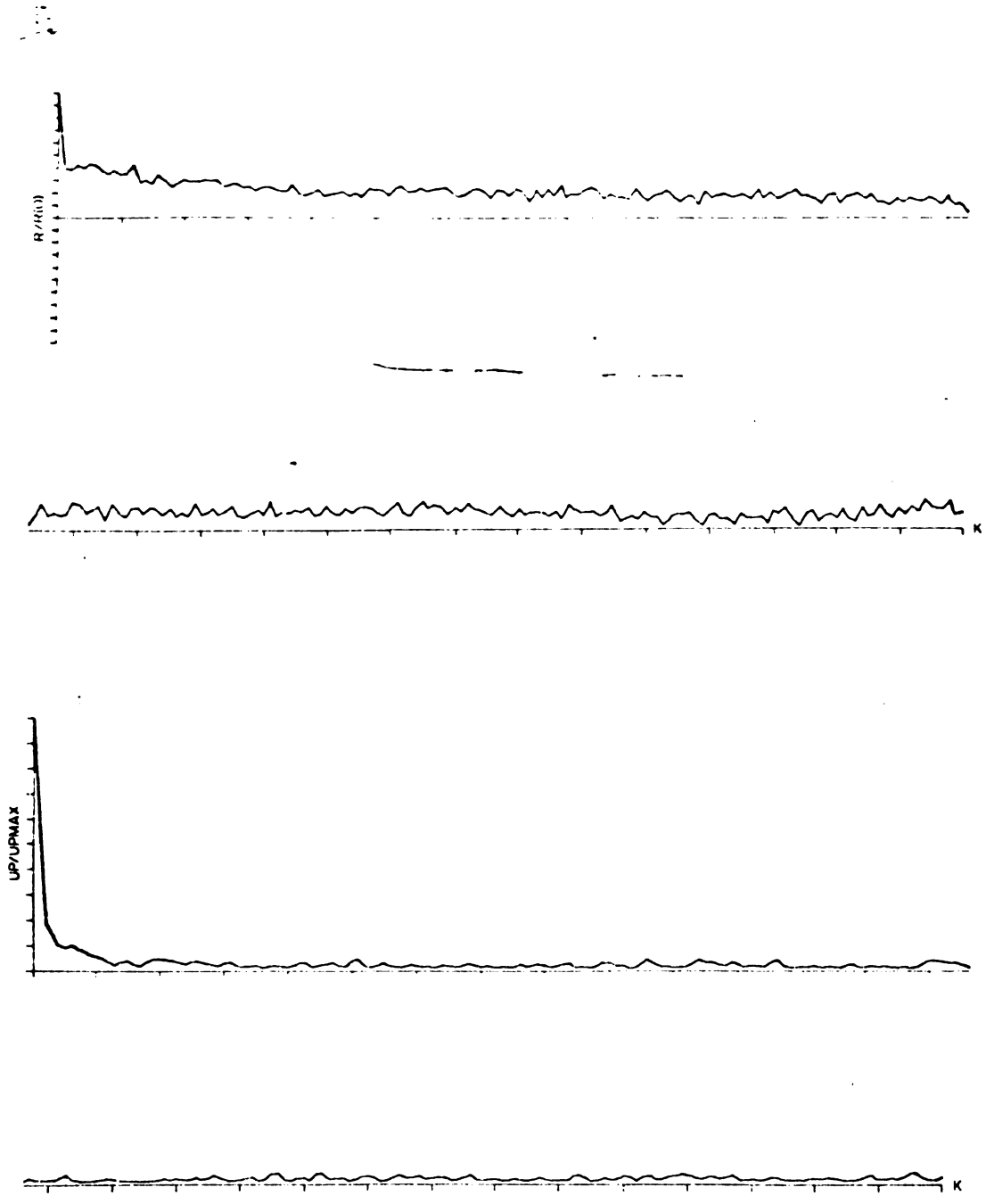

Figure IV.36.1. Subject DJ: Δt = 3 msec., T[a,b] = T[571,2080], m* = m'* = .5 and S* = 6.4 responses/interval.

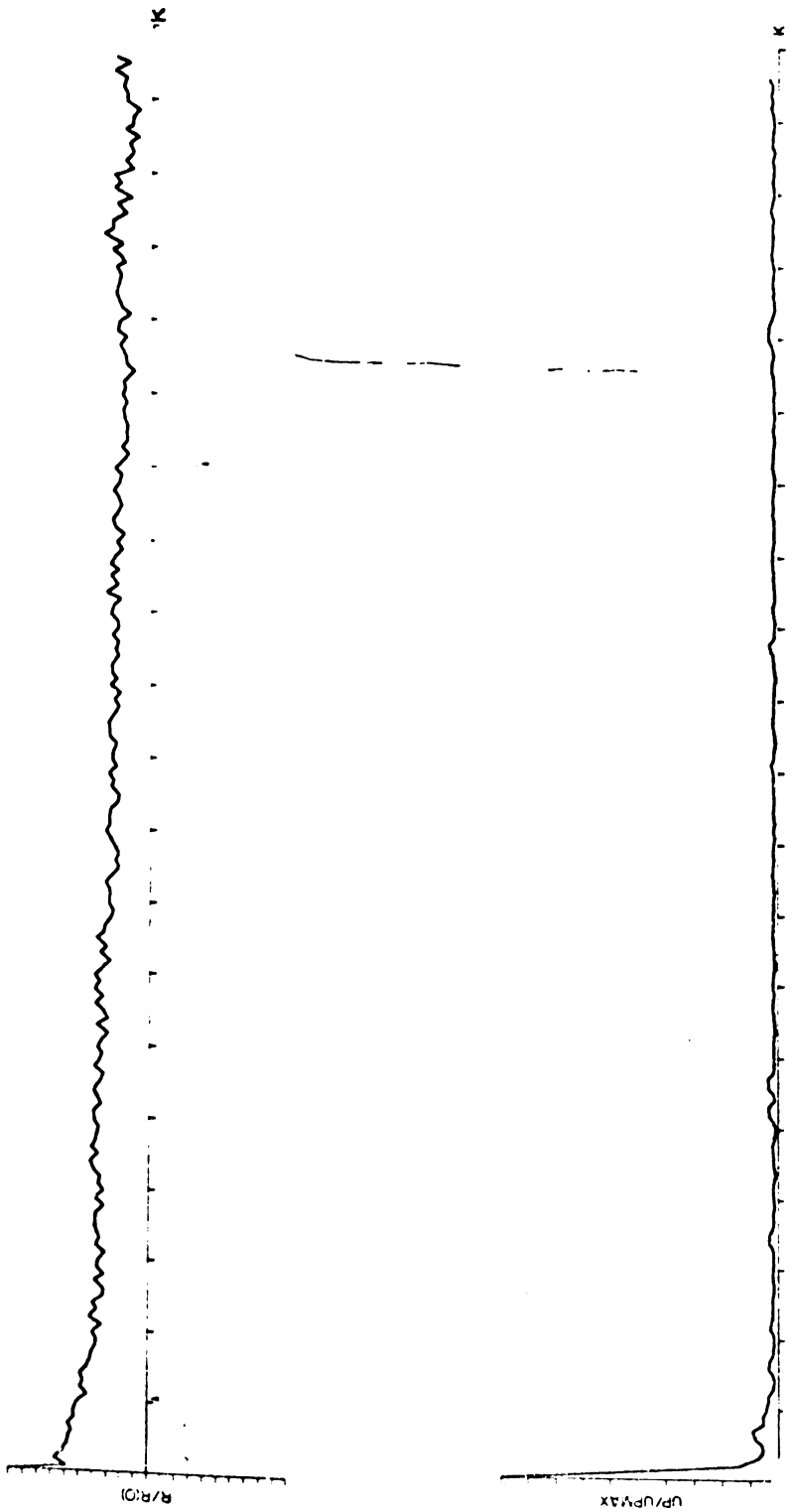

Figure IV.30.2. Subject DF: Δt = 5 msec., T[a,b] = T[551,2510], m*= m'* = .5 and S* = 12.7 responses/interval.

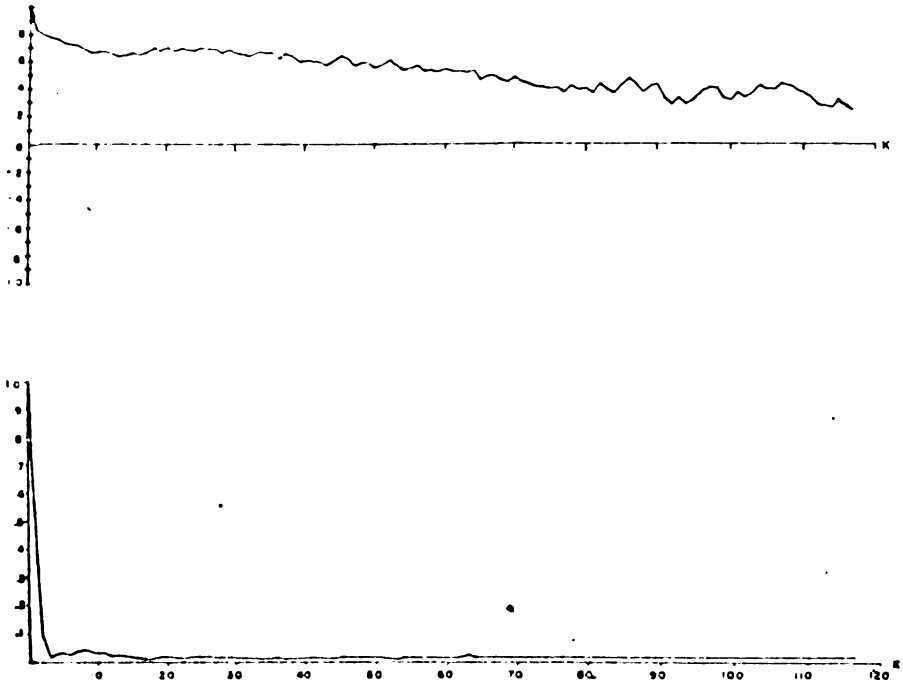

Figure IV-30-3. Subject DJ: Δt = 10 msec., T[a,b] = T[550,2879], m* = m'* = .5 and S* = 21.7 responses/interval.

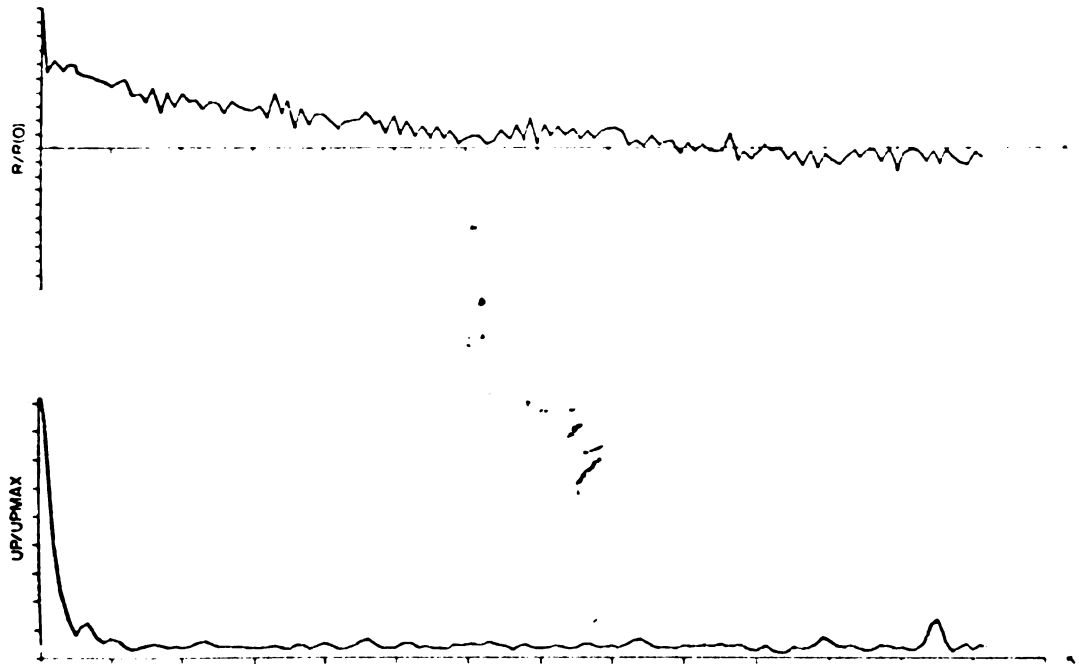

Figure IV.30.4. Subject GR: Δt = 5 msec., T[a,b] = T[535,1934], m* = m'* = .5 and S* = 19 responses/interval.

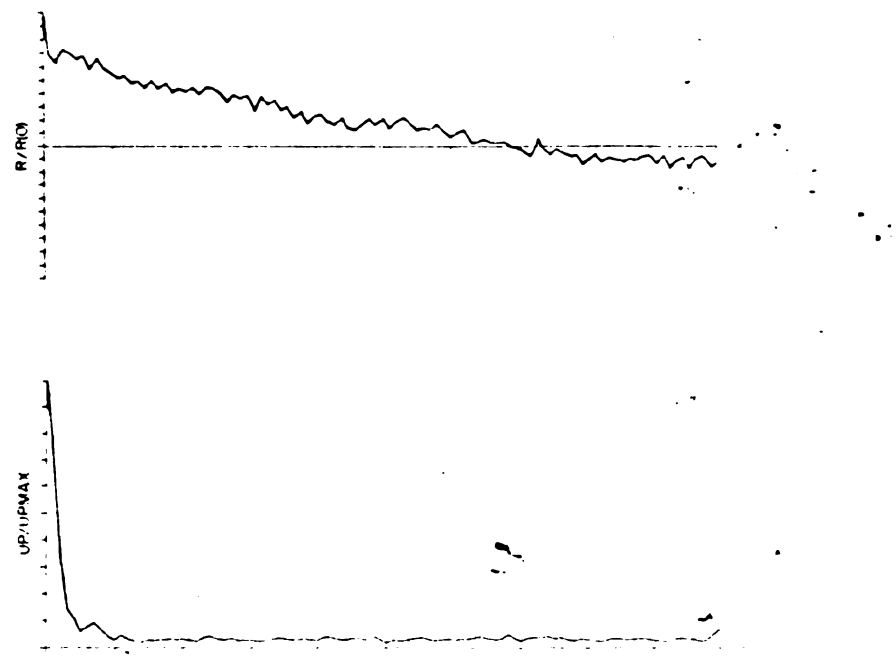

Figure IV.30.5. Subject GR: Δt = [illegible], T[a,b] = T[535,1931], m* = m'* = .5 and S* = 37.3 responses/interval.

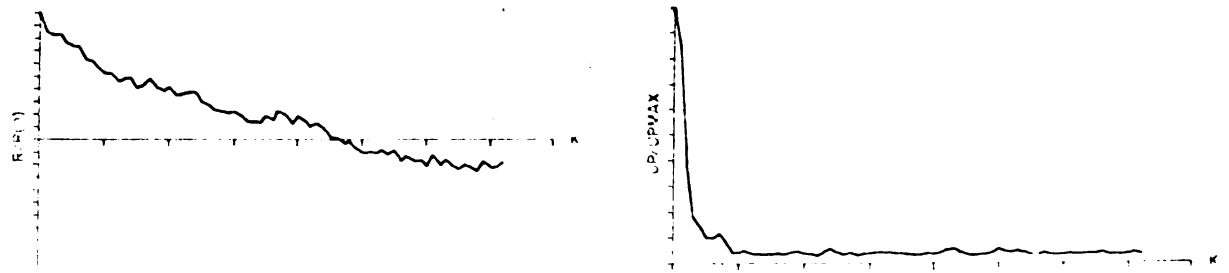

Figure IV.30.6.
Subject GR:
t = 10 msec.,
T[a,b] = T[510,1939],
m* = m'* = .5 and
s* = 32.8 responses/
interval.

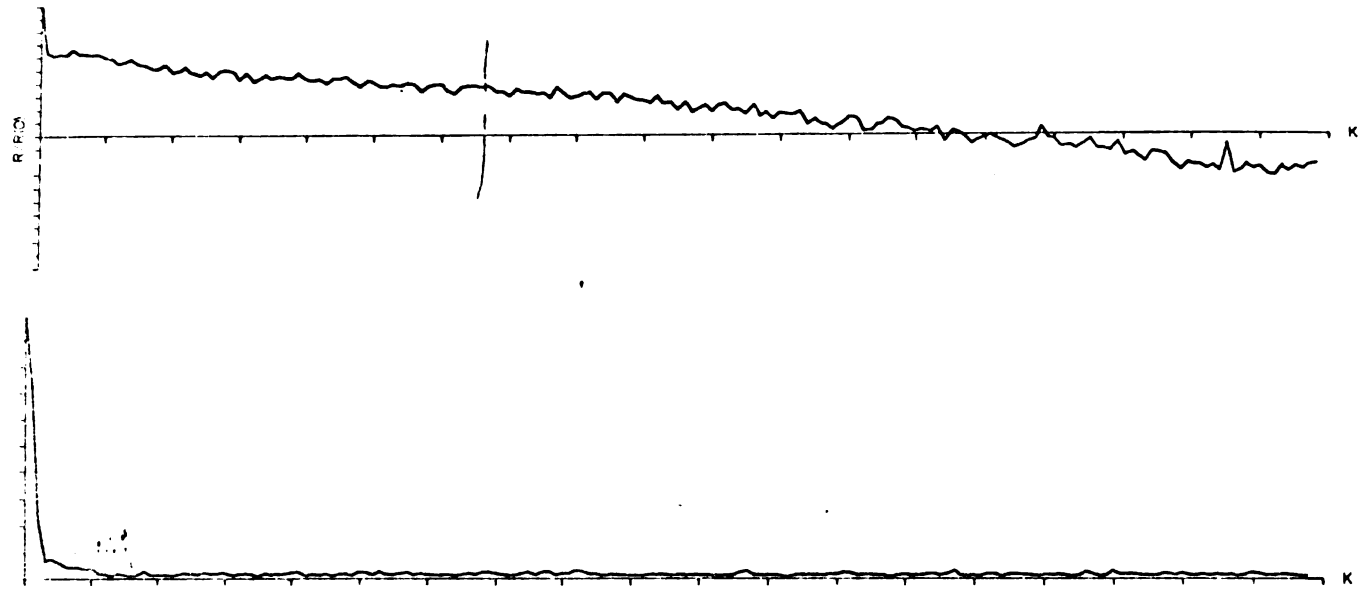

Figure IV.30.7. Subject PA: Δ t = 5 msec.,
T[a,b] = T[561,1628], m* = m'* = .5 and
s* = 14.5 responses/interval.

Figure IV.30.8. Subject PA: Δt = 5 msec., ↓ T[a,b] = T[435,1604], m* = m'* = .5 and S* = 22.1 responses/interval.

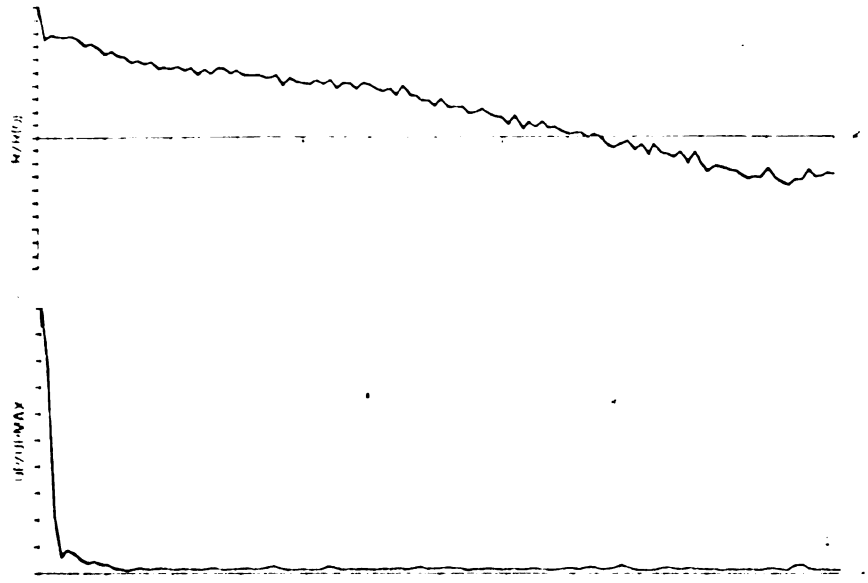

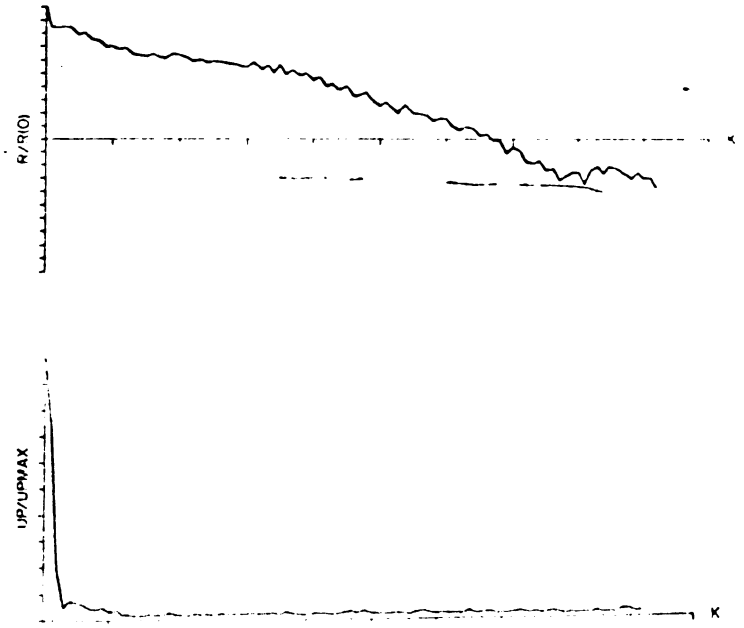

Figure IV.30.9. Subject PA: Δt = 7 msec, T[a,b] = T[1033,1763], m* = m'* = .5 and S* = 29.4 responses/interval.

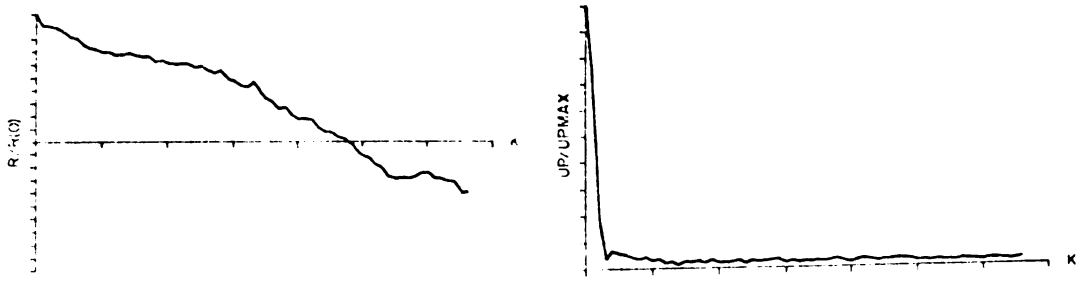

← Figure IV.30.10. Subject PA:
Δt = 10 msec.,
T[a,b] = T[400,1789],
m* = m'* = .5 and
S*=39 responses/interval.

Figure IV.30.11. Subject JM: Δt = 7 msec., T[a,b] = T[406,1700],
⇩ m* = m'* = .5 and S* = 27 responses/interval.

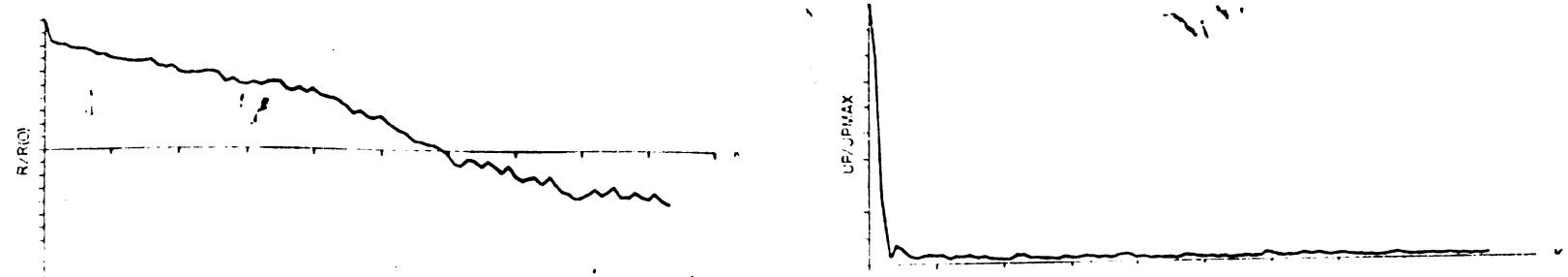

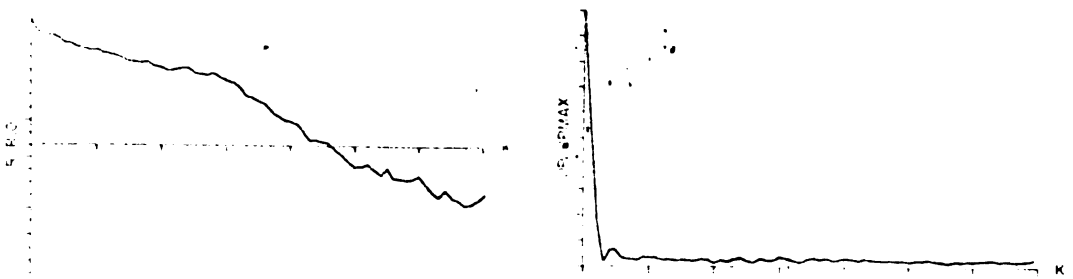

⇦ Figure IV.30.12. Subject JM:
Δt = 10 msec.,
T[a,b] = T[400,1779],
m* = m'* = .5 and
S* = 34 responses/interval.

of all of these, and indeed all the PSE's, is their lack of feature. They are unlike most of the PSE's obtained by Augenstein. Figure II.50, a PSE from SHN, is one of those that was somewhat similar.

IV.20.30. The average time per symbol.--The response times corresponding to the situation where the target element was in the 3rd position of the sequence were edited from each subject's data and 10 msec. interval histograms of these response times were constructed. The same prodecure was used for the 8th, 13th, 18th and 23rd positions,** two of these sets of histograms are shown in Figures IV.40 and IV.50. The average response time per symbol was obtained by plotting the average response time for each of the five positions and calculating the slope of the straight line of approximate mean square best fit. Only one subject, DJ, with an average response time per symbol of 68 msec., had a nonzero value. The other three subjects were taking as much time to process a sequence with a target element in the third position as it took them to process a sequence with a target element in the 23rd position.

**Recall that these positions had three times the number of target elements in them as in the other positions. Therefore, there were a significant number of data points corresponding to each of these positions.

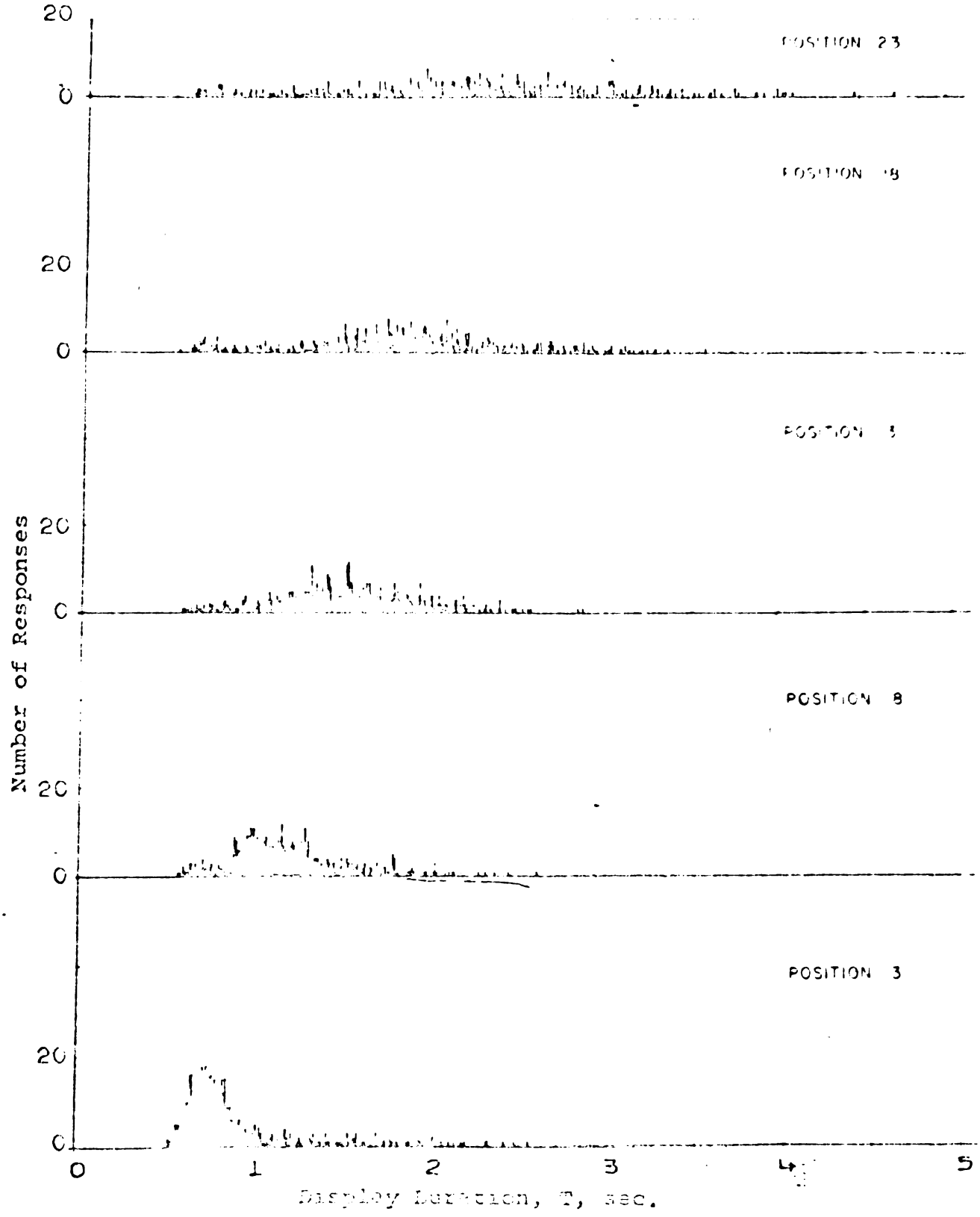

Figure IV.40. Histograms of response times for selected positions: Subject DJ.

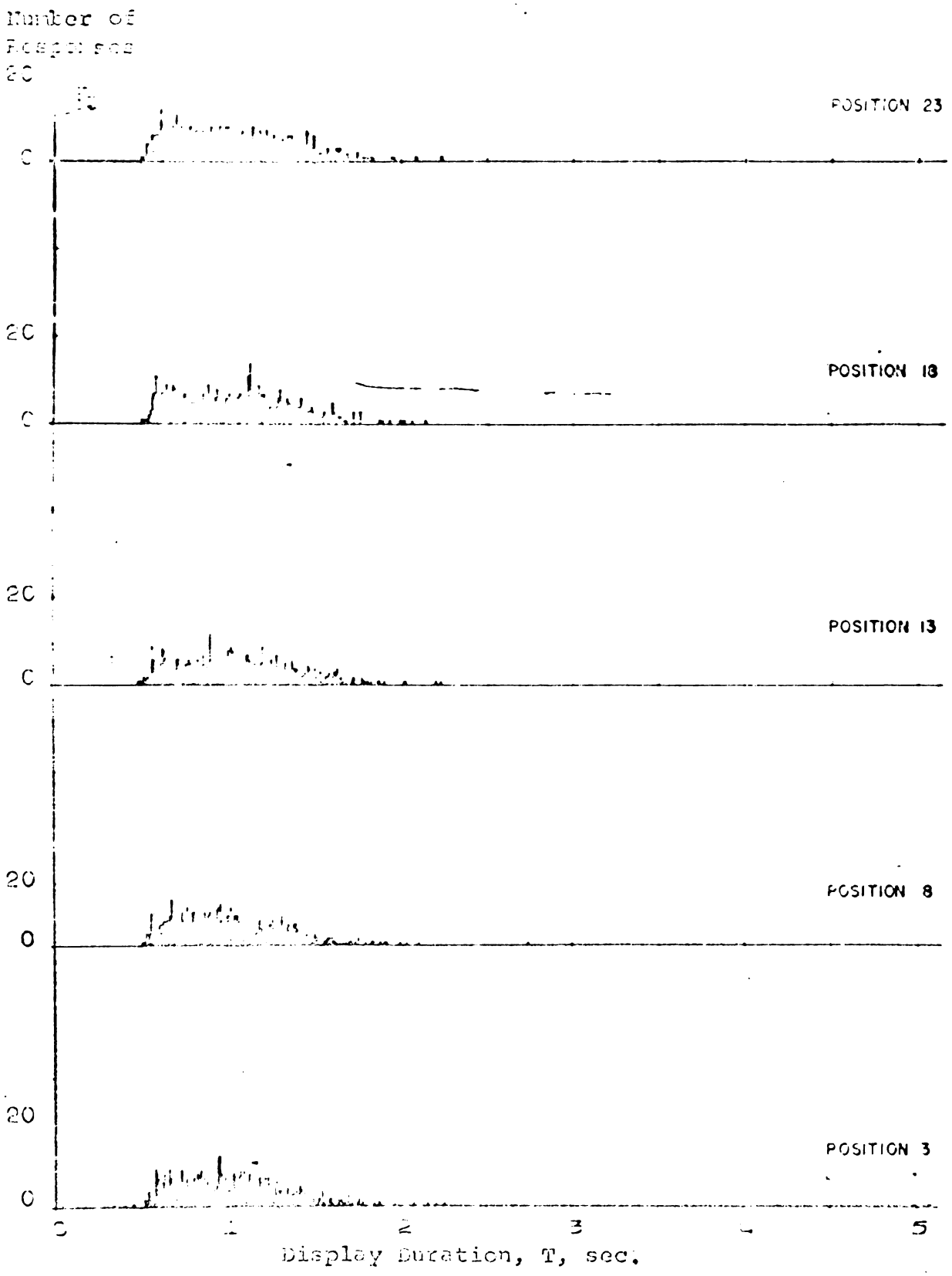

Figure IV.50. Histograms of Response Times For Selected Positions: Subject PA.

IV.20.40. A history of response times for selected positions.--While pondering the reasons for the discrepancies between the results of SHN and the results of this experiment, it was noticed that subject DJ's data seemed to fall into two classes: the data collected during the first part of the experiment were a function of position, the data collected during the last part were not. The data from the other subjects did not have this property. To construct the graphs in Figure IV.60 the data were arranged by position and in the correct chronological order of their generation. The data were then grouped into sets of 25 and the averages of these sets were calculated. Figure IV.60.1 indicates that DJ began the experiment by using the anticipated scanning procedure: she appears to have scanned the sequence from left to right at a constant rate. However, as the experiment progressed something began to happen to DJ's processing technique. This change is illustrated by Table IV.1, where the average time per symbol drops from 122 msec. at the beginning of the experiment to 0 near the end.

Accompanying the decrease in average time per symbol, there is an increase in the average time necessary to process the sequences with target elements in the first eight or so positions. The net result is that by the end of the experiment, DJ appears to have used the same processing technique that the other subjects used.

Figure IV.60.1.

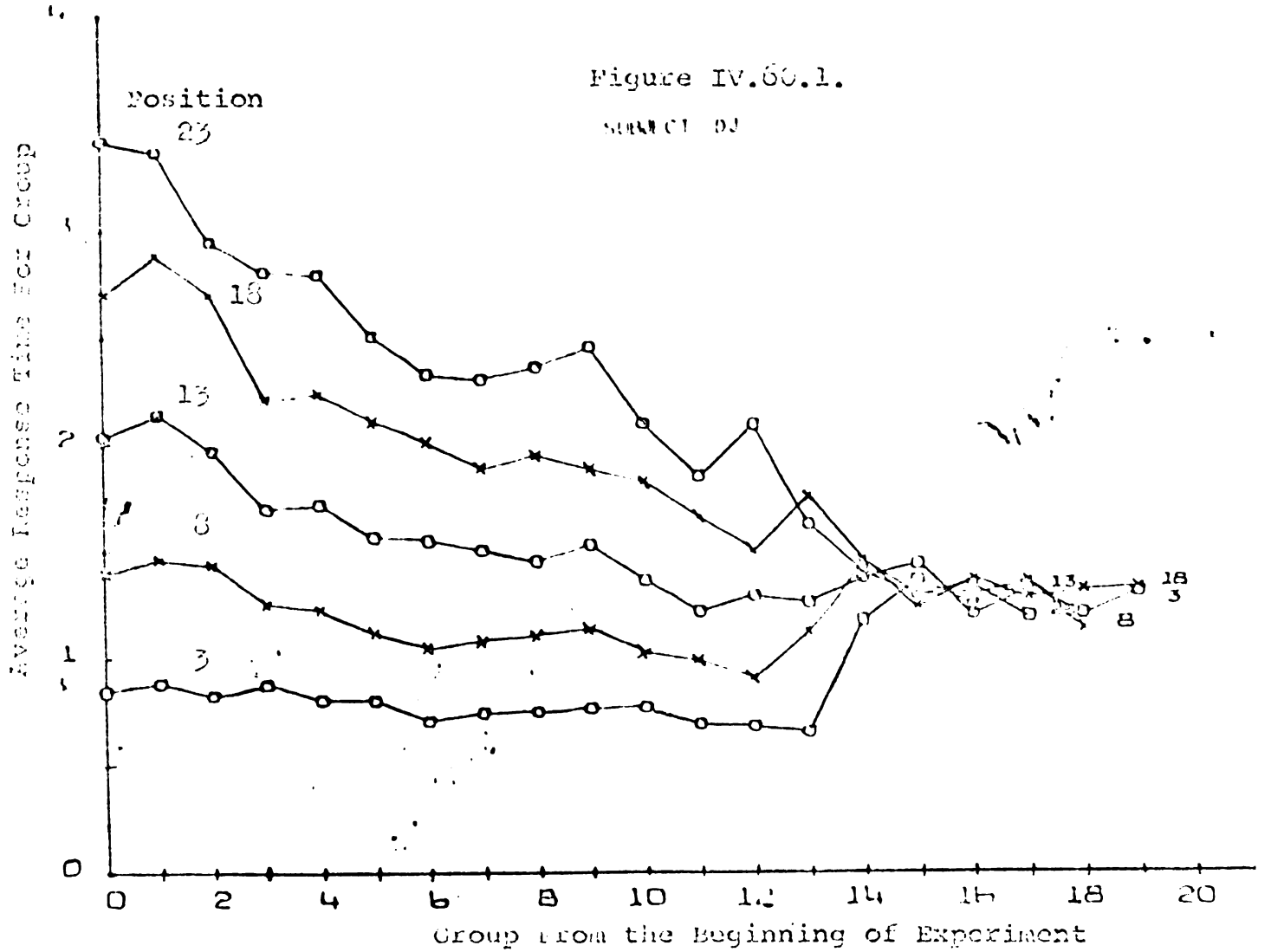

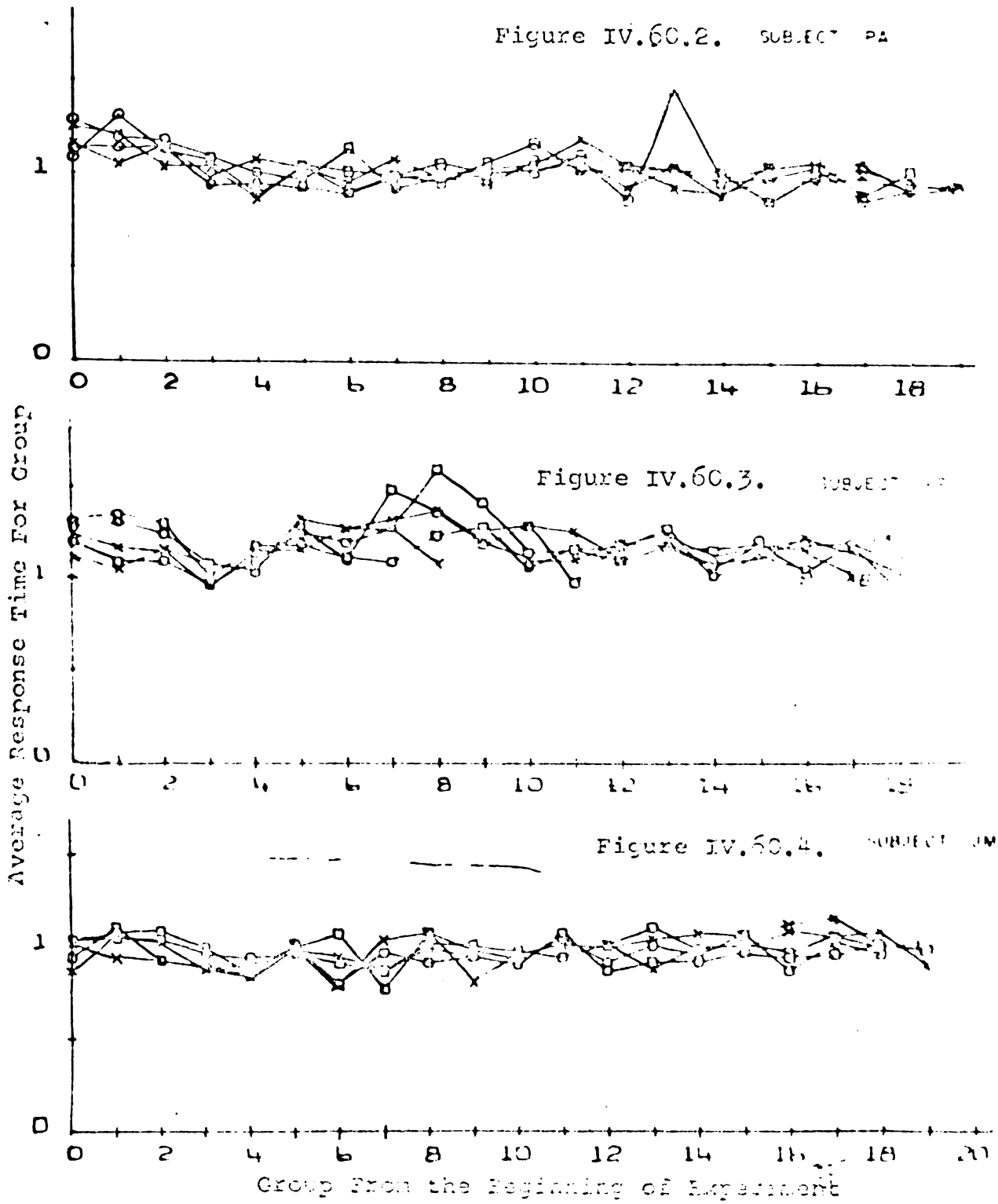

Figure IV.60. A history of response times for selected positions. The data were lumped into groups of twenty-five.

TABLE IV.1.--Average time per symbol during the course of experiment B-1: Subject DJ.

Set of data points averaged*	Average time per symbol (msec.)
1-75	122
76-175	98
176-275	82
276-350	61
351-425	0
remaining	0

*For instance, 1-75 signifies that the first 75 data points (chronologically ordered) from each position were used.

IV.30. Experiment B-2

IV.30.10. Experimental design and procedure.

--With very few exceptions, the power spectral estimates of Exp. B-1 did not have the expected "bumpy" form. Augenstein suggested that this discouraging lack of bumpiness might have been due to an experimental variable that was not identified at the conception of Exp. B-1, the amount of time between trials.

It is known that a periodically varying electrical potential, called the alpha rhythm, can be recorded from the scalp (most strongly above the occipital lobes of the brain) of most persons who are awake but whose mind is in a resting state. Furthermore, if this resting state is

disturbed, say by presenting something interesting into the visual field, the alpha rhythm disappears. In the experimental procedure of SHN there was an unintentional 30 second interval between trials. Conceivably, boredom with the whole procedure could have imposed an alpha rhythm during these intervals. On the other hand, in B-2 there was only a very brief (the subjects averaged four seconds per slide) interval between trials. Hence, the probability of an alpha rhythm being present during this interval is much smaller than during a 30 second interval. Could it be that the same phenomenon which generates the alpha rhythm is also responsible for the periodic nature of the histograms? This was pure speculation, but it did indicate a previously unforeseen difference between the two experimental procedures: the time between trials.

The experiments developed to test this difference were straightforward. In an experiment called B-2F, each of five subjects* was given 1120 trials with a minimal time between trials; this procedure duplicated that of B-1. Then, in an experiment designated B-2S, each of the subjects was given 1120 trials with a mandatory 30 second

---

*Subjects TJ, MV and DF were American. JT was from the Far East and IK from the Middle East. All the subjects were males. DF was very impatient and his data contained many errors. He had a reputation for being very intelligent. JT did not speak English as well as IK.

rest period between trials; this procedure was an attempt to duplicate the procedure of SHN.

IV.30.20. Power spectral analysis.--The analytical procedure for B-2F and B-2S was identical to that of B-1. To enumerate the steps:

1. The raw data were edited.
2. Histograms of one millisecond intervals were formed (10 histograms altogether, five from B-2F and five from B-2S).
3. Histograms with three, five, seven and ten millisecond interval histograms (there were a total of five histograms per subject per experiment). Examples of the 10 msec. interval histograms are shown in Figure IV.70.
4. Sections, T[a,b] of each of the histograms except those with one millisecond intervals were chosen.
5. Parameter values of $m'^* = m^* = m/N\Delta t = .50$, .33 and .25 were chosen and PSE's calculated using Eqns. II.40.70 and II.40.80.

Figures IV.80 and IV.90 contain examples of the PSE's of Exp. B-2F and B-2S respectively. After an inspection of these and the other PSE's it has been concluded that the only visible qualitative difference between the PSE's of the two experiments is that the PSE's calculated

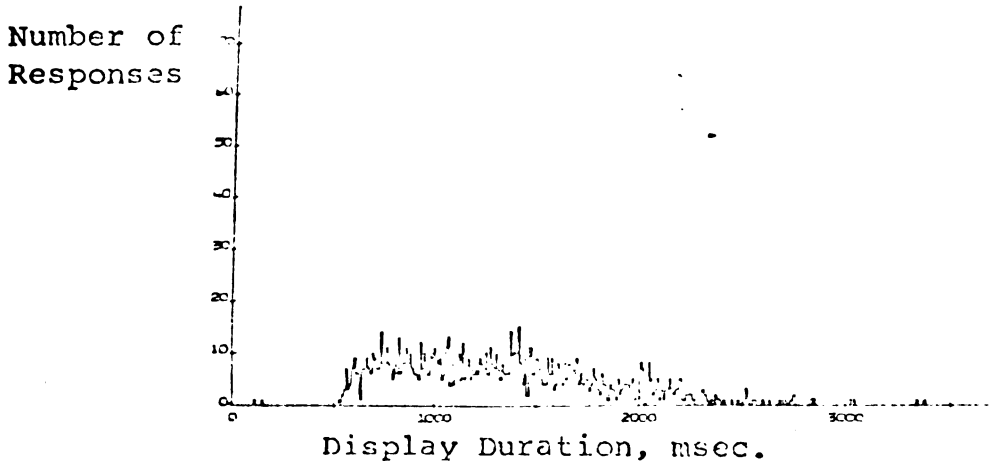

Figure IV.70.1. Histogram with 10 msec. intervals: Subject TJ in Experiment B-2S.

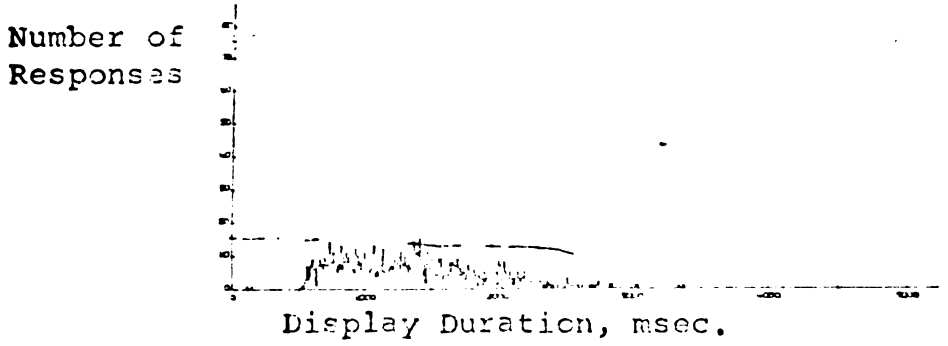

Figure IV.70.2. Histogram with 10 msec. intervals: Subject TJ in Experiment B-2F.

Figure IV.80. Examples of power spectral estimates and their autocorrelations calculated from histograms of Experiment B-2F. The autocorrelation is the upper or leftmost of the two graphs that make up each subfigure. The abscissa for the autocorrelation is the lag number k. The ordinate is $\hat{R}(k\Delta T)$. See Eqn II.40.70. Conversion to time lag ΔT can be made using $\Delta T = K\Delta t$. The abscissa for the power spectrum is p, which is related to frequency by $f = p/2m\Delta t$. The ordinate is $P_o(p)$. See Eqn II.40.80. T[a,b] denotes the histogram interval analyzed, Δt is the histogram interval size, $m^* = m.\Delta t/(b-a-1)$, $m'^* = m'.\Delta t/(b-a-1)$, and s^* is the average number of responses/interval in the histogram over T[a,b].

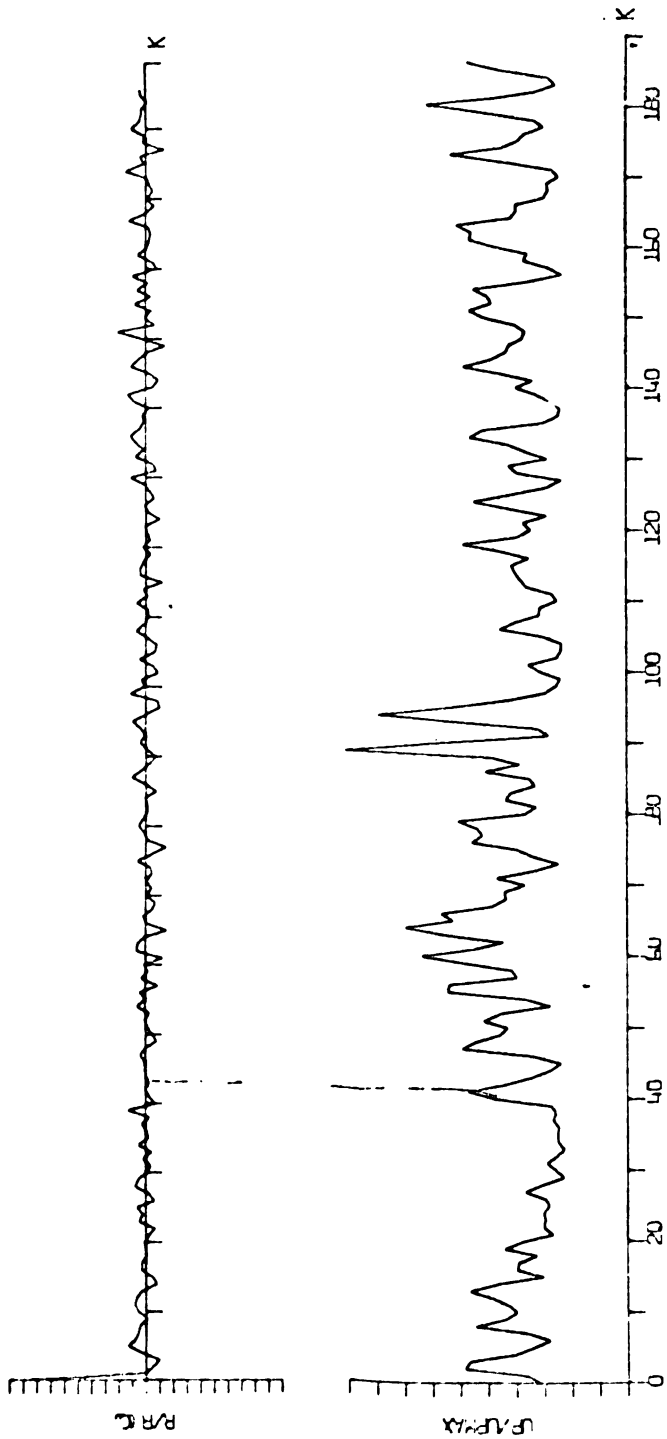

Figure IV.30.1. Subject TJ: Δt = 3 msec., T[a,b] = T[594,1709], m* = m'* = .5 and s* = 2.5 responses/interval.

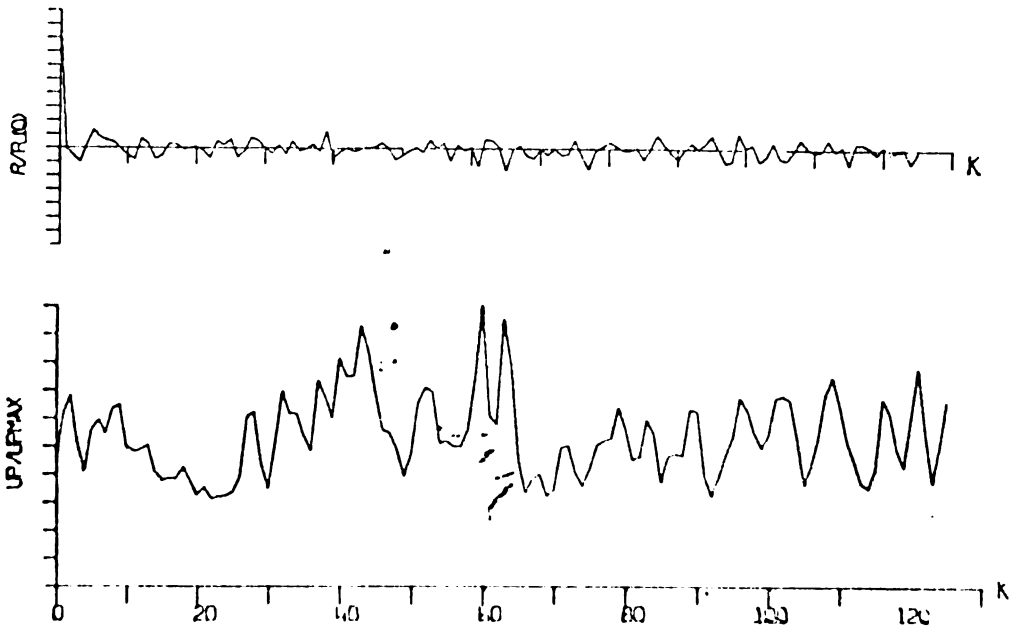

Figure IV.30.2. Subject TJ: Δt = 3 msec., T[a,b] = T[594,1709], m* = m'* = .34 and S* = 2,5 responses/interval.

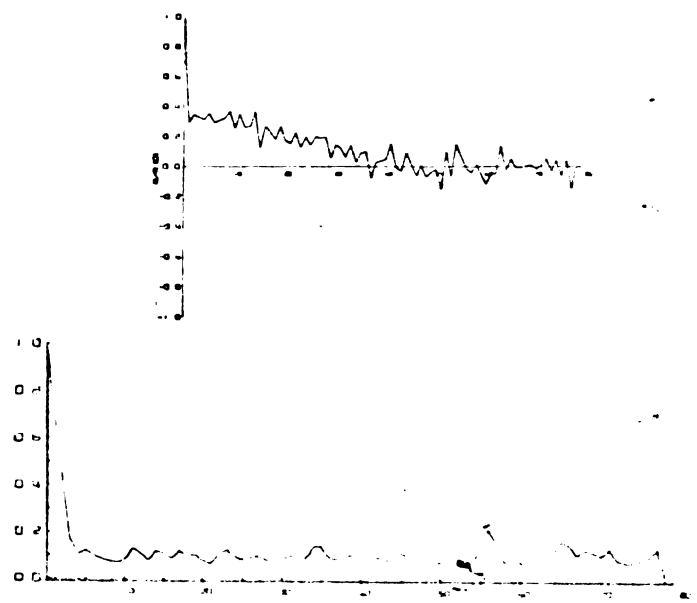

Figure IV.30.3. Subject TJ: Δt = 10 msec., T[a,b] = T[560,2099], m* = m'* = .5 and S* = 6 responses/interval.

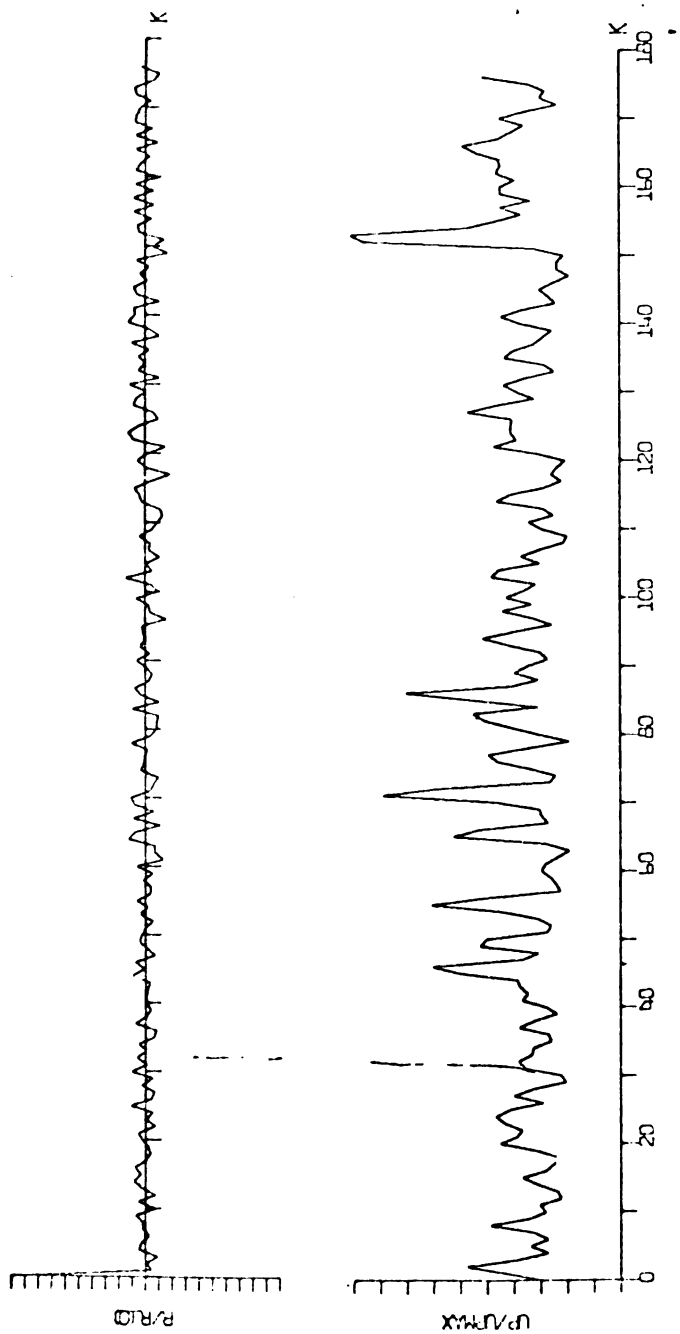

Figure IV.80.4. Subject MV: Δt = 3 msec., T[a,b] = T[793,1850], m* = m'* = .5 and S* = 2 responses/interval.

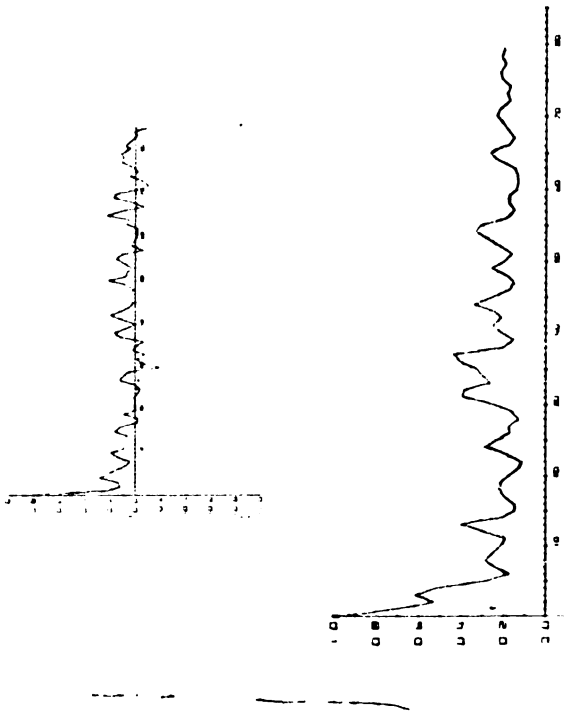

Figure IV.80.5. Subject MV: Δt = 10 msec., $T[a,b] = T[720,2409]$, $m^* = m'^* = .5$ and $s^* = 5.9$ responses/interval.

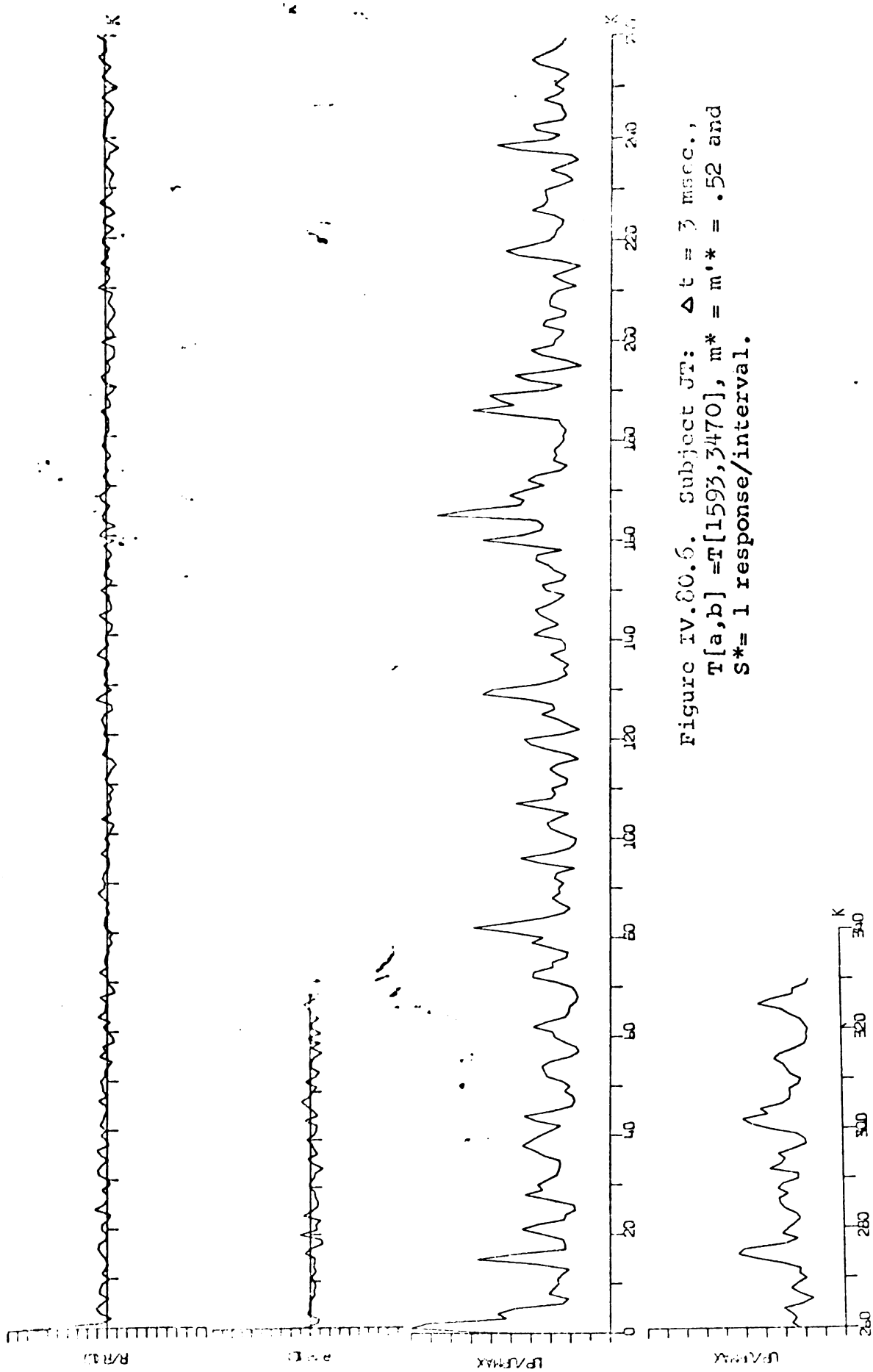

Figure IV.60.6. Subject JT: Δt = 3 msec., T[a,b] =T[1593,3470], m* = m'* = .52 and S*= 1 response/interval.

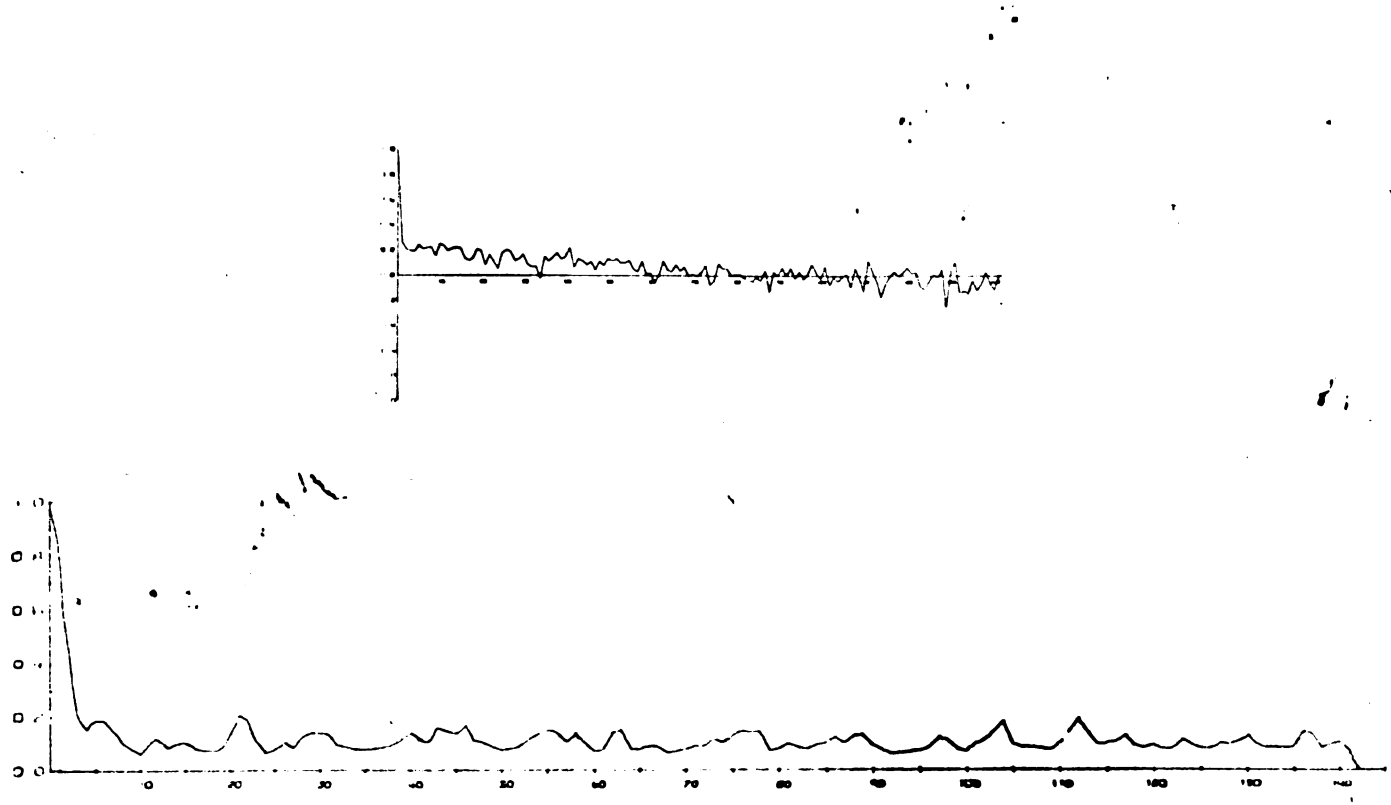

Figure IV.20.7. Subject JT: Δt = 10 msec., T[a,b] = T[1600,4419], m* = m'* = .5 and S* = 2.7 responses/interval.

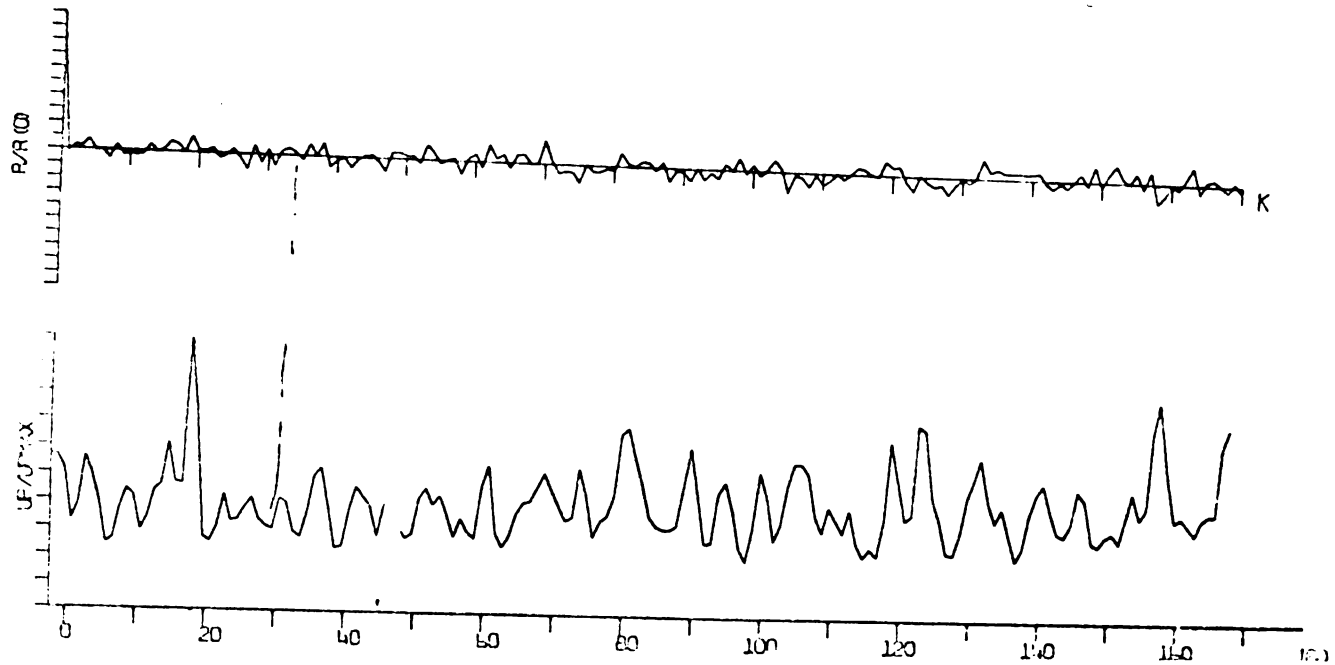

Figure IV.80.8. Subject IK: Δt = 3 msec., T[a,b] = T[1314,2327], m* = m'* = .5 and S* = 2.2 responses/interval.

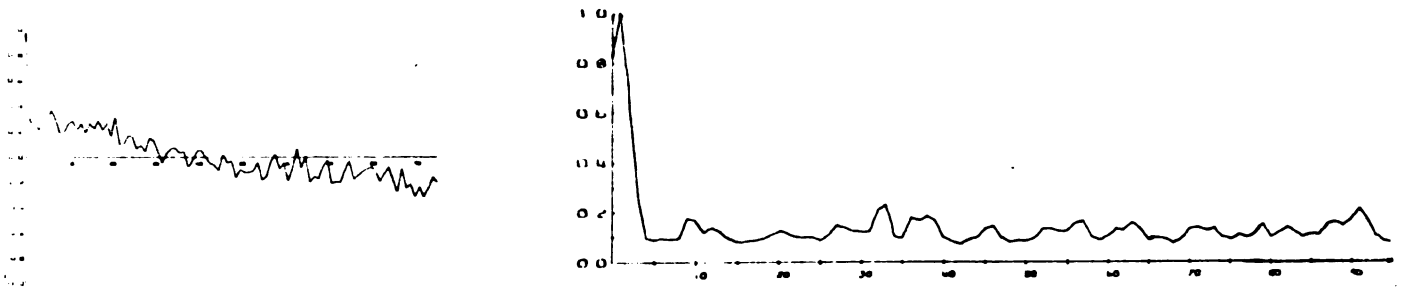

Figure IV.80.9. Subject IK: Δt = 10 msec., T[a,b] = T[860,2739], m* = m'* = .5 and S* = 5 responses/interval.

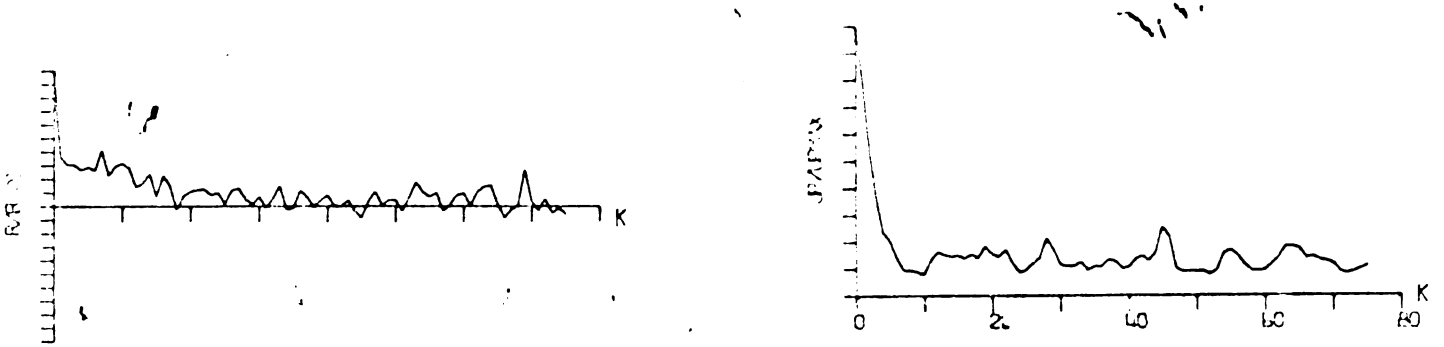

Figure IV.80.10. Subject DF: Δt = 3 msec., T[a,b] = T[672,1118], m* = m'* = .5 and S* = 5.8 responses/interval.

Figure IV.90. Examples of power spectial estimates and their autocorrelations calculated from the histograms of Experiment B-2S. The autocorrelation is the upper or leftmost of the two graphs that make up each subfigure. The abscissa for the autocorrelation is the lag number k. The ordinate is $\hat{R}(k\Delta T)$. See Eqn II.40.70. Conversion to time lag ΔT can be made using $\Delta T = K\Delta t$. The abscissa for the power spectrum is p, which is related to frequency by $f = p/2m\Delta t$. The ordinate is $P_o(p)$. See Eqn II.40.80. T[a,b] denotes the histogram interval analyzed, Δt is the histogram interval size, $m^* = m \cdot \Delta t/(b-a-1)$, $m'^* = m' \cdot \Delta t/(b-a-1)$, and s^* is the average number of responses/interval in the histogram over T[a,b].

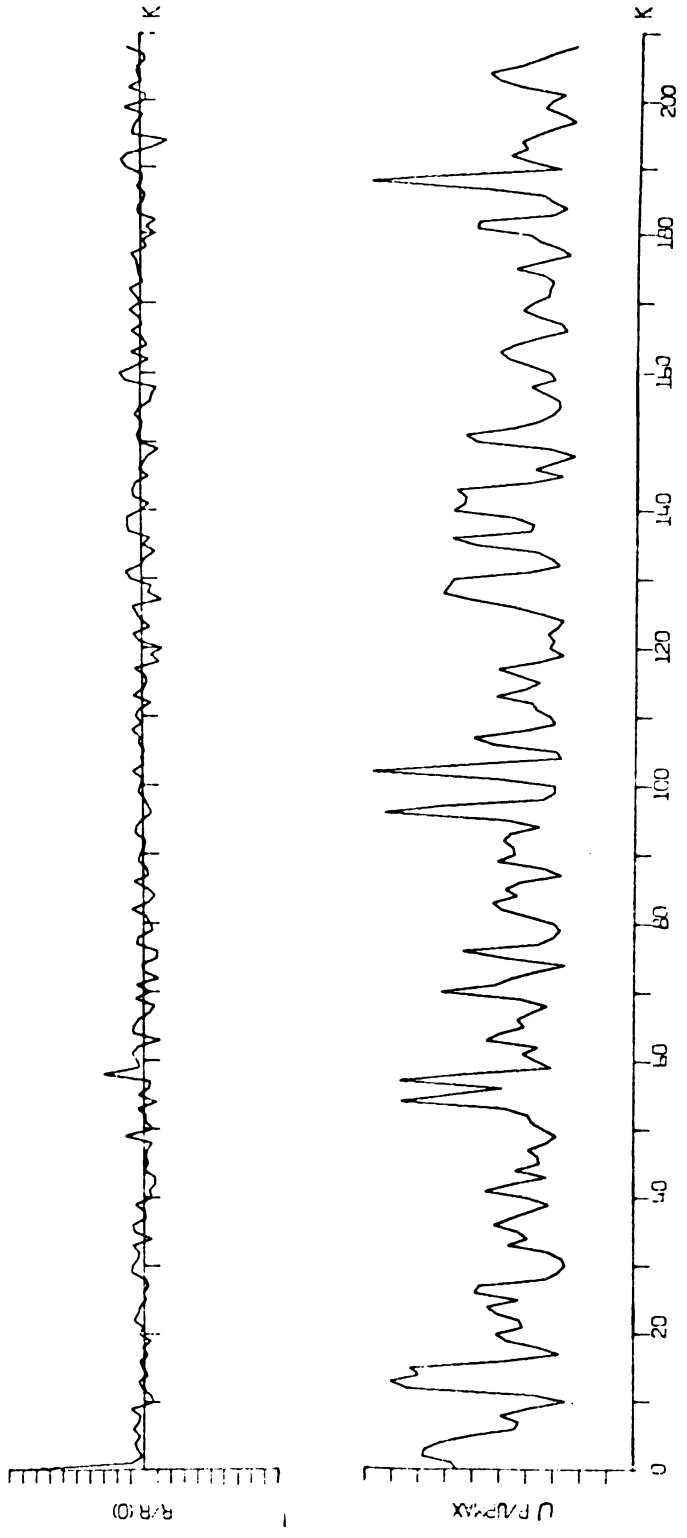

Figure IV.90.1. Subject TJ: Δt = 3 msec., T[a,b] = T[627,1874], m* = m'* = .5 and S* = 3.2 responses/interval.

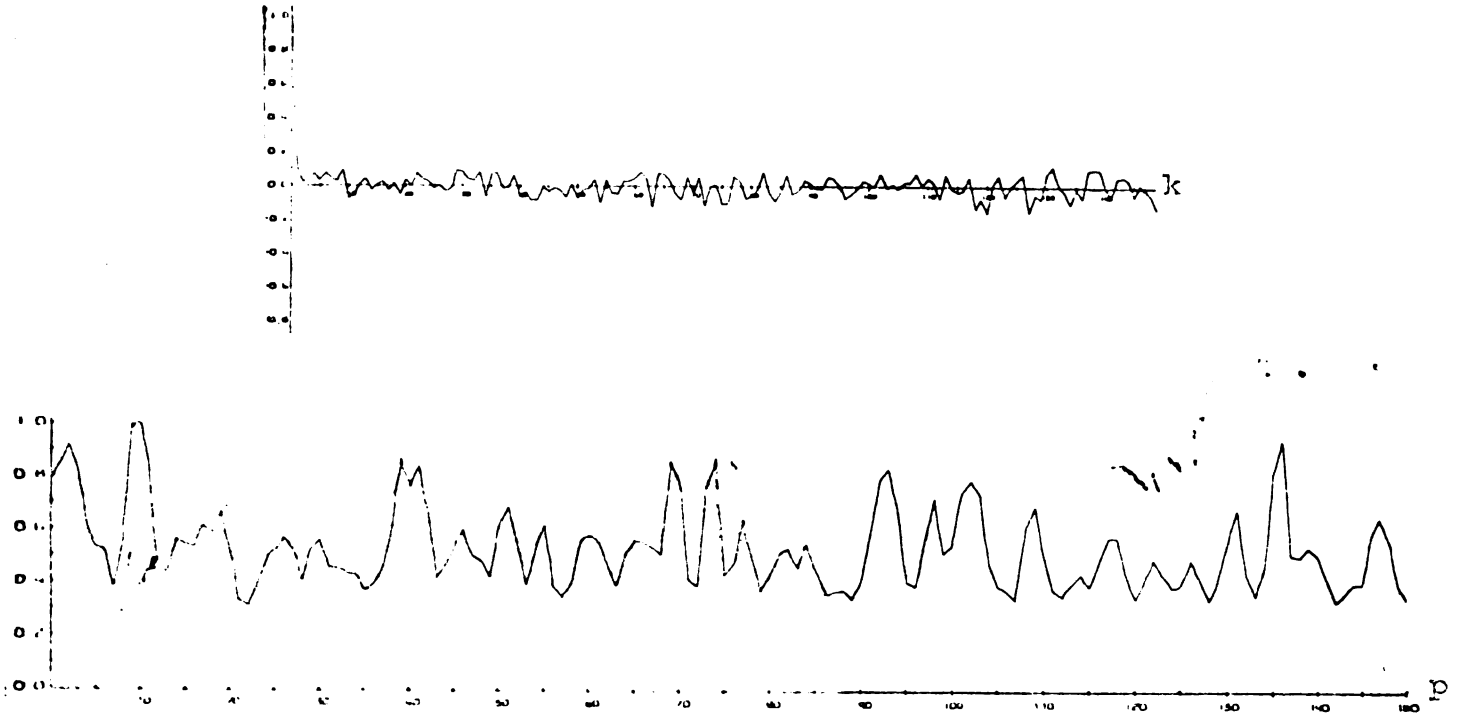

Figure IV.90.2. Subject TJ: Δt = 3 msec., T[a,b] = T[627,1374], m* = m'* = .36 and S* = 3.2 responses/interval.

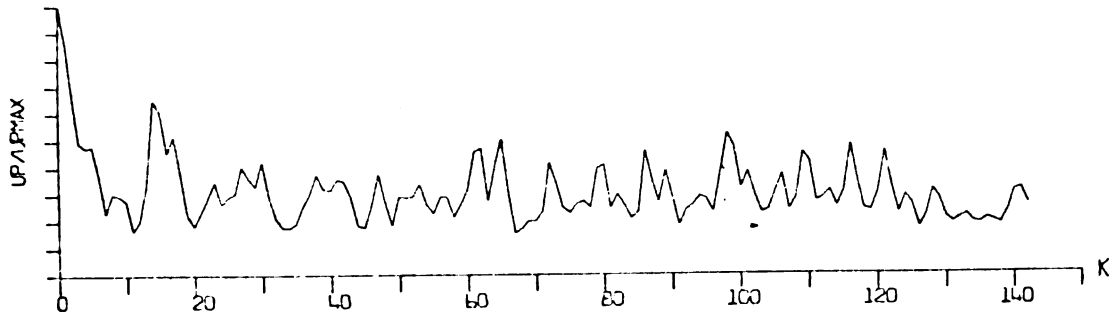

Figure IV.90.3. Subject TJ: Δt = 5 msec., T[a,b] = T[620,2039], m* = m'* = .5 and S* = 3.9 responses/interval.

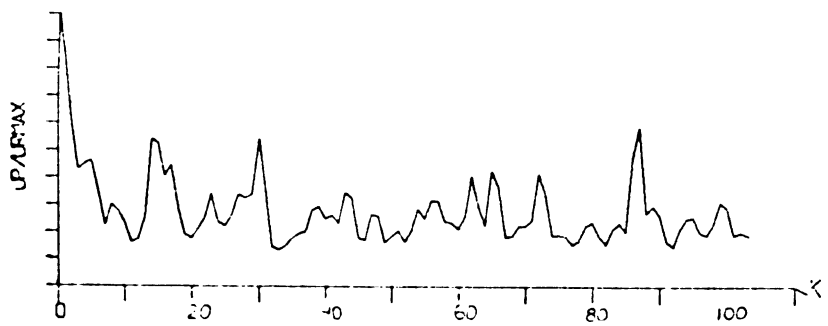

Figure IV.90.4. Subject TJ: Δt = 7 msec., T[a,b] = T[616,2043], m* = m'* = .5 and S* = 5.1 responses/interval.

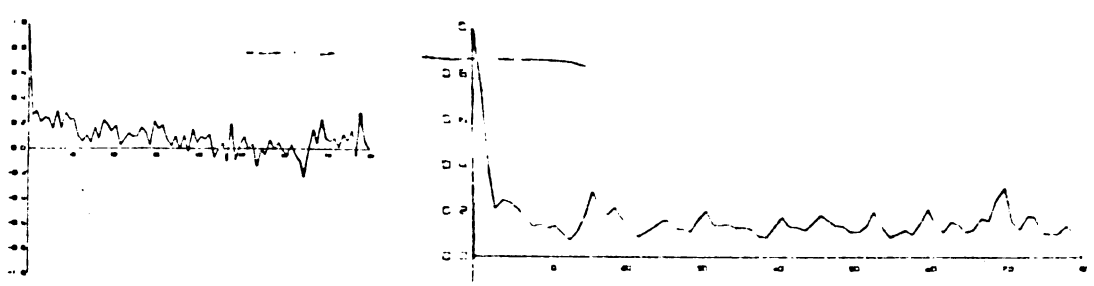

Figure IV.90.5. Subject TJ: Δt = 10 msec., T[a,b] = T[620,2159], m* = m'* = .5 and S* = 6.9 responses/interval.

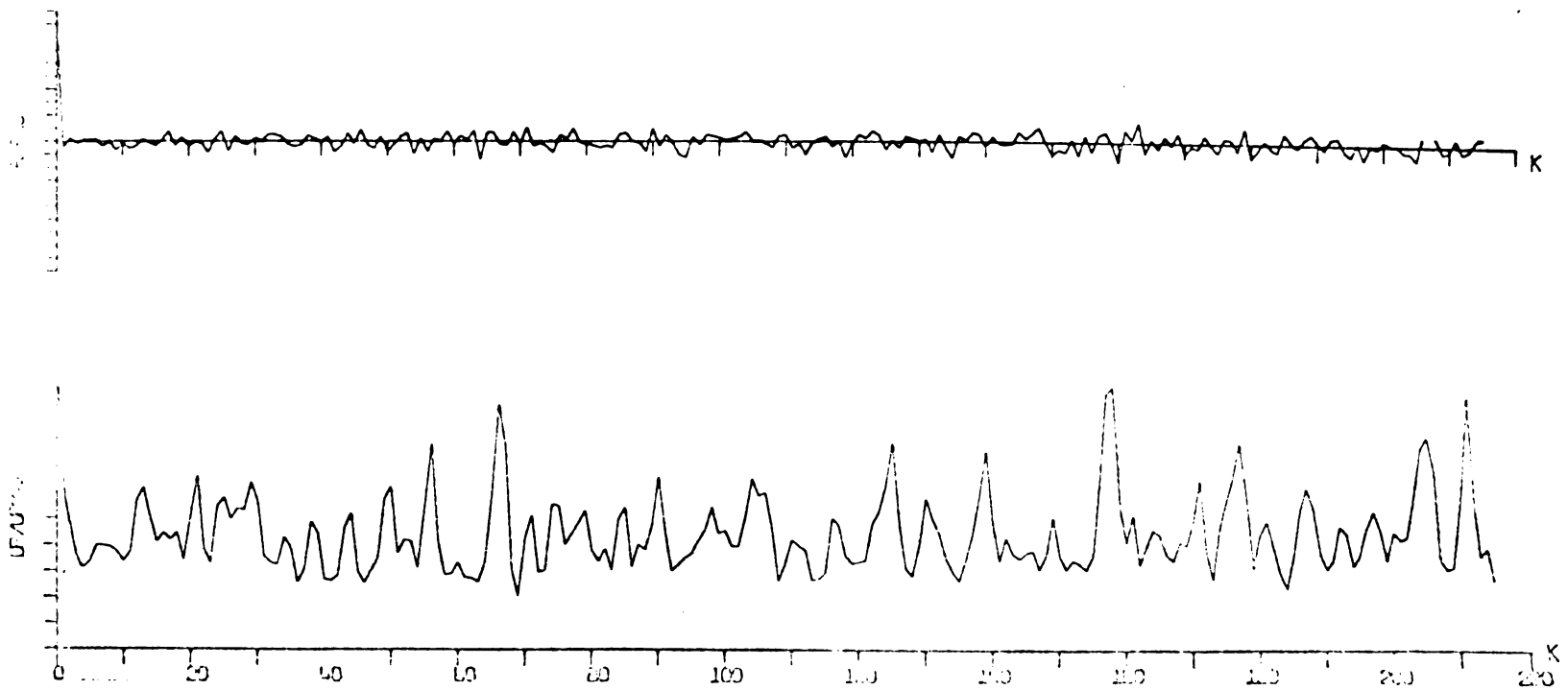

Figure IV.90.6. Subject MV: Δt = 3 msec., T[a,b] = T[600,1886], m* = m'* = .5 and S* = 2.1 responses/interval.

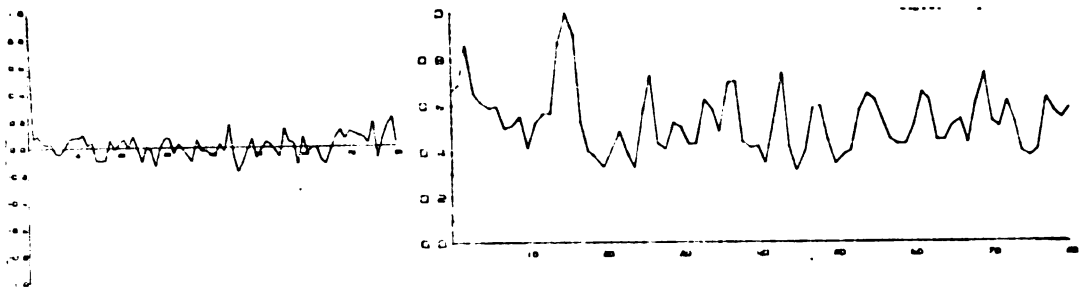

Figure IV.90.7. Subject MV:
Δt = 10 msec.,
T[a,b] = T[540,2139],
m* = m'* = .5 and
S* = 6 responses/interval.

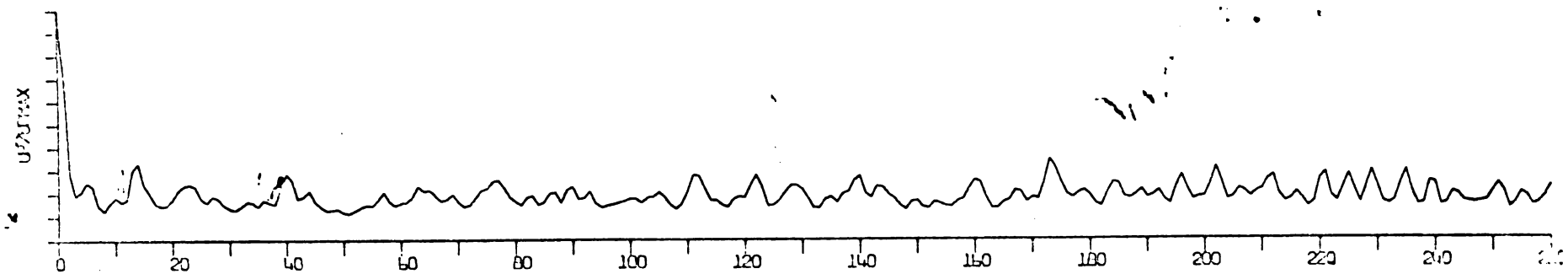

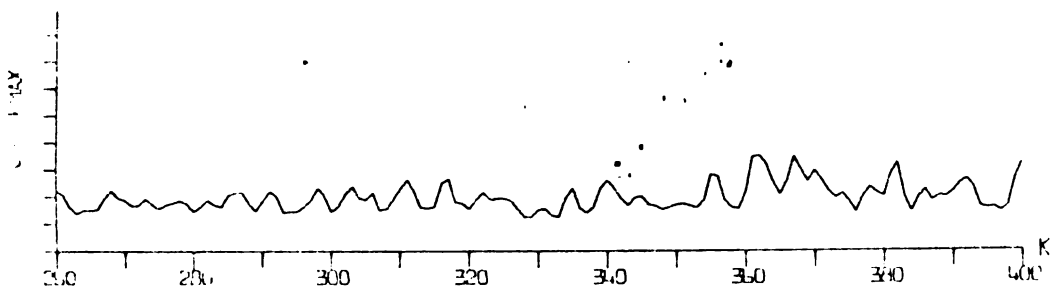

Figure IV.90.8. Subject JT:
Δt = 3 msec.,
T[a,b] = T[1650,6629],
m* = m'* = .25 and
S* = 1 response/interval.

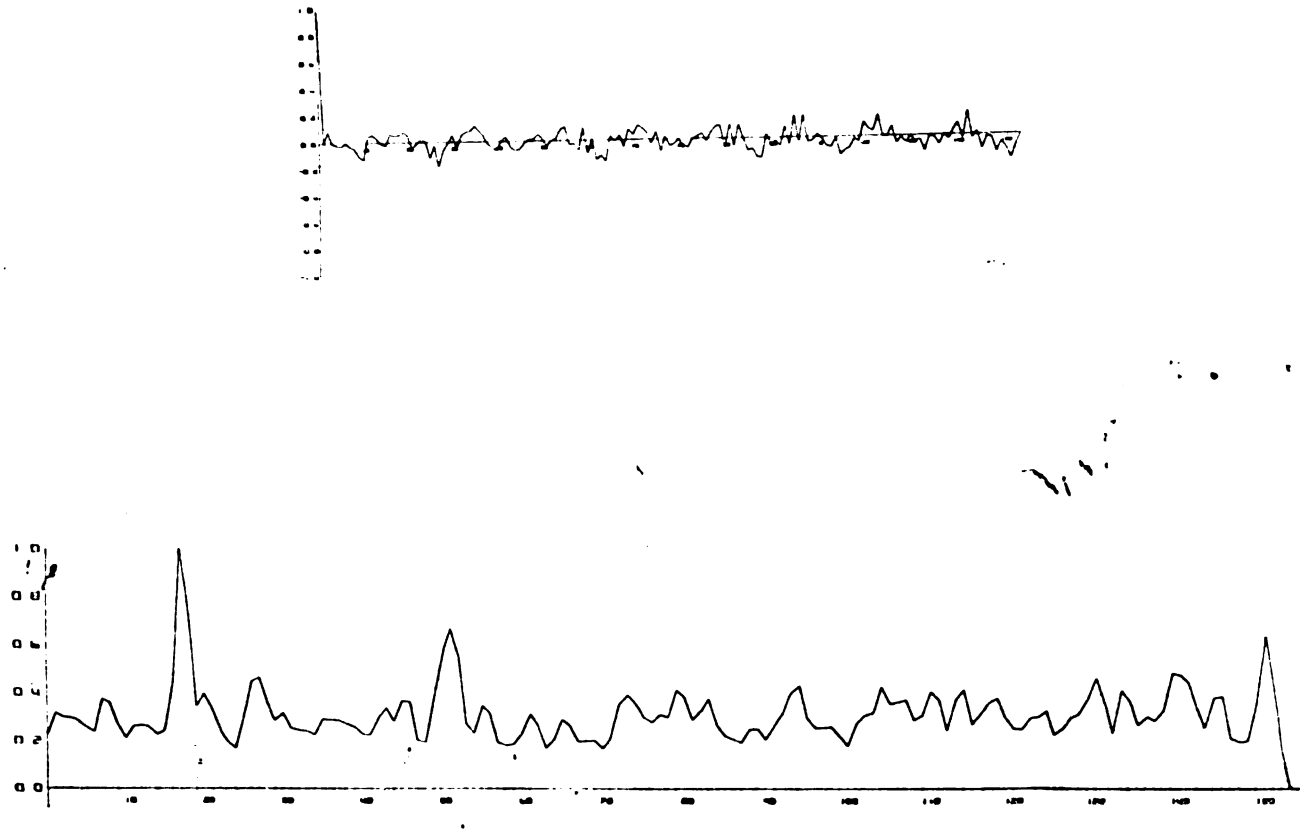

Figure IV.90.9. Subject JT: Δt = 10 msec., T[a,b] =T[2750,5789], m* = m'* = .5 and S* = 2.4 responses/interval.

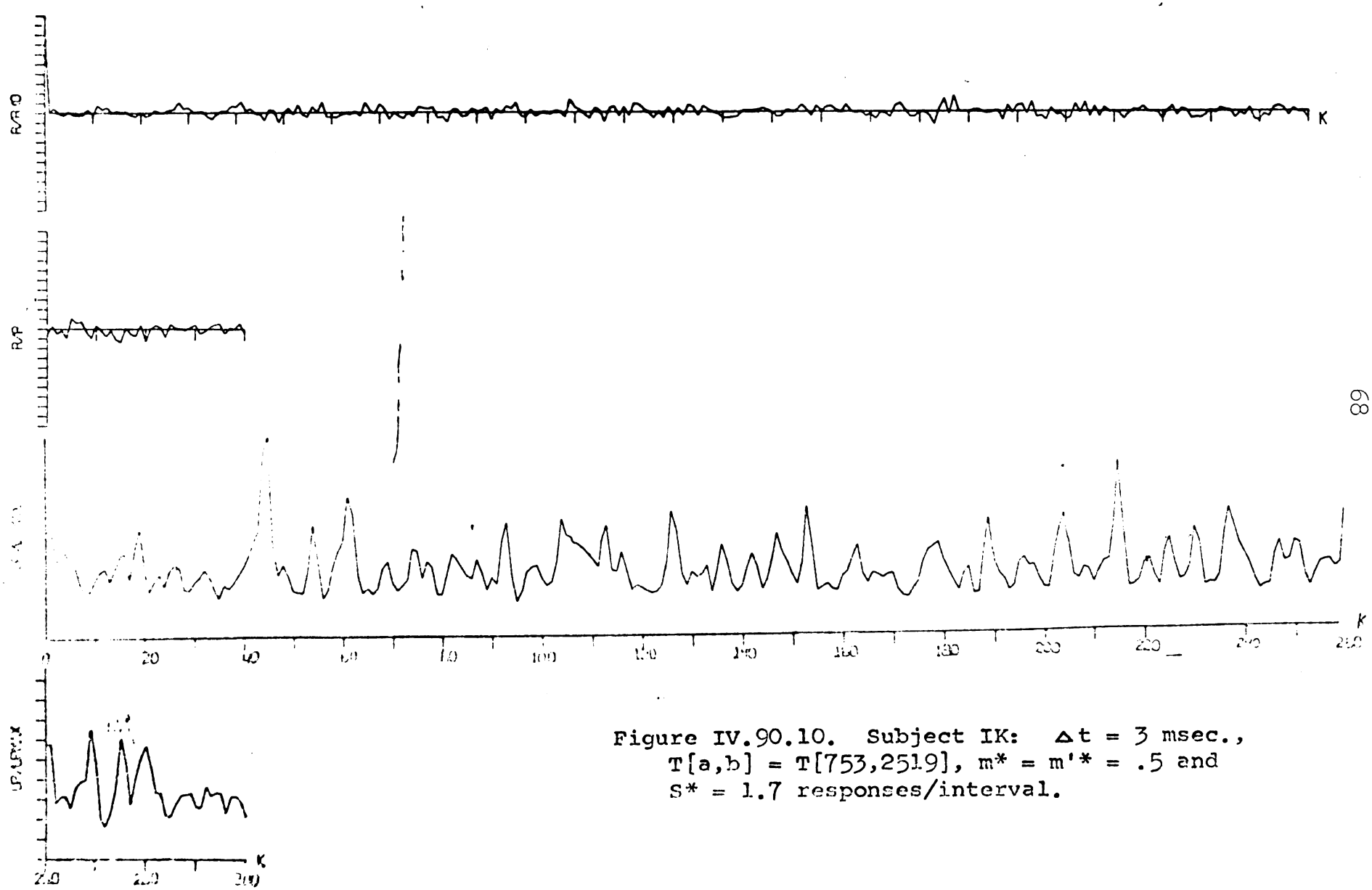

Figure IV.90.10. Subject IK: Δt = 3 msec., T[a,b] = T[753,2519], m* = m'* = .5 and S* = 1.7 responses/interval.

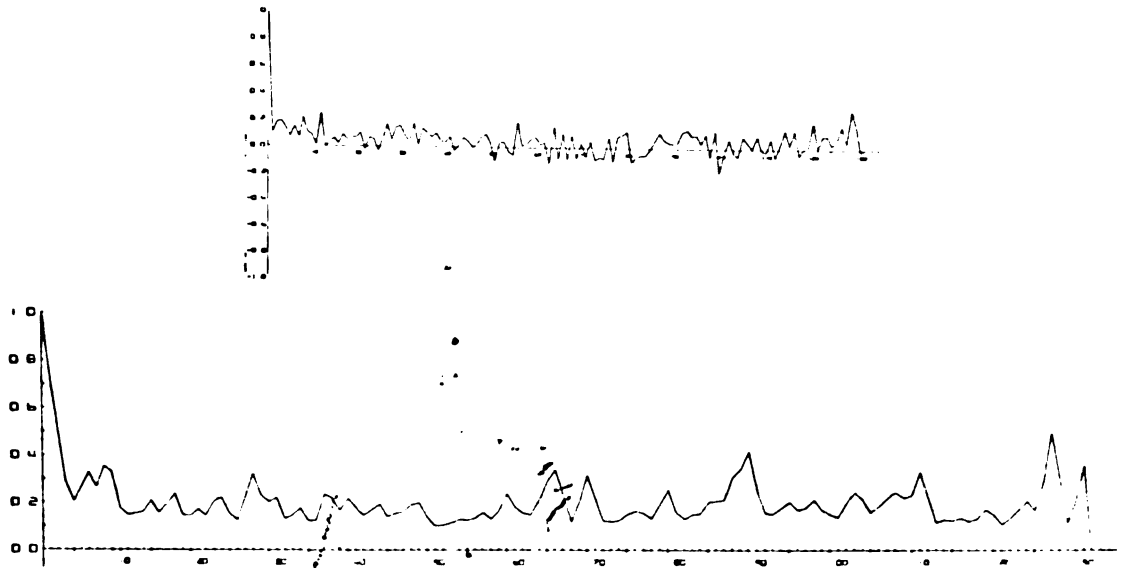

Figure IV.90.11. Subject IK: Δt = 10 msec., T[a,b] = T[710,3309], m* = m'* = .5 and S* = 4.3 responses/interval.

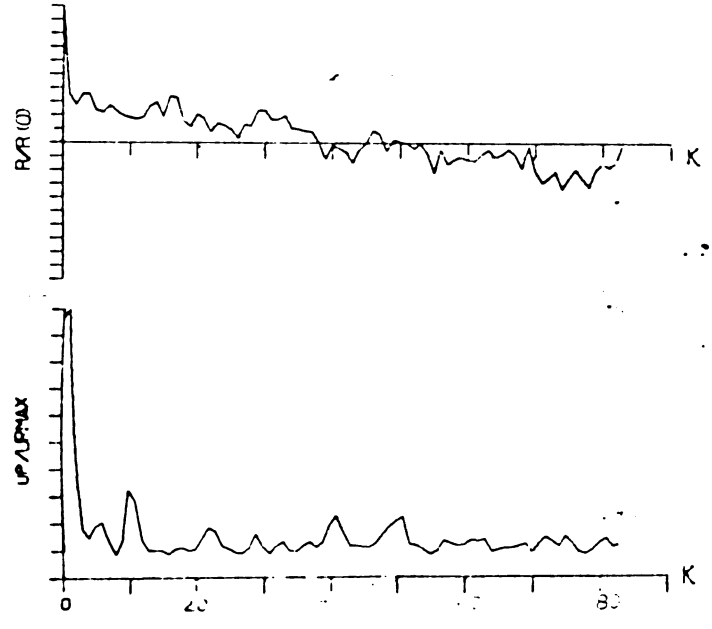

Figure IV.90.12. Subject IK: Δt = 3 msec., T[a,b] = T[484,987], m* = m'* = .5 and S* = 5.8 responses/interval.

from the histograms of B-2F with 10 msec. intervals tend to be slightly less bumpy than their counterparts in B-2S. Note that the PSE's of B-2F are, for the most part, not similar to those of Exp. B-1. However, the PSE's of the histograms with 10 msec. intervals from both B-2F and B-2S are similar to the PSE's obtained by Augenstein.

The qualitative interpretations of the PSE's of B-2S and B-2F (also B-1 and SHN) will be made in the next chapter. Whatever interpretative method is used, it will have to in some way contend with the following:

1. For a given subject, as the value of Δt increases, the bumpiness of the PSE's decreases (e.g., Figures IV.90.1, IV.90.3-IV.90.5).
2. As the value of m' decreases there can be a change in the relative magnitudes of the peaks of PSE's, all other parameter values being equal (for instance, see Figures IV.90.11 and IV.90.12).
3. For a given subject, the frequencies of the largest peaks of the PSE's from the histograms of one interval size usually do not correspond to the frequencies of the largest peaks of the PSE's from another interval size.

IV.30.30. The average time per symbol.--Using the same procedure that was used in Exp. B-1, 10 msec. interval histograms were constructed of the response times corresponding to target elements falling in each of the positions

3, 8, 13, 18 and 23. Typical sets of histograms of a subject for both B-2F and B-2S are shown in Figure IV.100. Note in both sets the increase in both average response time and dispersion of the data with increasing position.* However, the dispersion of the B-2F set is greater position by position than the dispersion of the B-2S set. This indicates that if the model T(·) does hold true, the values of the parameters σ_s and σ_p of the density functions are different (however, the difference is not great enough to noticeably affect the shape of the PSE's).

The relationship between the position and the average response time of that position was approximately linear for most subjects and for both B-2S and B-2F. The slope of the line which is the approximate mean square best fit of the average response time vs. position data is the average time per symbol. These values are recorded in Table IV.10 for each subject and for both experimental conditions.

TABLE IV.10.--The average time per symbol, Experiment B-2.

Subject	Value (msec.)	
	Exp. B-2F	Exp. B-2S
TJ	44	53
MV	64	57
JT	-large-	233
IK	67	67
DF	22	13

*This is also a property of the statistical model T(·).

Figure IV.100. Histograms of response times for selected positions: Subject TJ.

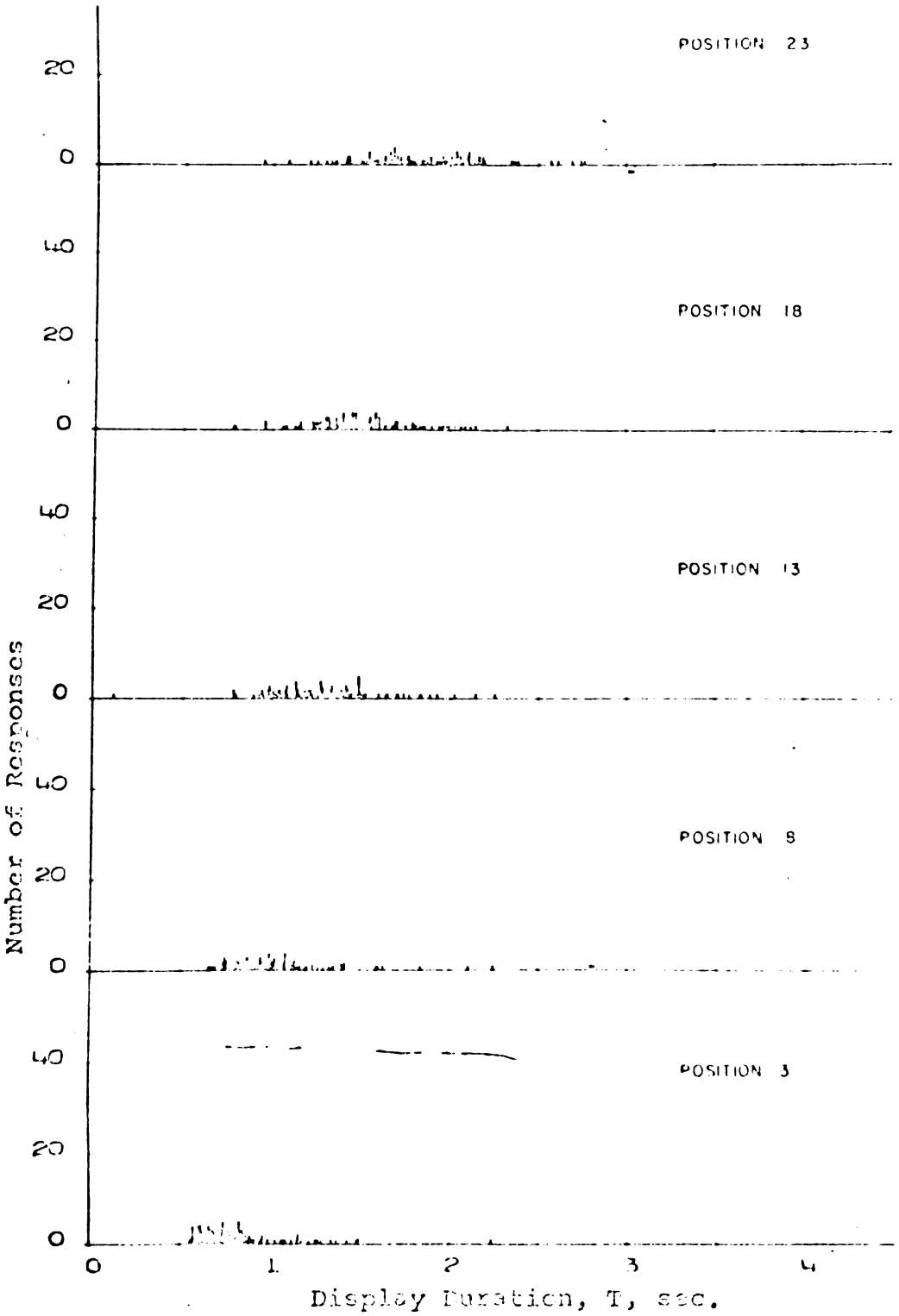

Figure IV.100.1. Experiment B-2F.

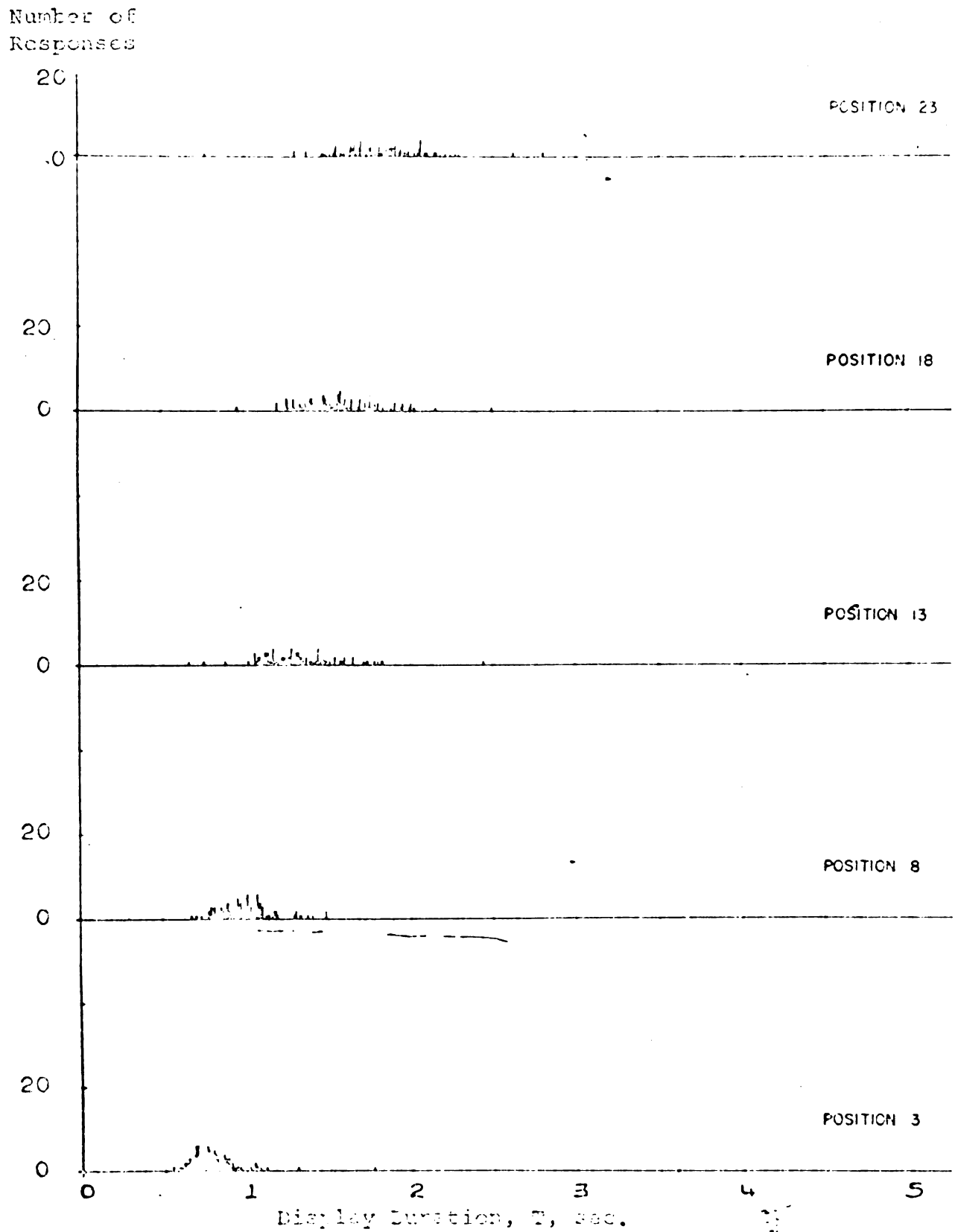

Figure IV.100.2. Experiment D-26.

There are no appreciable differences in the values of the two experiments for each subject. Furthermore, the values are in the general range of those reported by Augenstein for SHN.

Two of the subjects have average times per symbol that are not in the general range Augenstain reported. However, in both cases there is a logical explanation for this discrepancy. Subject JT was an Oriental and was not accustomed to scanning from left to right. It would be expected, therefore, that his average time per symbol is greater. Subject DF had a large number of errors (saying the wrong number). He seemed to be more interested in maintaining a fast, constant time than in accuracy or obeying the rules of the experiment. (See Figure IV.110.)

IV.30.40. A history of response times for selected positions.--The graphs in Figure IV.120 were obtained using the same procedure which was used to obtain the graphs of Figure IV.60. Note that there are no significant common differences between histories of each subject obtained from B-2F and the histories obtained from B-2S. Also, in no case does the subject require, during the course of the experiment, as much time to notice the target element when it is in the third position as he does to notice the target element when it is in the 23rd position.

Figure IV.110. Histograms of response times for selected positions: Subject DF.

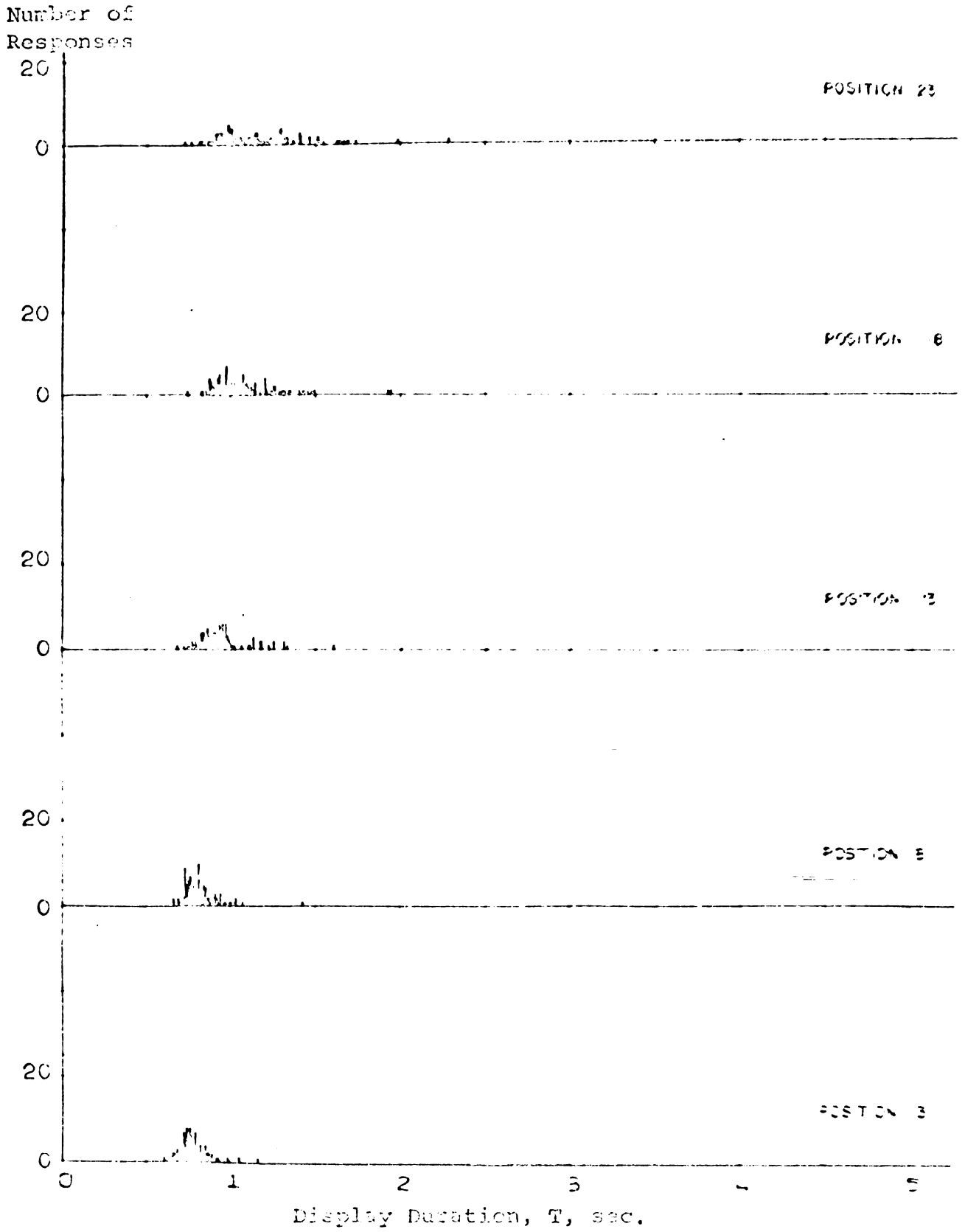

Figure IV.110.1. Experiment B-2F.

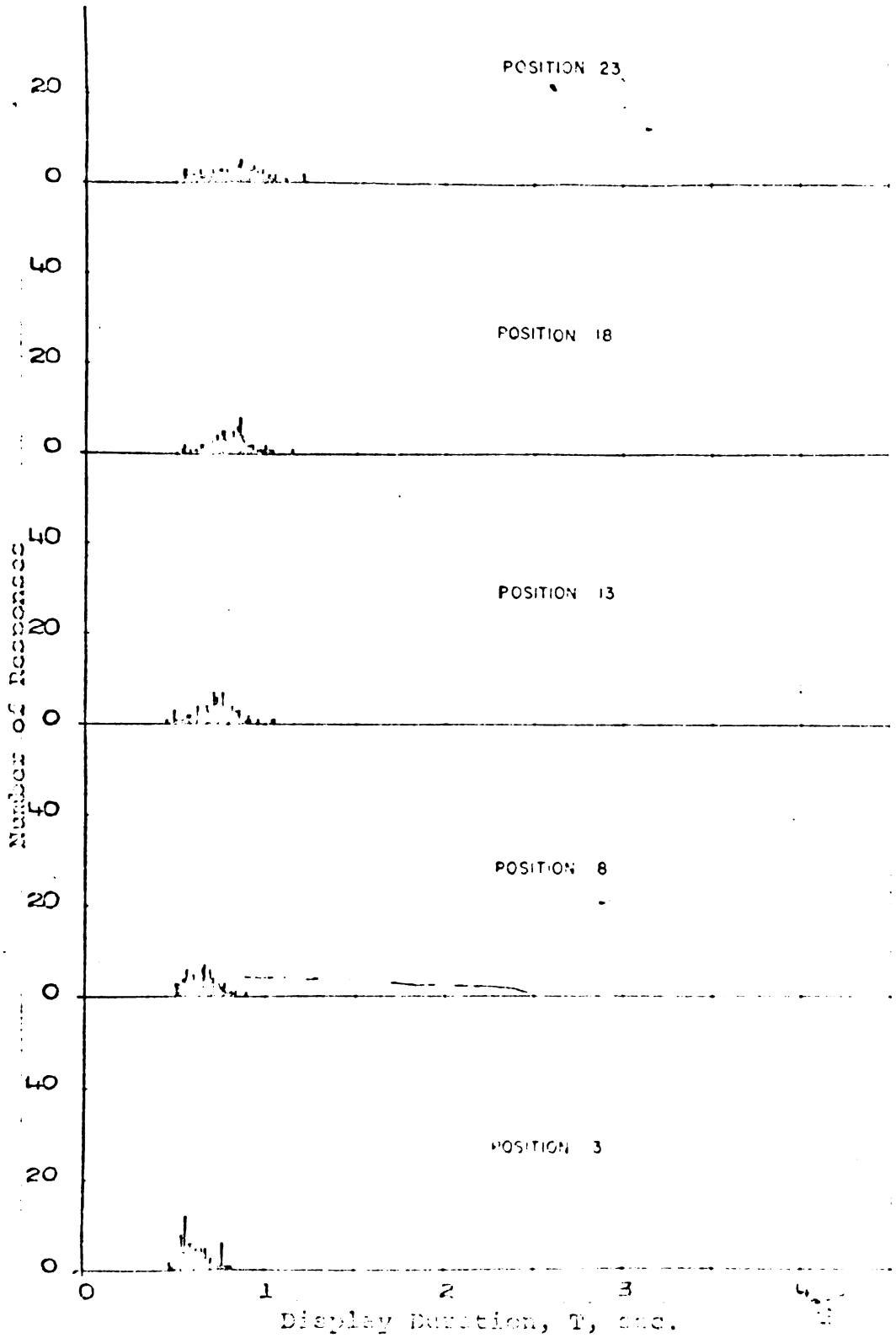

Figure IV.110.2. Experiment D-28.

Figure IV.120.--Histories of response times for selected positions: Experiment B-2. The data are lumped into groups of twenty-five.

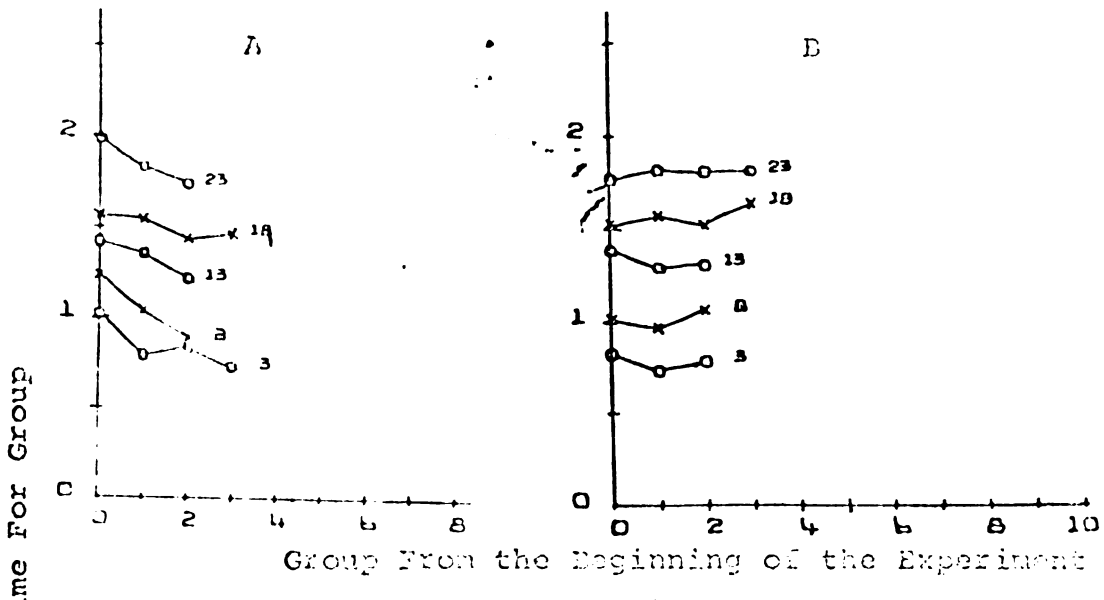

Figure IV.120.1. Subject TU. (A) is Exp. B-2F and (B) is Exp. B-2S.

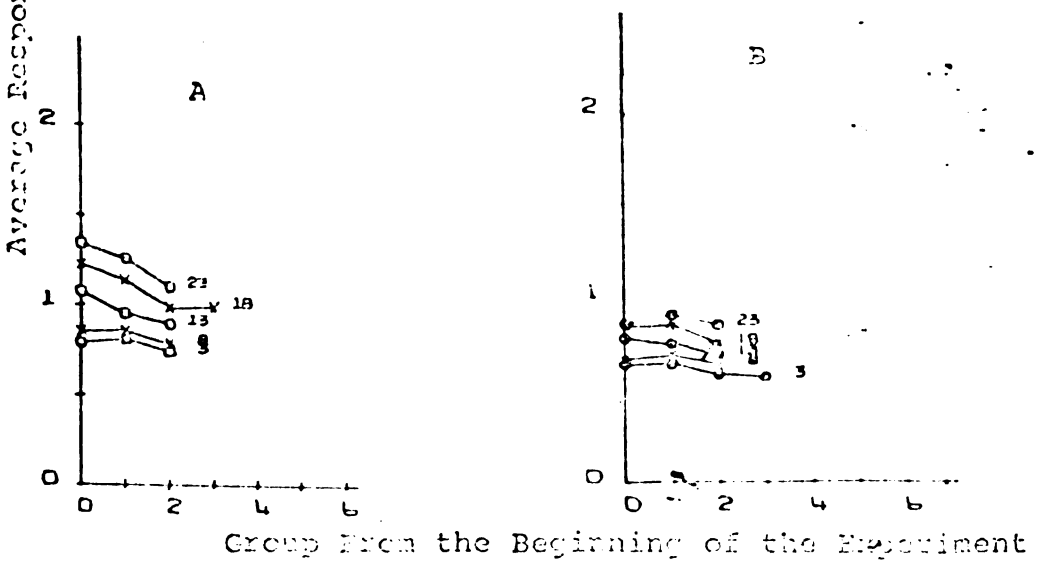

Figure IV.120.2. Subject DF. (A) is Exp. B-2F and (B) is Exp. B-2S.

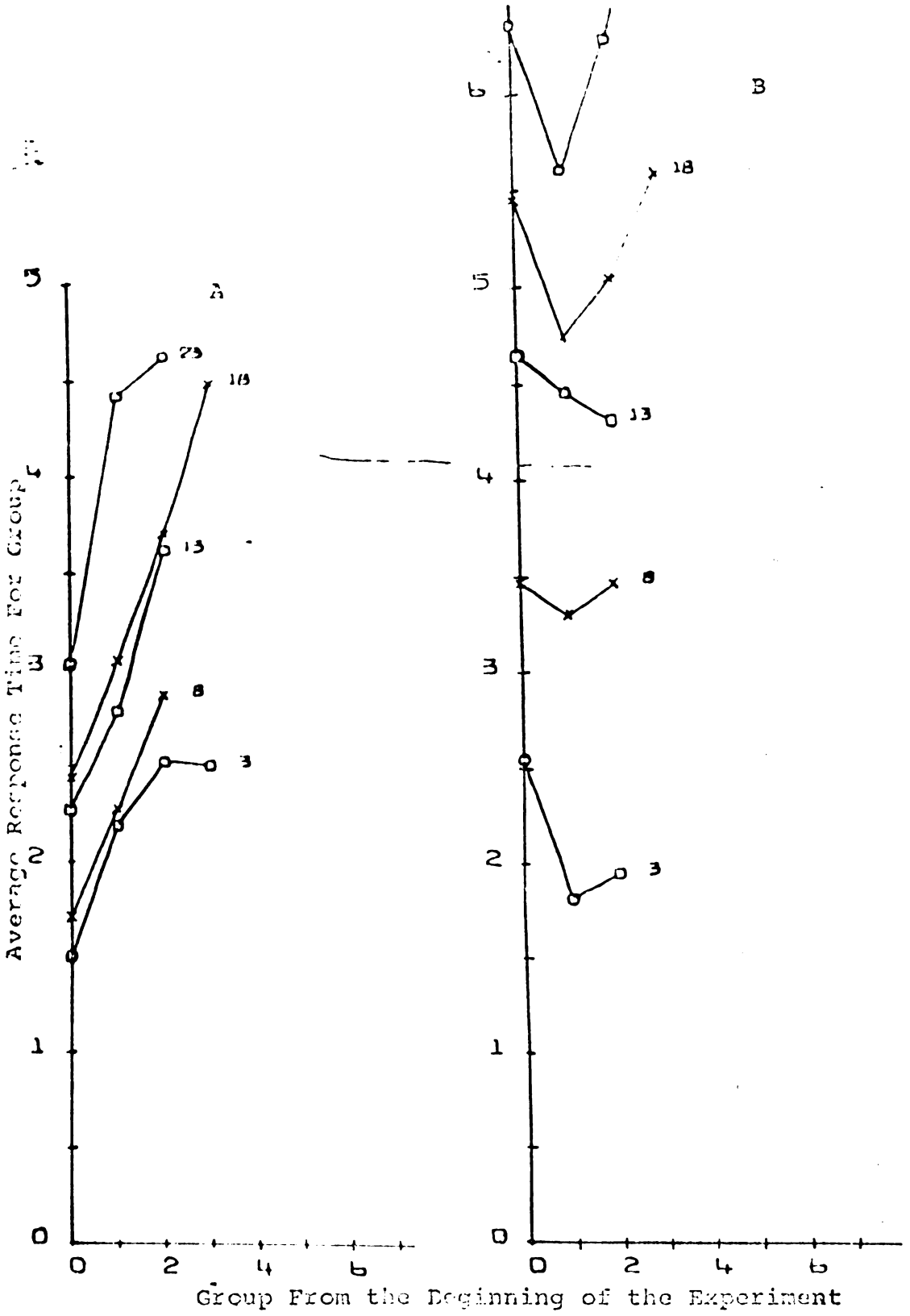

Figure IV.120.3. Subject JT. (A) is Exp. B-2F and (B) is Exp. B-2S.

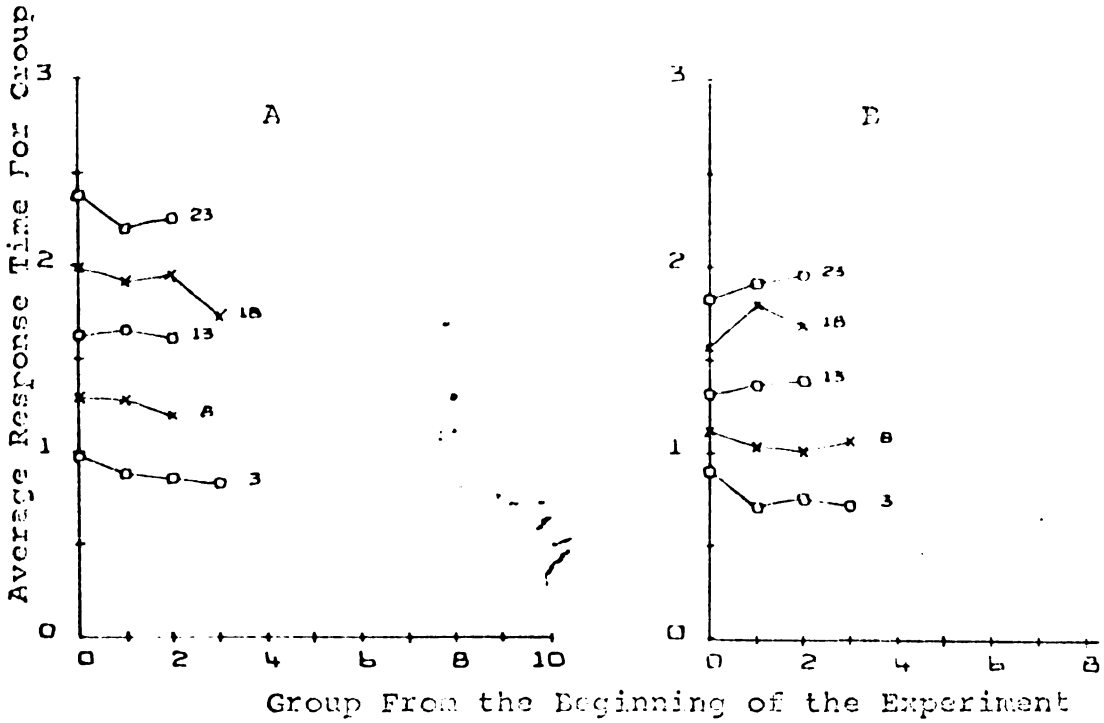

Figure IV.120.4. Subject MV. (A) is Exp. B-2F and (B) is Exp. B-2S.

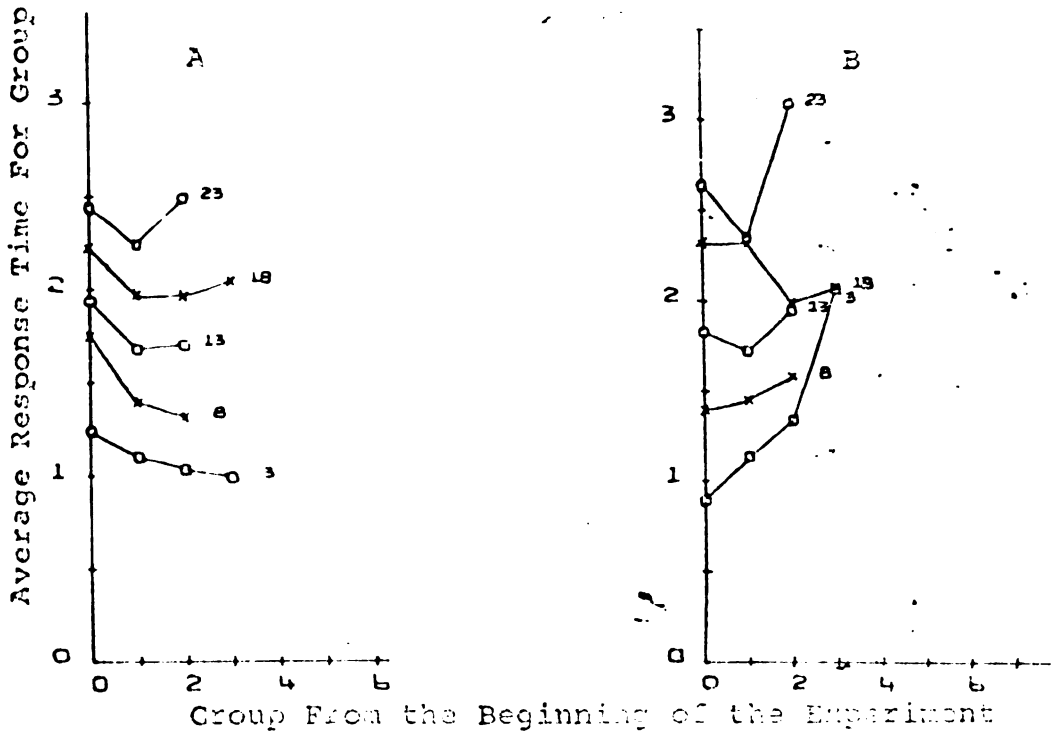

Figure IV.120.5. Subject TK. (A) is Exp. B-2F and (B) is Exp. B-2S.

CHAPTER V

EXPERIMENT B-3

V.10 Introduction

The analytical procedure used in the previous experiments consisted of constructing histograms appoximating unknown density functions and calculating power spectral estimates (PSE's) from these histograms. Recall that the power spectrum transformation was chosen because inductive reasoning suggested that the value of the parameter t_p of the density function $f_T(\cdot)$ would correspond to the frequency in the power spectrum with the greatest power density. There is, however, no proof that this is the case for PSE's. The purpose of this experiment, therefore, was to attempt to establish definite properties to be used to interpret the PSE's obtained in experiments SHN, B-1 and B-2. More specifically, the purpose of Experiment B-3 was to determine properties associated with the shape and frequency of maximum power density by which the following questions concerning an arbitrary experimental PSE can be answered:

Q1. Is the power spectral estimate a member of the set Q' of all power spectral estimates of the $f_T(\cdot)$ defined next?

Q2. If it is, does the frequency of maximum power density correspond to the value of t_p?

Two computer programs were used in this experiment. One program generated histograms from the density function $f_T(\cdot)$ with the component density functions

Eqn V.10.1. $$f_{T_s}(t_1) = N(t_s,\sigma_s),$$

Eqn V.10.2. $$f_{T_p}(t_2) = N(t_p,\sigma_p),$$

and

Eqn V.10.3. $$P_A(a) = 1/30,\ a=1, 2, \ldots, 30.$$

This program required the specification of the values of the parameters Δt (the resolution of the histogram), t_s, t_p, σ_s, σ_p and S (the total sample size) in order to generate a histogram. The other program calculated the PSE from a given histogram. To do this it was necessary to specify the parameters T[a,b] (the interval of histogram used for the estimate), m (the maximum lag of the autocorrelation) and m' (the maximum resolution of the PSE).

V.20 The Experimental Procedure and Results

The experimental technique used to develop the properties of Q' associated with question Q2 was to generate PSE's for various combinations of the nine parameters

specified above and then, through trial and error classification, to develop a set of properties which allowed the experimenter to place an arbitrary PSE generated from the model into one of three groups. Evaluation of the members of each of these groups revealed that one group consisted entirely of PSE's whose maximum power density occurred at the frequency corresponding to t_p, f_p. It was concluded, assuming the generated set of PSE's was representative of the entire set Q', that these properties can be used to classify any experimentally derived PSE such that if the PSE is placed in the first group the value of the parameter t_p can be stated with some confidence.

The technique used to answer question Q1, was to examine the PSE's generated in conjunction with question Q2 for a property common to all of them. Assuming the generated PSE's are representative of the set Q', this property is a necessary condition for an experimental PSE to be a member of Q'.

The critical aspect of the experimental technique was the choice of the parameter values used to generate the PSE's. They had to be so chosen that the generated PSE's were representative of the set Q', while at the same time the number of PSE's generated had to be kept to a minimum. To see how this was accomplished, a brief description of the procedure used to choose the parameter values is in order.

The first step in the experiment was the selection of the values for the parameters t_s, Δt, T[a,b] and t_p. The value for Δt was set equal to 10 msec. in order that the results might be immediately applicable to an interpretation of Augenstein's PSE's. The value for T[a,b] was set equal to T[801,2900] because the histograms were expected to have substantial values in this interval. The value for t_p was set equal to 50 msec. because this value appeared to give the best balance between good resolution and the ability to detect harmonics. A value of t_s = 400 msec. was chosen because this seemed to be close to the true value. However, the value assigned to t_s will not have any effect on the PSE, since a power spectrum does not retain the phase information of the signal.

The next set of parameter values specified was S*, m* and m'*. These parameters are defined by

Eqn. V.20.1. $m^* = m \cdot \Delta t/(b-a-1)$

Eqn. V.20.2. $m'^* = m' \cdot \Delta t/(b-a-1)$

and

Eqn. V.20.3. $S^* = S \cdot \Delta t/(b-a-1)$

Also define

Eqn. V.20.4. $\sigma_s^* = \sigma_s/t_p$

Eqn. V.20.5. $\sigma_p^* = \sigma_p/t_p$

for future convenience.

The computer programs were used to empirically determine the best values for these. First, PSE's were calculated for the following parameter settings; $S^* = 3.6$, $m^* = m'^* = 0.5$, $\sigma_s^* = 0$ and $\sigma_p^* = 0.02$, 0.06, 0.10. 0.16 and 0.26. These PSE's are Figures A.1, A.2, A.10, A.12 and A.18 of Appendix A. Note that the PSE corresponding to $\sigma_p^* = 0.02$ has maximum power density at the frequency corresponding to the value of the parameter $t_p(f_p)$ and very little power density at the other frequencies (the background). As σ_p^* increases, the average magnitude of the background increases and becomes more irregular. For $\sigma_p^* \geq 0.10$ the PSE is very irregular and the maximum power dentiy no longer occurs at f_p. Furthermore, the same trend was found for the parameter combinations $S^* = 3.6$, $m^* = m'^* = 0.33$, $\sigma_p^* = 0.1$, 0.2, 0.3, 0.5, 0.7 and 0.9. In this case, the PSE corresponding to $\sigma_s^* = 0.5$ had many large peaks, the largest being at f_p. The PSE's corresponding to $\sigma_s^* \geq 0.5$ did not have maximum power density at f_p.

The effect of S^* on the shape of the PSE's was tested by using the parameter combinations $\sigma_p^* = 0$, $\sigma_s^* = 0.3$, $m^* = m'^* = 0.33$ and $S^* = 3.6$, 7.2, 10.8, 14.3 and 17.9. The results were that as the number of samples per interval increased, the irregularity and average power density of the background decreased.

Finally, the effect of m* on the shape of the PSE's was noted. It was observed that as the autocorrelation lag parameter increased, the AC became more irregular and the average magnitude decreased. This was accompanied by increasing irregularity and higher average power density in the background of the PSE's.

S*, m* and m'* are parameters whose values are specified by the experimenter. Nothing more can be asked of their values than that they give the best possible resolution; i.e., a sharp peak at f_p and lower power density elsewhere. Therefore, m'* and S* should be as large as possible and m* should be as small as practical. The value chosen for S* was 17.9. From experience, this is the largest practical number of trials to run on any one subject. The conditions that m'* be large and m* be small are antagonistic. The reason for this can be seen from the expression for a given frequency in a power spectrum, $f = p/2m\Delta t$. The largest possible frequency which can be detected in the histogram is $f_c = 1/2\Delta t$. This corresponds to p = m in the frequency expression. Therefore, the largest p possible, and hence the largest m' possible, is m. The best compromise that could be found was m* = m'* = 0.5.

With these parameters so specified, the current five dimensional system was reduced to an easily visualized two dimensional system. Appendix A contains the majority

of the PSE's generated from the parameter combinations $S^* = 17.9$, $m^* = m'^* = 0.5$, $t_p = 50$ msec., $t_s = 400$ msec., $T[a,b] = T[801, 2900]$ or $T[401, 2900]$, $\Delta t = 10$ msec. and σ_s^* and σ_p^* variable. (The reason two different histogram intervals were used is that midway through the calculations it was found that sticking only to the front of the histogram improved the resolution.)

At this point in the experiment some tentative properties were established for use with question Q2. They were tentative because of conditions under which these properties were applicable: $T[a,b]$ could only be the entire histogram, $f_{T_s}(\cdot)$ and $f_{T_p}(\cdot)$ could only be Gaussian, t_p could only be around 50 msec., $t_s = 400$ msec., $s^* = 17.9$, $p_A(a) = 1/30$, $m^* = m'^* = 0.5$ and $\Delta t = 10$ msec. It should be noted that these restrictions are not as severe as they might seem. As a matter of fact only the restraints on t_p, Δt, $T[a,b]$ and $p_A(a)$ are serious. PSE's were generated and analyzed for various combinations of values of the first three of these parameters and the tentative properties revised until the restrictions on these parameters were lifted (the restriction on $p_A(\cdot)$ remains). Appendices A and B contain the majority of the PSE's generated and Appendix C outlines some of the miscellaneous properties observed during this portion of the experiment.

The next step in the experiment was to use these revised properties to demonstrate that the generated

subset of Q' was indeed representative of the entire set. Section V.40 is this demonstration. Finally, the property common to all of the generated PSE's was defined.

V.30. The Properties Established to Interpret an Experimental PSE

The necessary property for a PSE to be a member of Q' is that it be irregular, or bumpy. However, just how bumpy a PSE has to be is difficult to define. An equivalent property for a sufficient condition for a PSE not to be a member of Q' is that the PSE should be non-bumpy. This property is more easily defined: By non-bumpy is meant a shape where the maximum power density occurs at zero frequency and low and reasonably uniform power density is found at all other frequencies. The PSE's of Experiment B-1 are good examples.

The properties established to determine the value of t_p in an arbitary PSE were the sharpness of the peak of greatest power density and the average value and bumpiness of that portion of the background. These properties place the PSE in one of three groups:

Group A--The maximum power density occurs at a non-zero frequency. The associated peak is sharp and there is low and fairly regular power density at other frequencies. "Fairly regular" is defined to mean no peak in the background greater than about 0.2 above the average power density. The value considered to be "low depends on Δt. The larger the value of Δt, the higher this low.

Group B--The PSE has two or more peaks with a power density of at least 0.8. The topology of the PSE is generally irregular and the average power density high.

Group C--The maximum power density occurs at a non-zero frequency. There may be other peaks of comparable magnitude (on the order of 0.8) but there is no doubt as to which is the principal peak.

Recall that the PSE is calculated from a histogram generated by a density function of the random function

$$T(s) = T_s(s) + \sum_{i=1}^{A(s)} T_{P_i}(s)$$

Also note that these properties assume that the density functions $f_{T_p}(\cdot)$ and $f_{T_s}(\cdot)$ are Gaussian and that $p_A(\cdot)$ is fairly uniform. In addition, it is advisable to have $m'^* = m^* = 0.5$, $S^* = 17.9$ and $T[a,b]$ equal to the first third of the histogram (if necessary) in order to obtain the best possible resolution.

V.40. A Demonstration of the Representative Nature of the Generated PSE's

In order to demonstrate that the PSE's generated during the course of Experiment B-3 were representative of the entire set Q', each of the generated PSE's was classified into one of the three groups defined in the previous section. Figures V.10-V.30 summarized the results of this classification. If a PSE has been classified, then

the symbol corresponding to the group the PSE was placed in is found at the coordinates of the values of S*, σp* and σs* associated with the given PSE. A square signifies that the PSE was placed in a group A, an ellipse signifies that the PSE was placed in group C, and no symbol signifies that the PSE was placed in group B. The number "inside" the symbol is the average power density of the background. Note that all of the PSE's in group A had their maximum power density at the frequency fp, all of the PSE's in group B did not have their maximum power density at fp and the PSE's in group C sometimes did and sometimes did not have their maximum power density at fp. An examination of Figures V.10-V.30 reveals that the properties under consideration are indeed well behaved over the parameter values covered by the figures. That is, close to the origin of the figures and close to each axis the PSE's classified in group A dominate. Near the fringes of the explored space, on the other hand, the PSE's placed in group B are dominant. There also appears to be a transitory space between these two extremes where group C PSE's are found. This well behavedness leads to the conclusion that the available PSE's are representative of the entire set Q'.

Figure V.10. Summary of PSE results, Experiment B-3. The histogram interval analyzed in all cases except those noted was T[a,b] = T[801,2900]. Other parameter values were $m^* = m'^* = .5$ (except where noted), $\Delta t = 10$ msec., $t_p = 50$ msec., and $t_s = 400$ msec. If a PSE has been calculated in Exp. B-3, a number, possibly inside a square or ellipse, appears at the coordinates $(\sigma_s^*, \sigma_p^*, S^*)$ corresponding to the values used in generating the PSE. The number is the average power density of the PSE. The square signifies that the maximum power density occurred at a non-zero frequency, the associated peak was sharp, and the remainder of the estimate (the background) was fairly regular. The ellipse signifies that the maximum power density occurred at a non-zero frequency and that, although there are peaks of comparable magnitude, there is no doubt as to which is the principal peak. See the text for details.

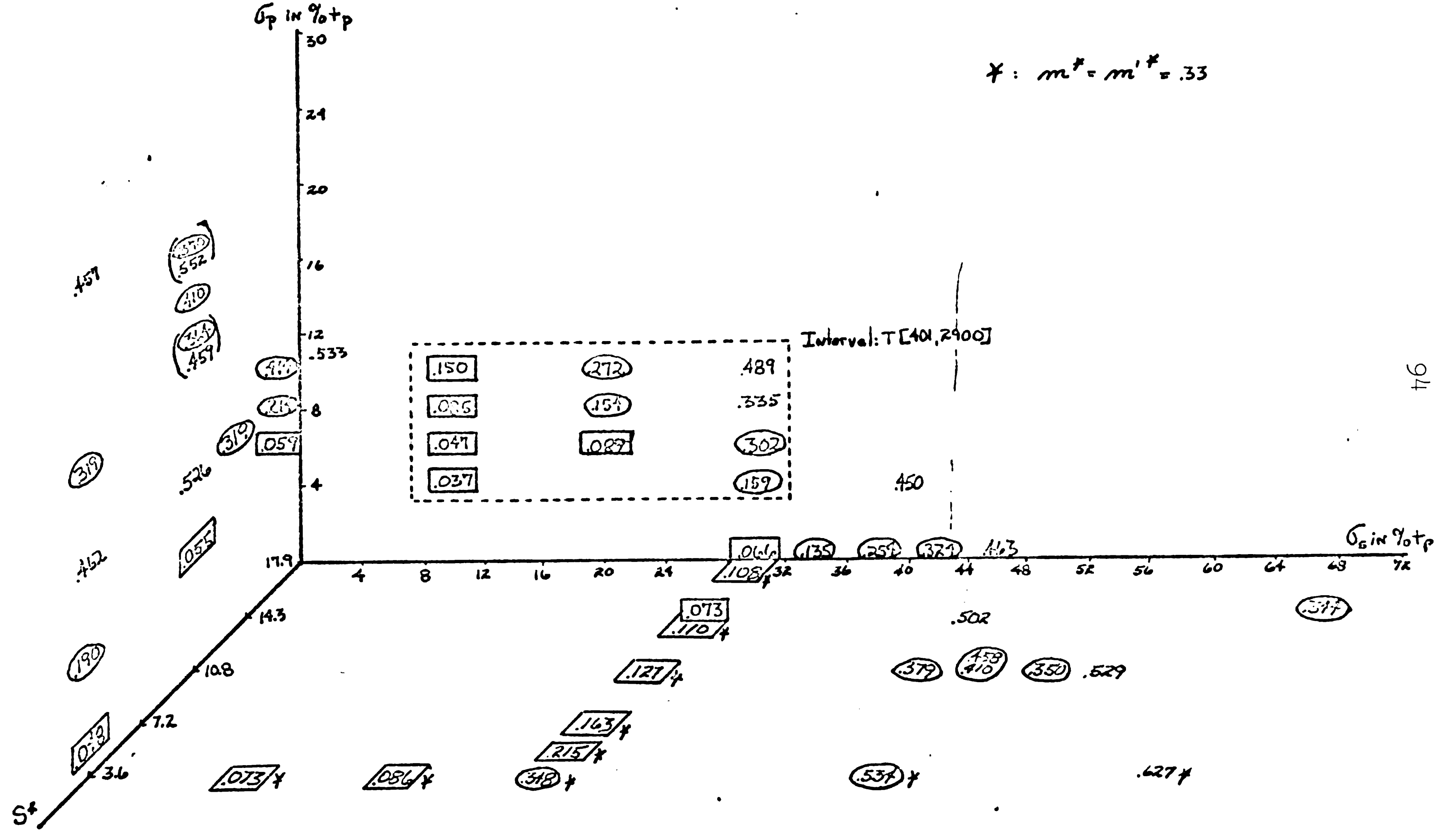
σ_p in % t_p
σ_G in % t_p
S^*
30
24
20
16
12
8
4
17.9
14.3
10.8
7.2
3.6
32
36
40
44
48
52
56
60
64
68
72
Interval: T[401,2900]
*: $m^* = m'^* = .33$

Figure V.20. Summary of PSE results, Experiment B-3. The histogram interval analyzed was T[a,b] = T[401,1400]. Other parameter values were $m^* = m'^* = .5$ (except where noted), Δt = 10 msec., t_p = 50 msec., and t_s = 400 msec. If a PSE has been calculated in Exp. B-3, a number, possibly inside a square or ellipse, appears at the coordinates (σ_s^*, σ_p^*, S^*) corresponding to the values used in generating the PSE. The square number is the average power density of the PSE. The square signifies that the maximum power density occurred at a non-zero frequency, the associated peak was sharp, and the remainder of the estimate (the background) was fairly regular. The ellipse signifies that the maximum power density occurred at a non-zero frequency and that, although there are peaks of comparable magnitude, there is no doubt as to which is the principal peak. See the text for details.

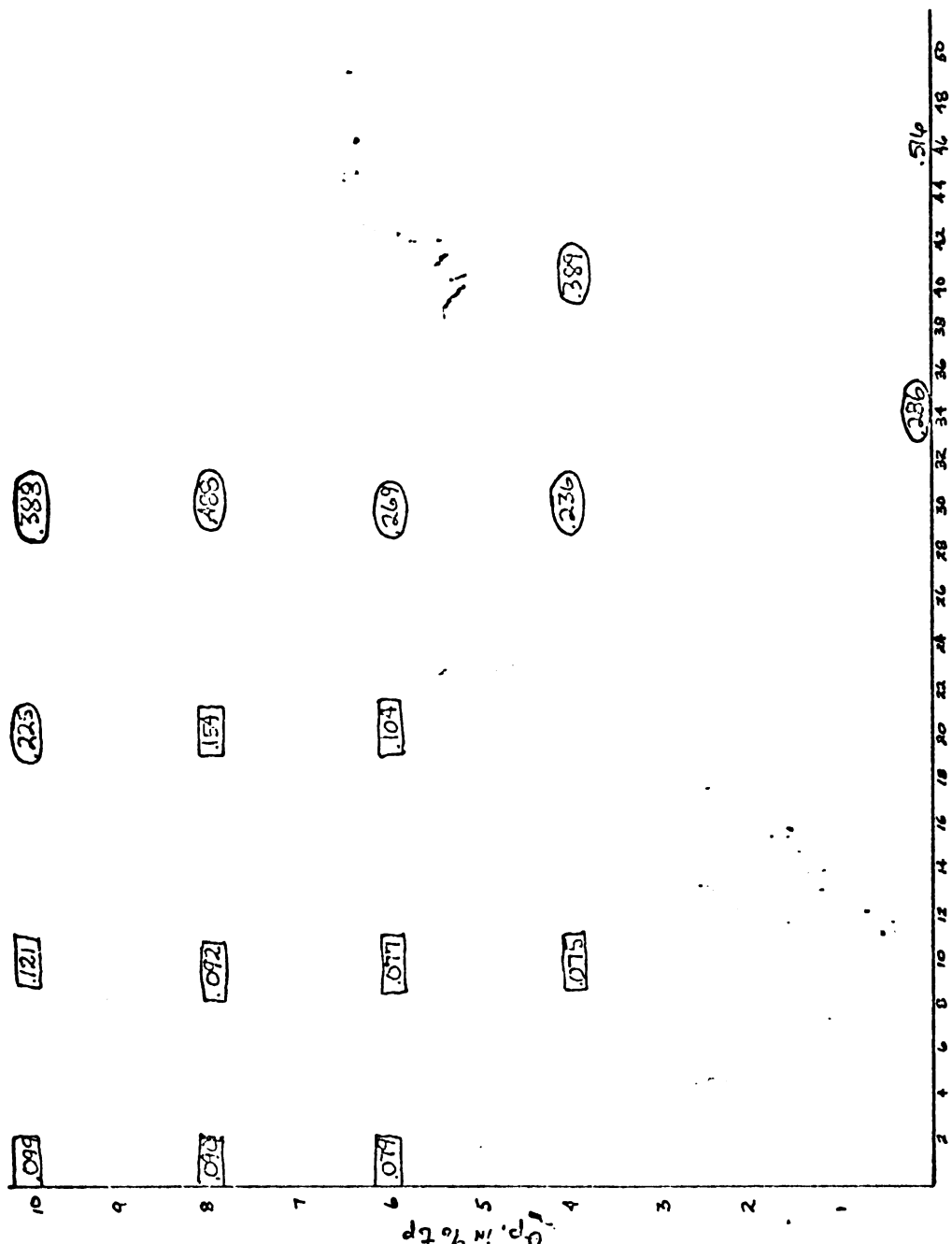
σ_p, in % tp
σ_ε, in % tp
.094
.045
.079
.121
.092
.140
.225
.154
.104
.388
.485
.269
.075
.236
.389
.286
.514

Figure V.30. Summary of PSE results, Experiment B-3. The histogram interval analyzed was T[a,b] = T[1401,2400]. Other parameter values were $m^* = m'^* = .5$ (except where noted), Δt = 10 msec., t_p = 50 msec., and t_s = 400 msec. If a PSE has been calculated in Exp. B-3, a number, possibly inside a square or ellipse, appears at the coordinates (σ_s^*, σ_p^*, S^*) corresponding to the values used in generating the PSE. The square number is the average power density of the PSE. The square signifies that the maximum power density occurred at a non-zero frequency, the associated peak was sharp, and the remainder of the estimate (the background) was fairly regular. The ellipse signifies that the maximum power density occurred at a non-zero frequency and that, although there are peaks of comparable magnitude, there is no doubt as to which is the principal peak. See the text for details.

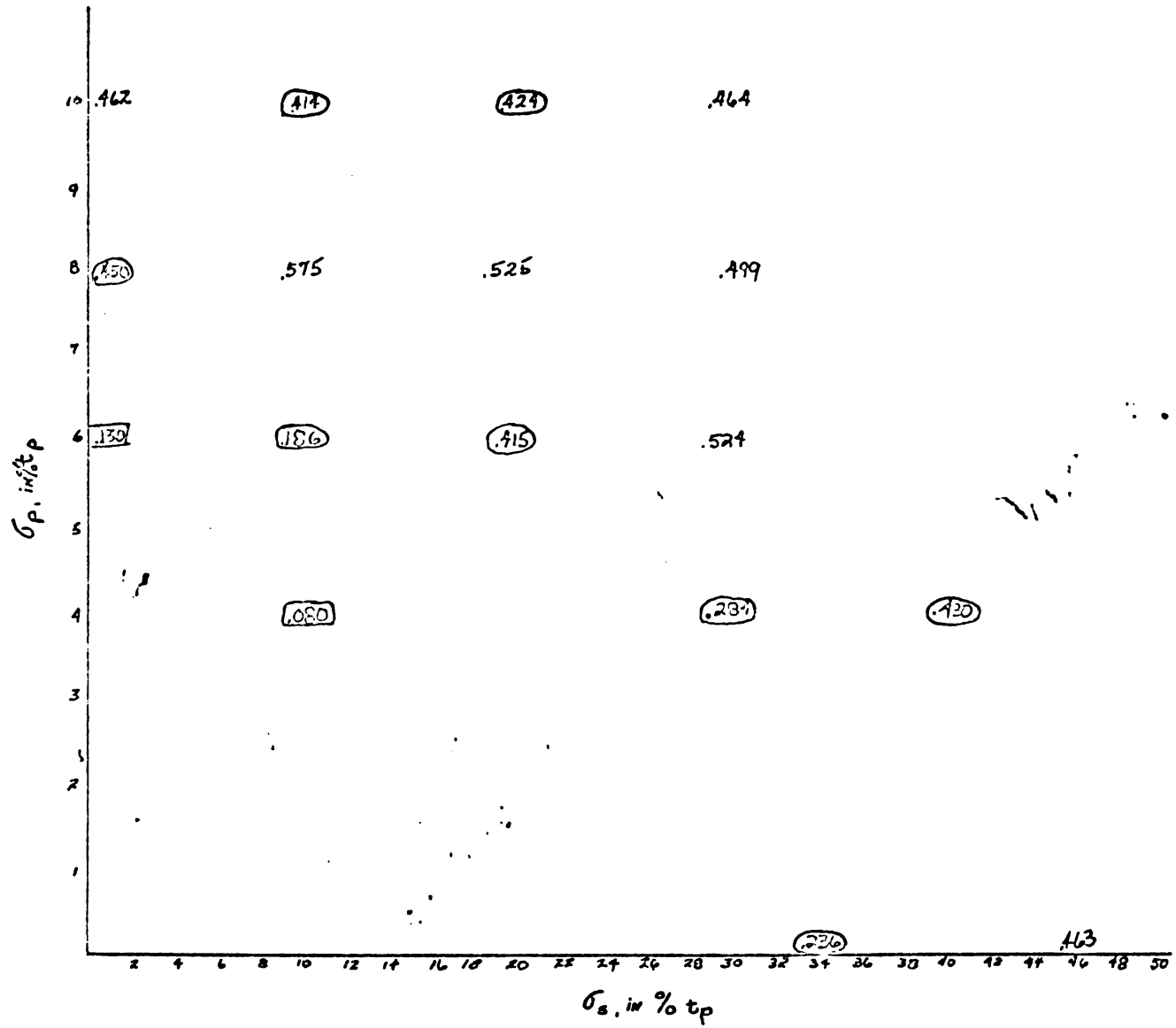
10
9
8
7
6
5
4
3
2
1
.462
.414
.424
.464
.150
.575
.526
.499
.130
.186
.415
.524
.080
.284
.420
.226
.463
2 4 6 8 10 12 14 16 18 20 22 24 26 28 30 32 34 36 38 40 42 44 46 48 50
σ_p, in % t_p
σ_s, in % t_p

V.50. An Interpretation of the Experimental Power Spectral Estimates

The properties and groups discussed in the previous chapters can be used to place an arbitrary experimental PSE into one of the following three categories:

Category A--The PSE was not calculated from a histogram generated by a $f_T(\cdot)$ with a reasonably uniform $p_A(\cdot)$.

Category B--The PSE was calculated from a histogram which could have been generated by a $f_T(\cdot)$ with a reasonably uniform $p_A(\cdot)$.

Category C--The PSE is a member of the set Q': the density function $f_T(\cdot)$ which generated the histogram has a fairly uniform component density function $p_A(\cdot)$. A legitimate value for the parameter t_p can be determined.

The PSE's published by Augenstein and the PSE's of Exps. B-1 and B-2 have been placed in one of these categories. The results are:

The PSE's published by Augenstein: All three categories are present. The PSE's of SHN (e.g., Figure II.50) were placed in category A. Two PSE's, one from Exp. WS4 and the other from Exp. SO (Figure II.40) were classified in category C. In both cases, the value for t_p was 100 msec. All other PSE's fell into category B.

The PSE's of Exp. B-1: All PSE's of this experiment were placed in category A.

The PSE's of Exp. B-2: There was no significant difference in the classification of PSE's from B-2S and B-2F. The PSE's calculated from the 3 msec. histograms were classified into category B. As the interval size increased, the PSE's began to be classified in category A. The PSE's calculated from the histograms with ten msec. intervals were placed, for the most part, in category A.

Two further comments can be made concerning the PSE's of Exp. B-2. First, the PSE's calculated from the histograms with ten msec. intervals were very similar to the PSE's of SHN. Second, the general behavior of the PSE's--i.e., the decrease in the bumpiness with increasing Δt--was seen in the behavior of the model, but the change was not drastic.

CHAPTER VI

DISCUSSION: PART II

VI.10. Summary

In an experiment SHN, designed by Augenstein, subjects were required to scan random sequences of 26 letters and numbers for the first number from the left in the sequence. The response time data collected from this and other experiments were used to form histograms and power spectral estimates (PSE's) were calculated from these. The PSE's were averaged to form an "experimental PSE." This PSE was compared to several PSE's calculated by substituting parameter values into an equation (II.10.14) expressing a statistical model and generating data in a Monte Carlo fashion. (This model was based on the thesis that the visual system of man can be thought of as an information processing system whose decision-making is performed in an essentially periodic* manner.) The value of the parameter t_p used in the generated data whose PSE most closely resembled the experimental PSE was said to be a reasonable estimate of the cycle time

---

*Periodic is used here in the intuitive sense and not in the rigorous mathematical sense.

associated with the periodic data processing in the visual system.

Three experiments, all modifications of SHN are described in this report. A fourth experiment examines the interpretation to be given to the resulting PSE's. The outcome of these experiments allow at least partial answers to some important questions. These questions and answers are now presented.

QUESTION: How should the power spectral estimates of the relevant experiments be interpreted?

The objective of any analytical method used on the response time data is to determine if the data are periodic and if so the time duration of the fundamental period. As has been pointed out in previous chapters, the power spectrum is the obvious choice for this analysis. However, reasons have also been given for the difficulties in confidently interpreting the power spectral estimate available from experimentation. In an experiment B-3 some heuristic rules were developed that partially eliminate the difficulty. A description of these rules and the conditions under which they apply are found in Section V.60.

QUESTION: What are the experimental variables and what are their effects on the results of the scanning experiments?

Four experimental variables have been examined or found to be important during the present experimentation.

The illumination

In an experiment B-2F, SHN was duplicated as closely as possible except that incandescent lighting was used in place of fluorescent lighting. The PSE's calculated from the data of B2F were similar to those of SHN. The conclusion is that the lighting is not a source of data artifacts.

The data resolution

The data of SHN were recorded to the nearest 10 msec., making reliable detection of any cycle times below 20 msec. impossible. Augenstein questioned whether the 100 msec. cycle time he detected might not be the result of ten 10 msec., or some other similar combination, cycle times being lumped together. The data of all experiments reported in this thesis were recorded accurate to 1 msec. No evidence of cycle times in the range of 2 to 20 msec. was found.

The trial interval

Because of the manual nature of the procedure of SHN, there was an interval of approximately 30 seconds between trials. In an experiment called B-2F this interval was shortened to 3 to 4 seconds. The PSE's of B-2F were not significantly different from the PSE's of either SHN or B-2S. The conclusion is that the interval between trials is not a significant source of data artifacts.

The type font and the method of scanning

The scanning method used by the subjects of SHN and the subsequent experiments was assumed to be to scan the stimulus sequence from left to right for the first number. That this method was indeed used by the subjects of B-2F and B-2S has been confirmed from two sources. The first source was by visual observation of the subjects: their eyes appeared to be moving from the left hand side of the sequence to the right. The other source is the histories of the response times for selected positions. These histories show that the average response time increased with increasing position of the target element to the right in the sequence, and that, almost without exception, this relationship was maintained throughout the course of the experiments. However, in an experiment that was a duplication of B-2F, the subjects' histories do not show this relationship: the average response time for stimuli with the target element in the first position is the same as that for stimuli with the target element in the last position. The subjects in B-1 were apparently not scanning from left to right.

A possible method that the subjects of B-1 were using depends on the fact that pica type was used in the construction of the stimuli. A characteristic of this type is that the tails of the numbers fall above or below the average top or bottom of the letters. Thus, the first

number from the left in the sequence literally sticks out like a "sore thumb." It is conceivable that the human visual system could be dynamically programmed to detect only the tail, disregarding most of the information that would be processed according to the anticipated scanning method. A random scan may well be the most efficient way to detect a tail. Furthermore, it is entirely possible that such a method would be performed using a separate, nonperiodic "primitive" processor.

The above method is also important in its effect on the data of the other experiments in the SHN series. If the primitive processor were used for only a small portion of the tasks by a given subject, the effects on the data of that subject would still be disastrous in terms of introducing noise into the data.

All things considered, the tails on the numbers in the pica type used in the stimuli is an important new candidate for a source of data artifacts. Unfortunately, this possibility was recognized only during the final analysis and thus was not tested explicitly.

QUESTION: Do humans show periodicity in the time required to perform a simple visual task, and if so, what is the period or cycle time?

Because of the stochastic nature of any available data, it is impossible to answer the question as it is written with any confidence. Therefore, the question has

been rephrased. A stochastic model has been constructed and the question is whether the data could have been generated by this model, and if so what is the period, or cycle time. Under all experimental conditions, including Augenstein's experiments, and using the methods of interpretation developed expressly for the analytical technique used, only a couple of instances were found (for instance, see Figure II.40) where it could be concluded that the data could have been generated by the model. The cycle time in these cases was about 100 msec. For the rest of the data it was concluded that although they might have been generated by the statistical model, it was impossible to determine the cycle time (see the rules in Section V.60).

VI.20. Suggestions for Further Experimentation

Future experimental efforts in this area of research will depend on the motivation of the experimenter. If the experimenter is motivated by the desire to determine, once and for all, the model to explain existing data, or if new experiments are planned that follow the basic procedures of SHN, then it will be necessary for him to use different density functions of $p_A(.)$ and attempt to generate more general rules for the interpretation of the power spectral estimates. There is a pessimistic note to be sounded if this course is pursued: a pattern recognition computer

program (learning with a teacher) was written (19) that could not separate histograms according to the different functions used for $p_A(\cdot)$ (no matter how different they were).

If the experimenter is motivated by the desire to determine both the sufficiency of the model and the value of the clock cycle time, but wants to use existing interpretational procedures then it will be necessary for him to design new experimental tasks or severely overhaul the old ones. For instance, he could use the basic procedure of SHN and attempt to decrease what amounts to σ_s by designing a system that would open the shutter on the projector with the movement of the subject's eyes and close the shutter at the beginning of the utterance of the name of the digit. Optimism for this approach is lessened by the problem of not knowing what went wrong with Exp. B-1.

Alternative experimentation might be to repeat some of the experiments Augenstein conducted that did produce good results (WS4 or SO). If these experiments are redone, it will be necessary to determine the reason these experiments produce the acceptable power spectral estimates while the others do not.

There was something about the presentation of the stimulus in Exp. B-1 that enabled the subjects (including DJ during the last twenty per cent of the experiment) to

detect the target element in about the same average time, regardless of the position of the target element. It is also interesting that the subjects developed the processing procedure independently and without any encouragement from the experimenter. The experimenter might attempt to determine the variables in the experimental procedure of the B series that enabled this phenomenon to express itself. A suggested initial experiment is to use ERG records to determine eye movements as a function of size of the sequence image on the retina.

APPENDIX A

APPENDIX A

The figures in this appendix are the power spectral estimates and their autocorrelations calculated in Experiment B-3. In each figure the autocorrelation is on the left and the power spectral estimate is on the right. The abscissa for the autocorrelation is k, the lag number. This axis can be converted to the lag time by multiplying each value by Δt. The abscissa for the power spectral estimate is p and can be converted to frequency using the relationship $f = p.2m\Delta t$.

Parameter values of Δt = 10 msec., t_p = 50 msec., t_s = 400 msec. and $m^* = m'^* = .5$ were used (unless otherwise indicated) for all the figures. The value of the parameter T[a,b] is T[801,2900] when $\sigma_s^* = 0$ or $\sigma_p^* = 0$ and T[401,2900] when $\sigma_s^* \neq 0$ and $\sigma_p^* \neq 0$ (unless otherwise indicated).

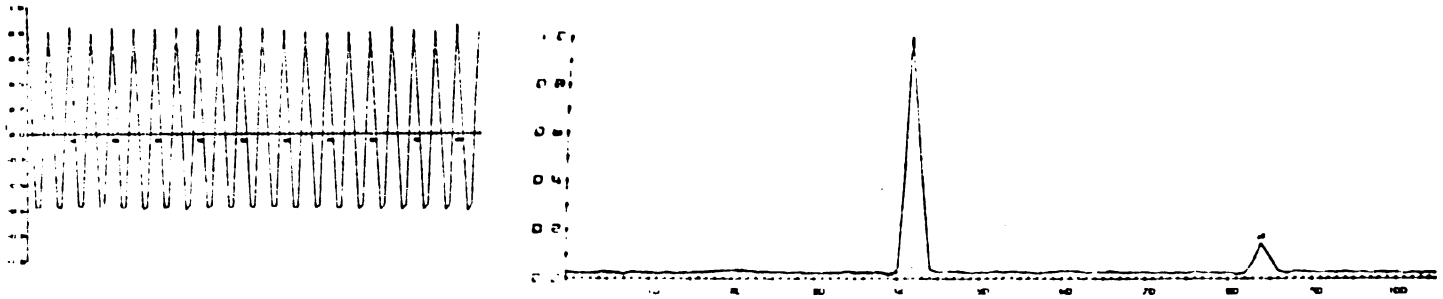

Figure A.1. $\sigma_s^* = 0$, $\sigma_p^* = .02$ and $S^* = 3.6$.

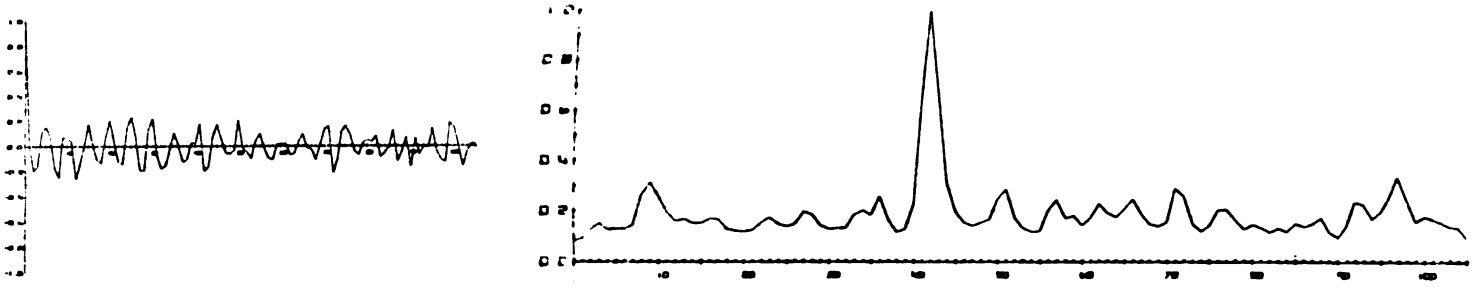

Figure A.2. $\sigma_s^* = 0$, $\sigma_p^* = .06$ and $S^* = 3.6$.

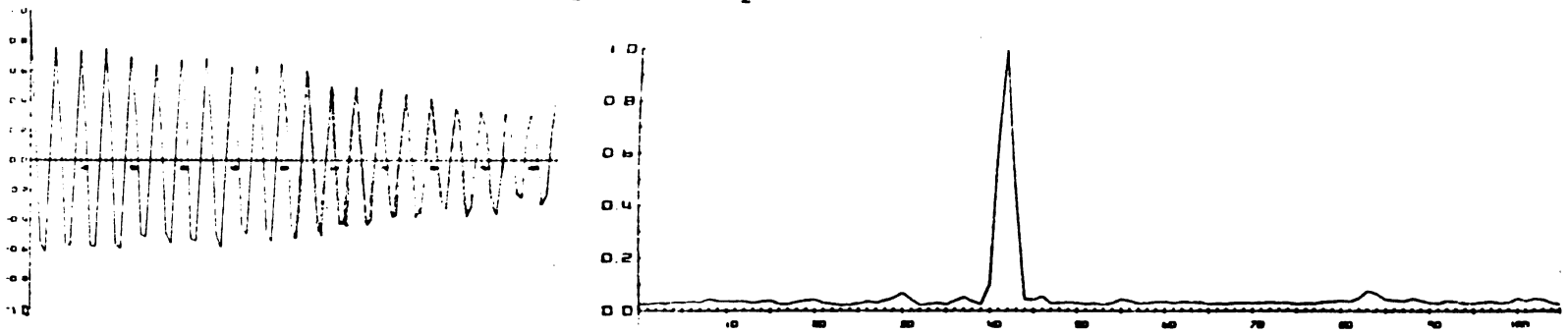

Figure A.3. $\sigma_s^* = 0$, $\sigma_p^* = .06$ and $S^* = 10.8$.

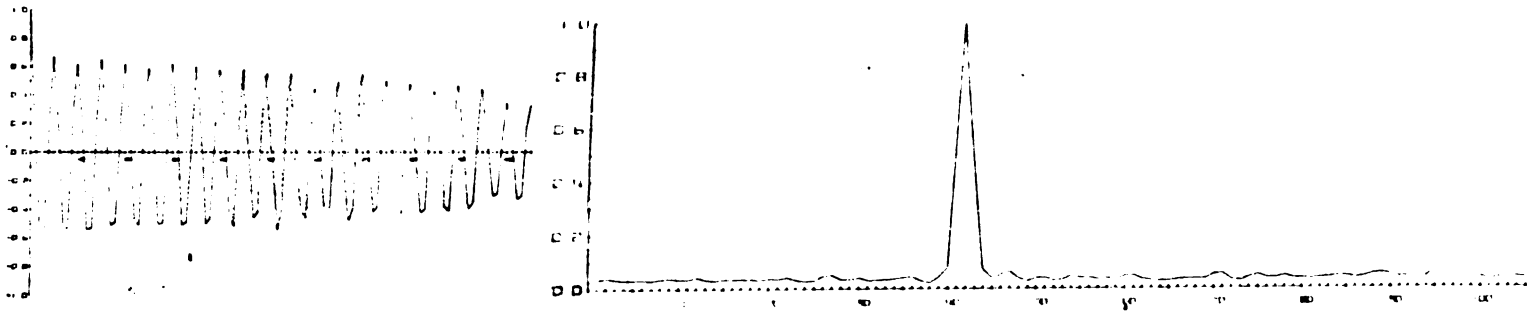

Figure A.4. $\sigma_s^* = 0$, $\sigma_p^* = .06$ and $S^* = 17.9$.

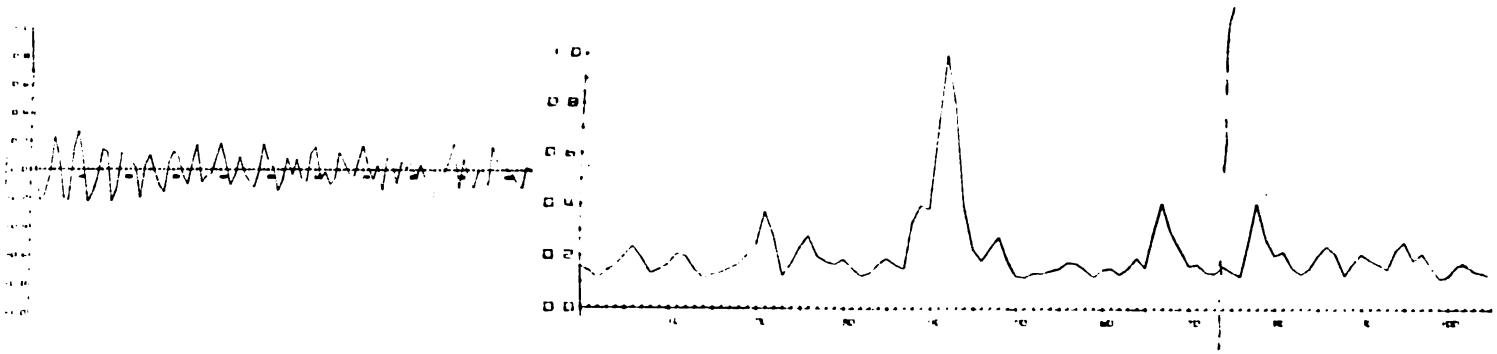

Figure A.5. $\sigma_s^* = 0$, $\sigma_p^* = .08$ and $S^* = 17.9$.

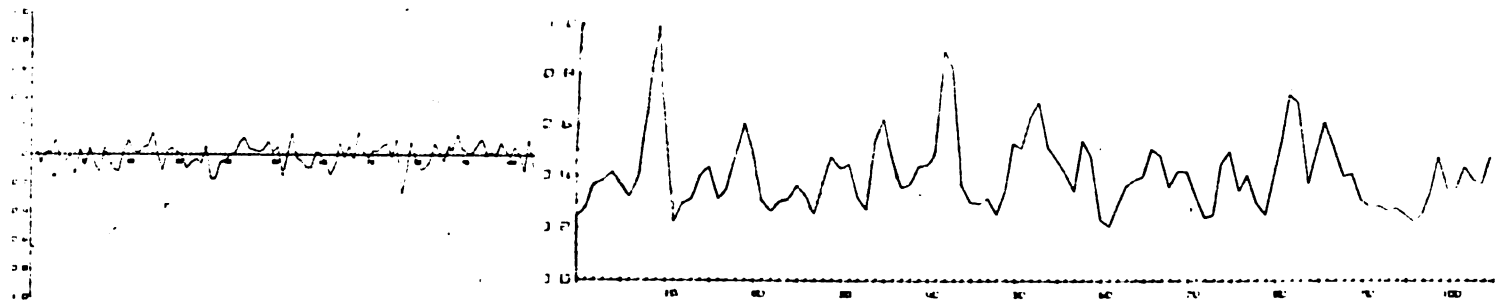

Figure A.6. $\sigma_s^* = 0$, $\sigma_p^* = .1$ and $S^* = 17.9$.

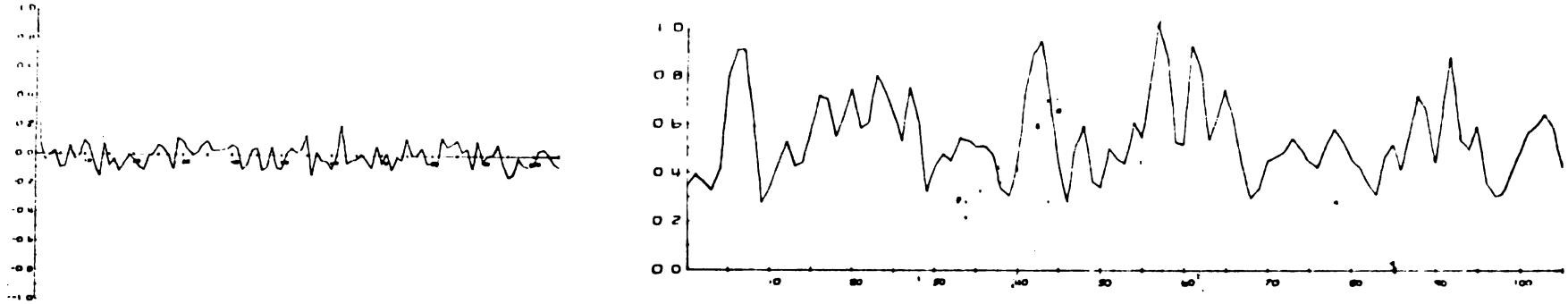

Figure A.7. $\sigma_s^* = 0$, $\sigma_p^* = .1$ and $S^* = 17.9$.

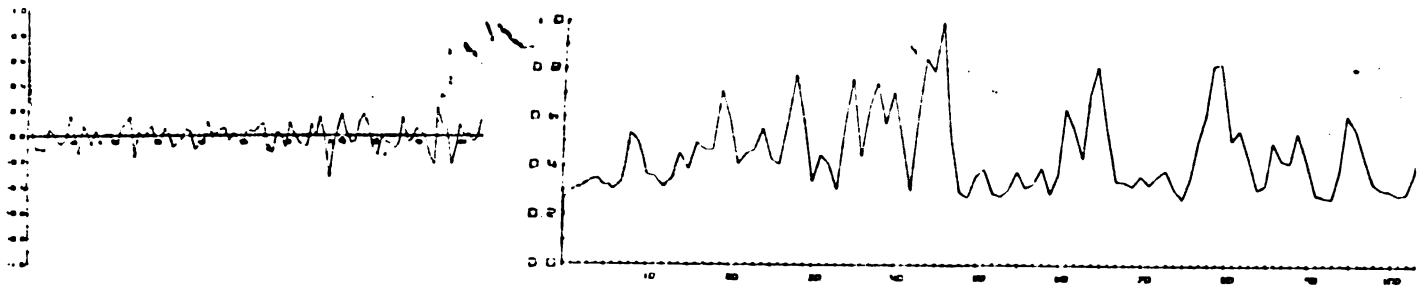

Figure A.8. $\sigma_s^* = 0$, $\sigma_p^* = .1$ and $S^* = 10.8$.

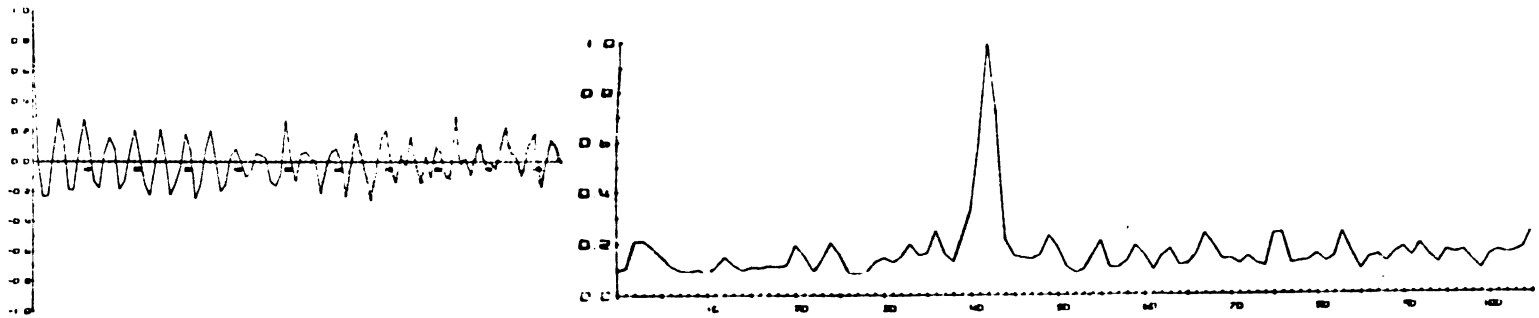

Figure A.9. $\sigma_s^* = 0$, $\sigma_p^* = .1$, $S^* = 10.8$, T[a,b] = T[510,2100] and $m^* = m'^* = .65$.

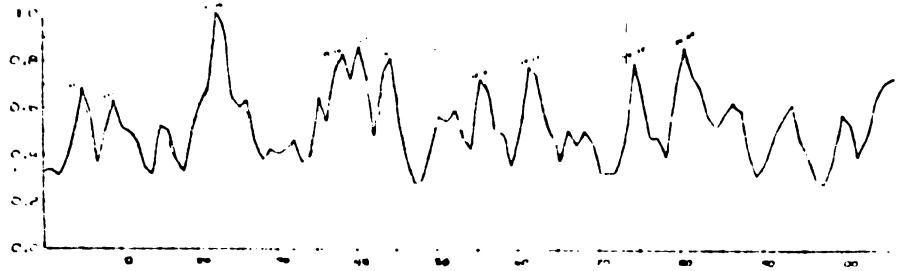

Figure A.10. $\sigma_s^* = 0$, $\sigma_p^* = .1$ and $S^* = 3.6$.

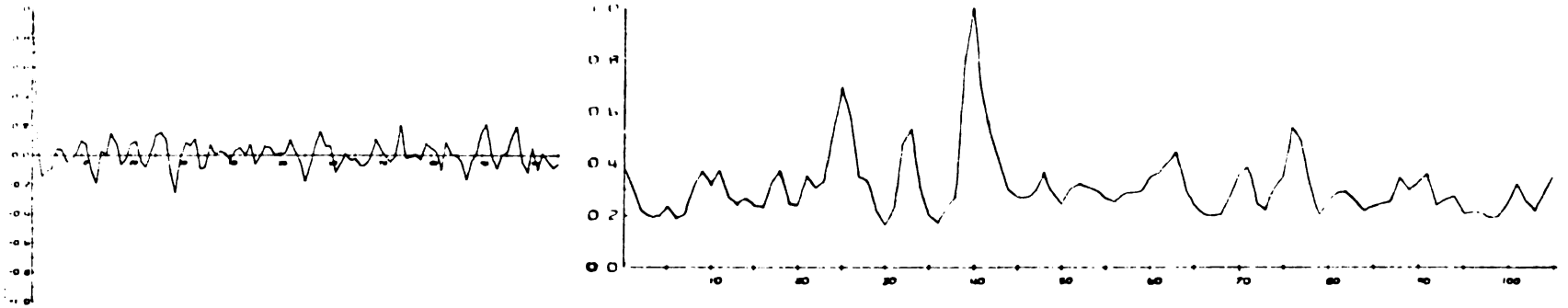

Figure A.11. $\sigma_s^* = 0$, $\sigma_p^* = .1$ and $S^* = 14.3$.

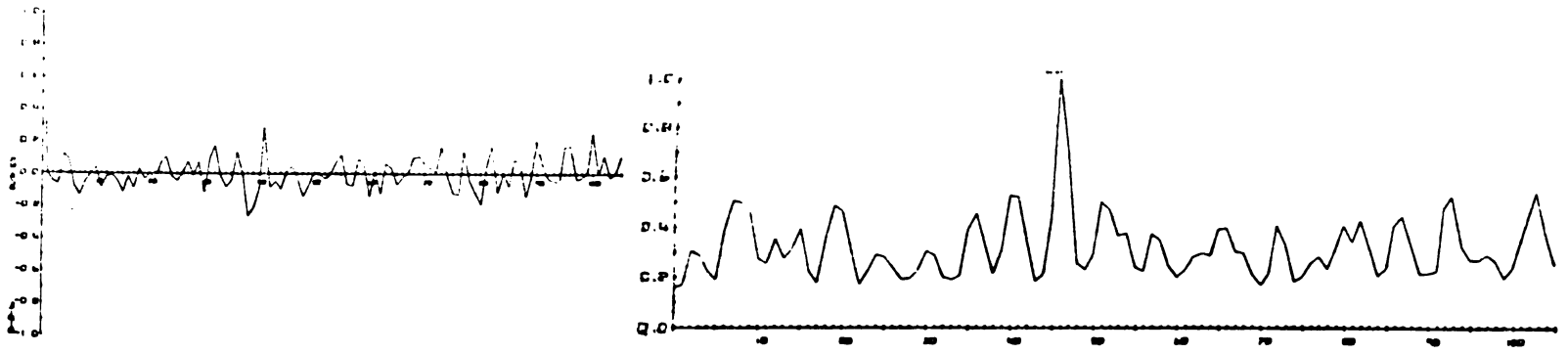

Figure A.12. $\sigma_s^* = 0$, $\sigma_p^* = .16$ and $S^* = 3.6$.

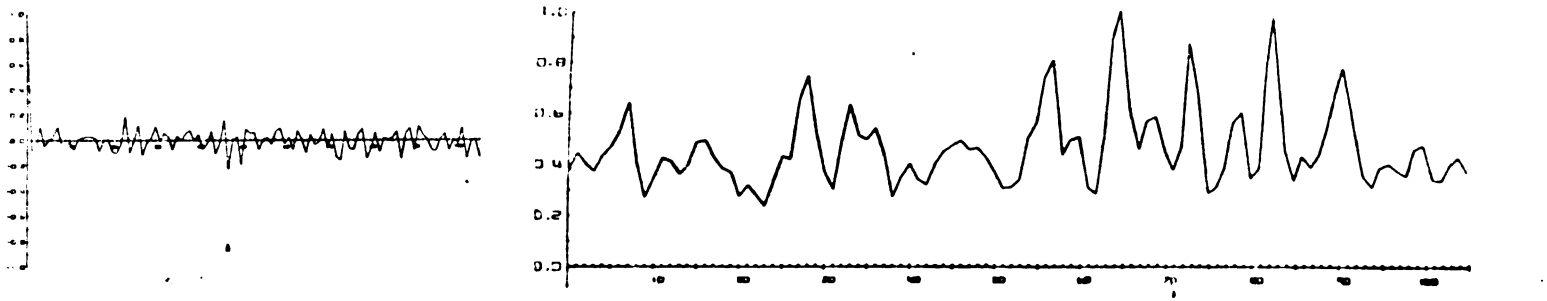

Figure A.13. $\sigma_s^* = 0$, $\sigma_p^* = .18$ and $S^* = 10.8$.

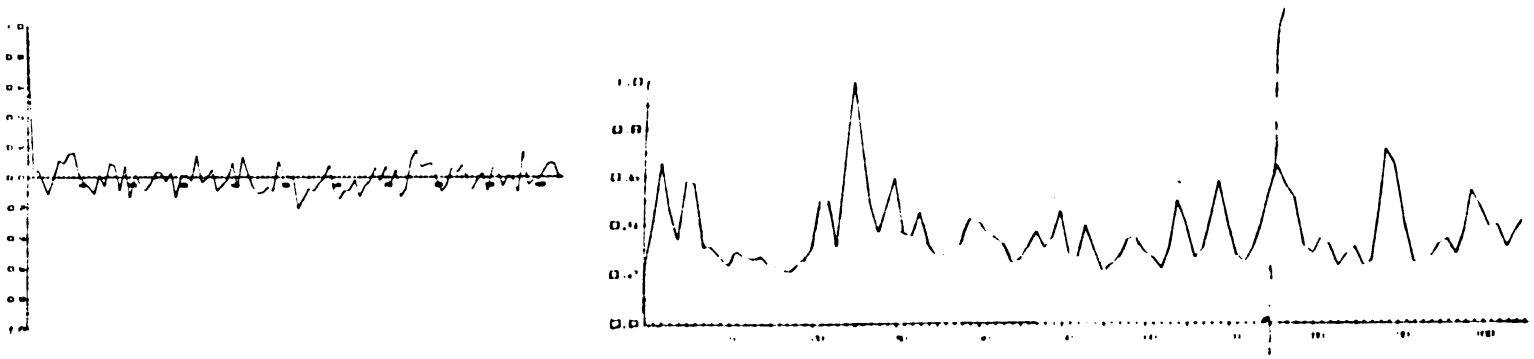

Figure A.14. $\sigma_s^* = 0$, $\sigma_p^* = .18$ and $S^* = 10.8$.

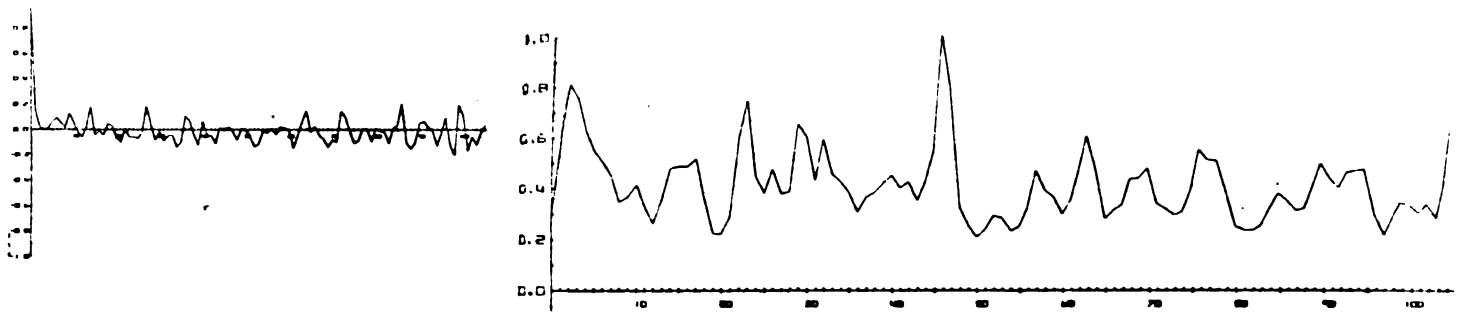

Figure A.15. $\sigma_s = 0$, $\sigma_p^* = .2$ and $S^* = 10.8$.

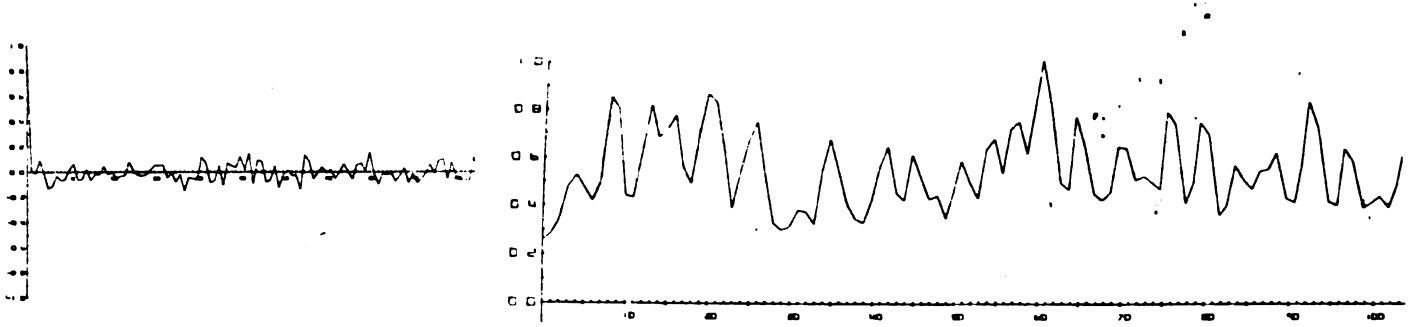

Figure A.16. $\sigma_s^* = 0$, $\sigma_p^* = .22$ and $S^* = 10.8$.

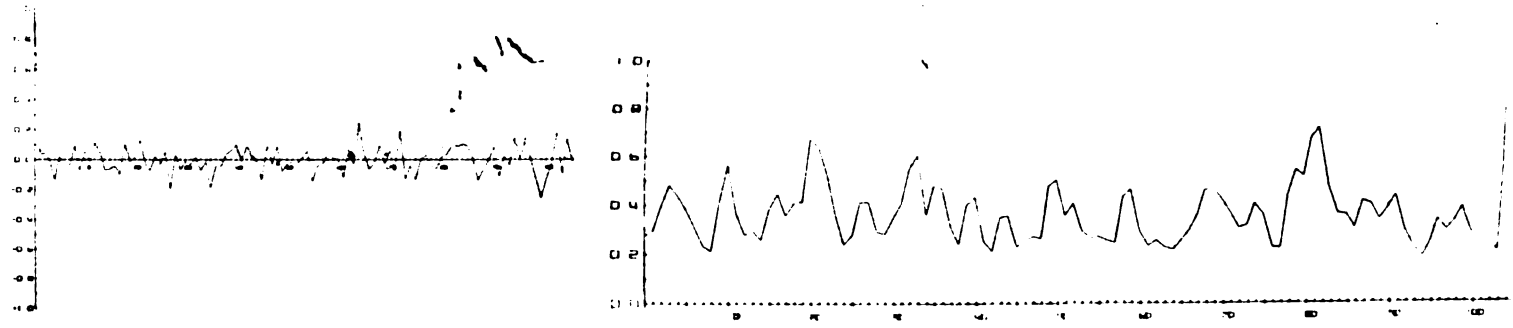

Figure A.17. $\sigma_s^* = 0$, $\sigma_p^* = .22$ and $S^* = 10.8$.

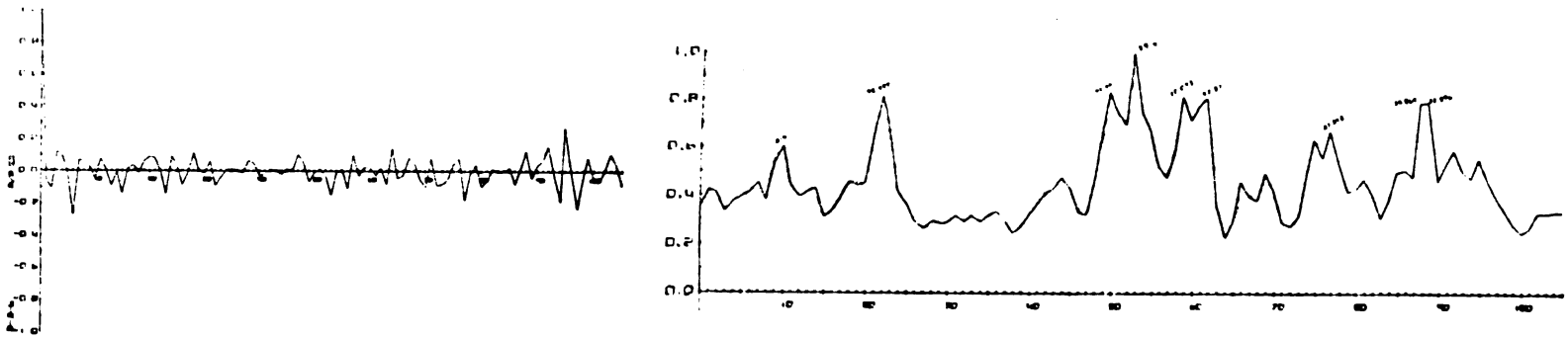

Figure A.18. $\sigma_s^* = 0$, $\sigma_p^* = .26$ and $S^* = 3.6$.

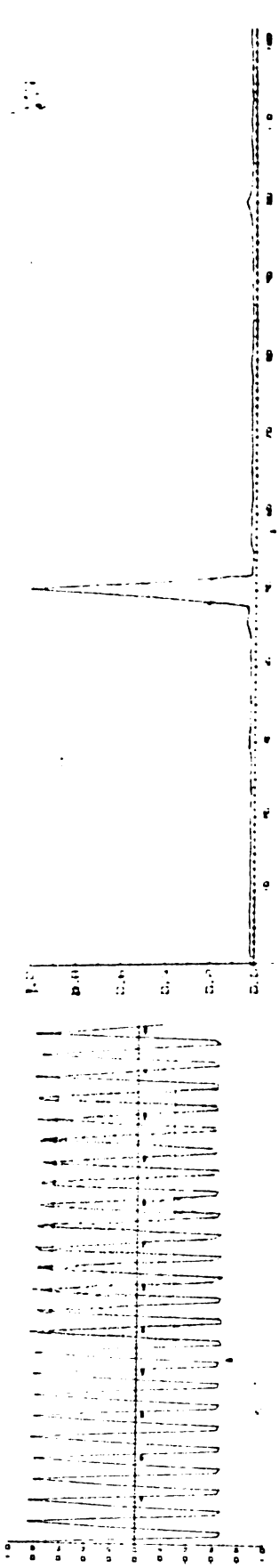

Figure A.19. $\sigma_s^* = .1$, $\sigma_p^* = .04$ and $S^* = 17.9$.

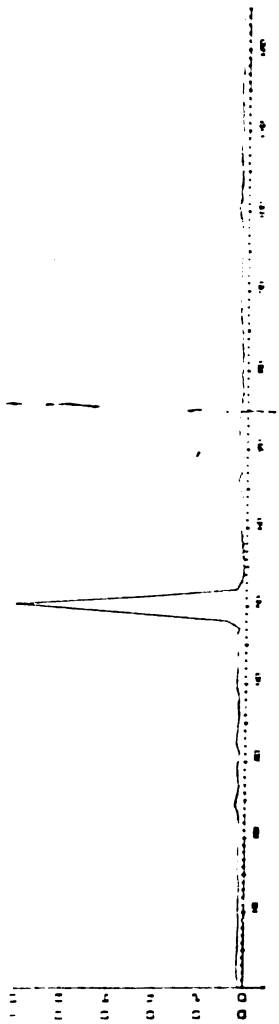

Figure A.20. $\sigma_s^* = .1$, $\sigma_p^* = .06$ and $S^* = 17.9$.

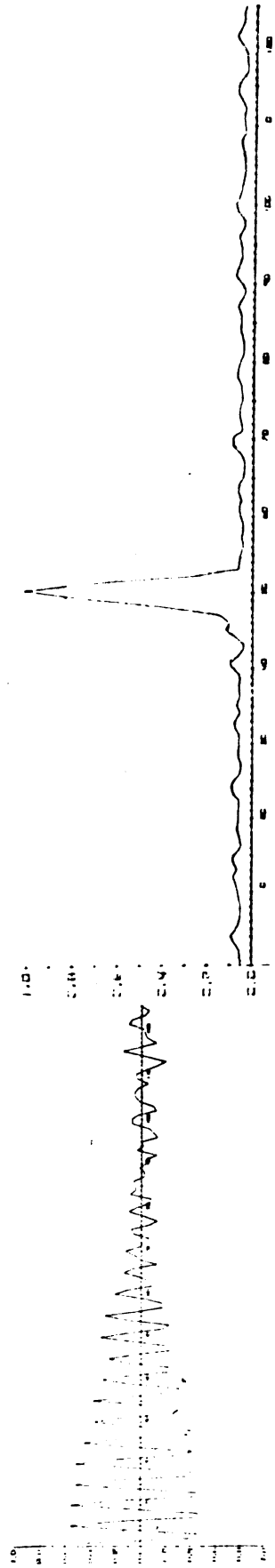

Figure A.21. $\sigma_s^* = .1$, $\sigma_p^* = .08$ and $S^* = 17.9$.

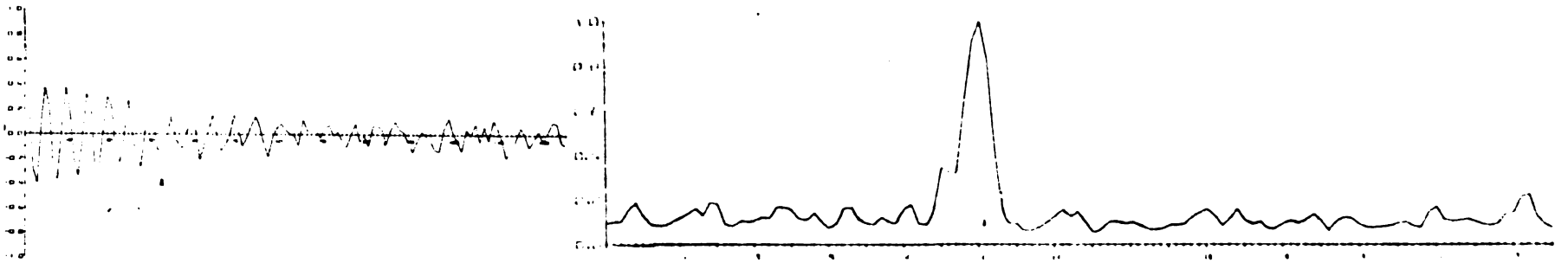

Figure A.22. $\sigma_s^* = .1$, $\sigma_p^* = .1$ and $S^* = 17.9$.

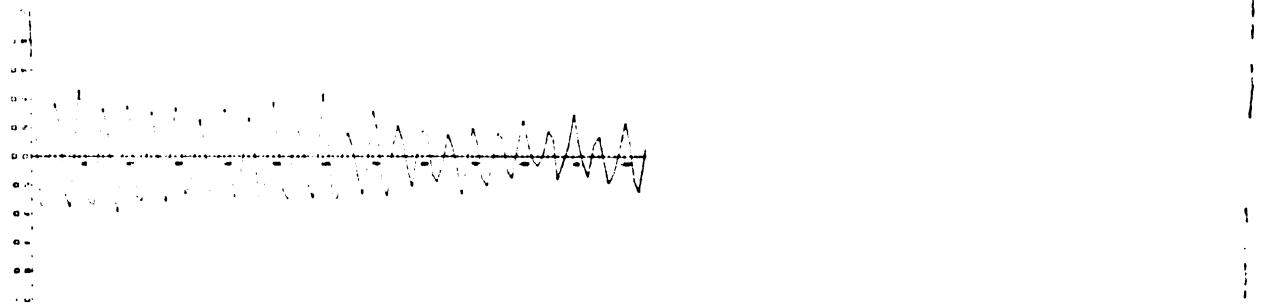

Figure A.23. $\sigma_s^* = .2$, $\sigma_p^* = .06$ and $S^* = 17.9$.

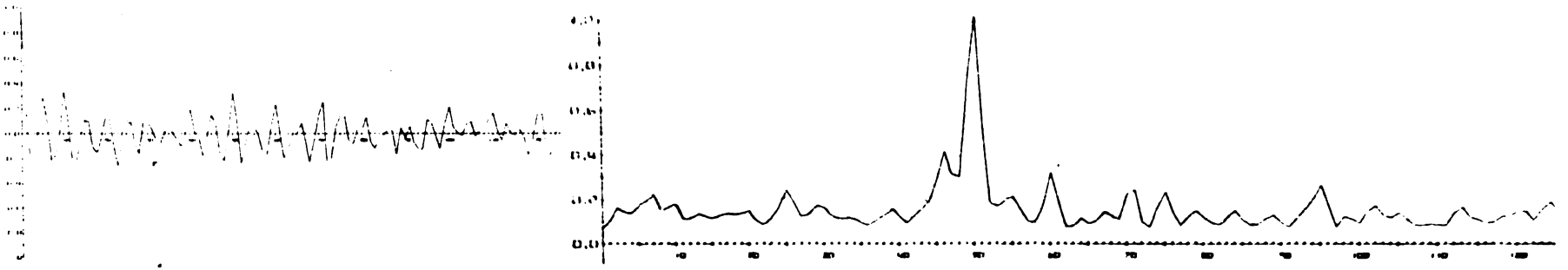

Figure A.24. $\sigma_s^* = .2$, $\sigma_p^* = .08$ and $S^* = 17.9$.

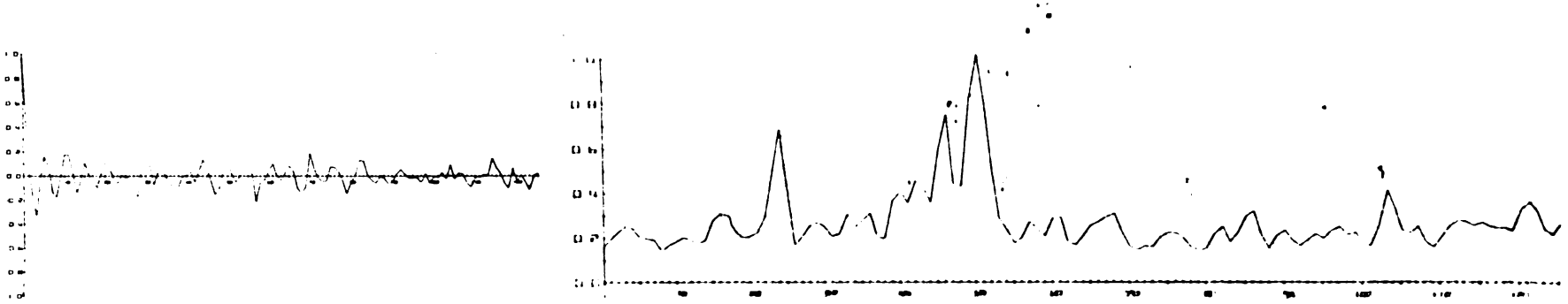

Figure A.25. $\sigma_s^* = .2$, $\sigma_p^* = .1$ and $S^* = 17.9$.

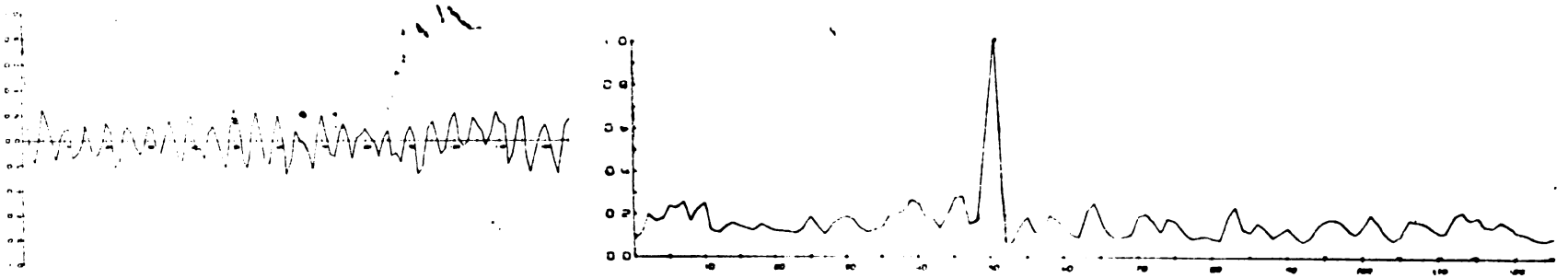

Figure A.26. $\sigma_s^* = .3$, $\sigma_p^* = .04$ and $S^* = 17.9$.

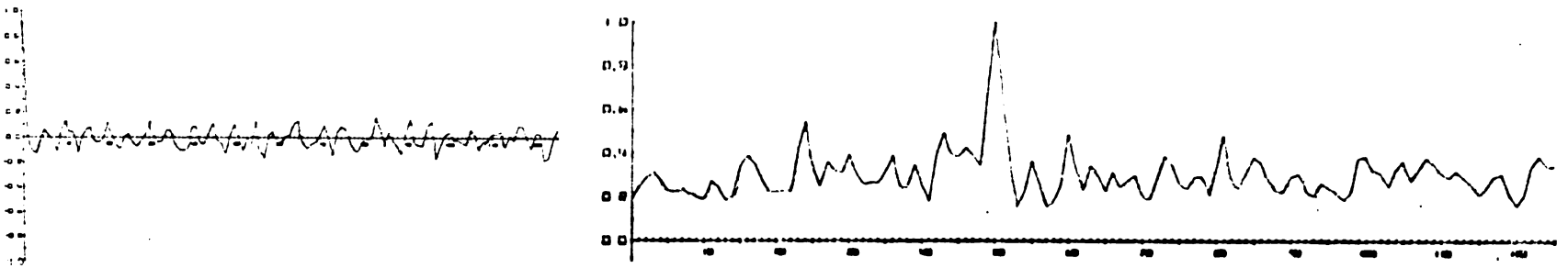

Figure A.27. $\sigma_s^* = .3$, $\sigma_p^* = .06$ and $S^* = 17.9$.

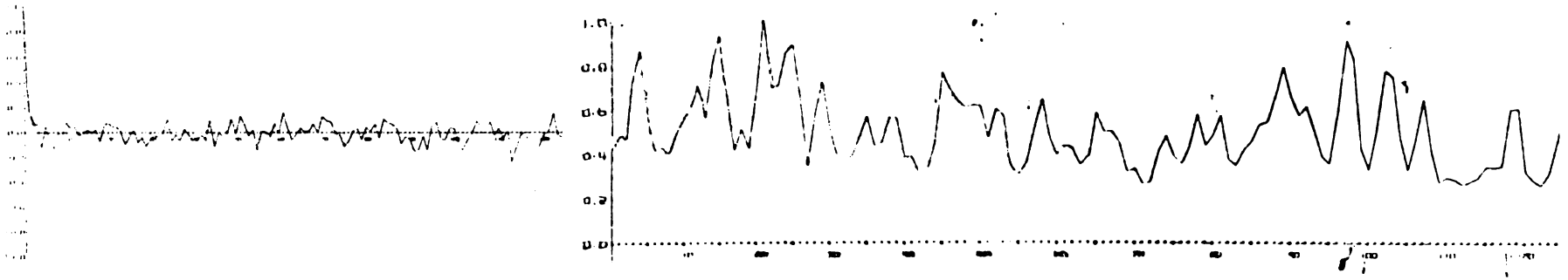

Figure A.28. $\sigma_s^* = .3$, $\sigma_p^* = .1$ and $S^* = 17.9$.

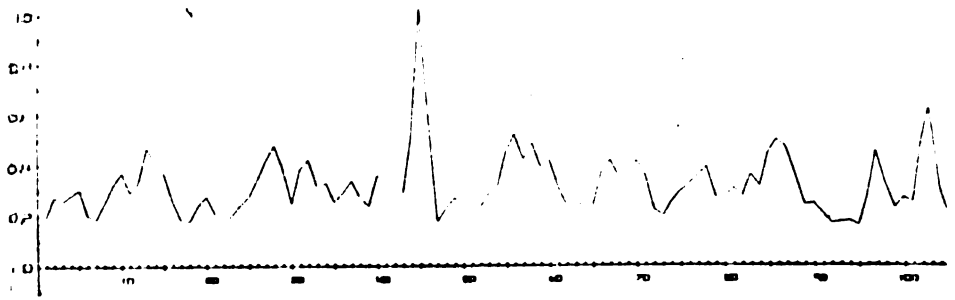

Figure A.29. $\sigma_s = 15$, $\sigma_p = 0$, $S^* = 3.6$ and $t_p = 46.667$.

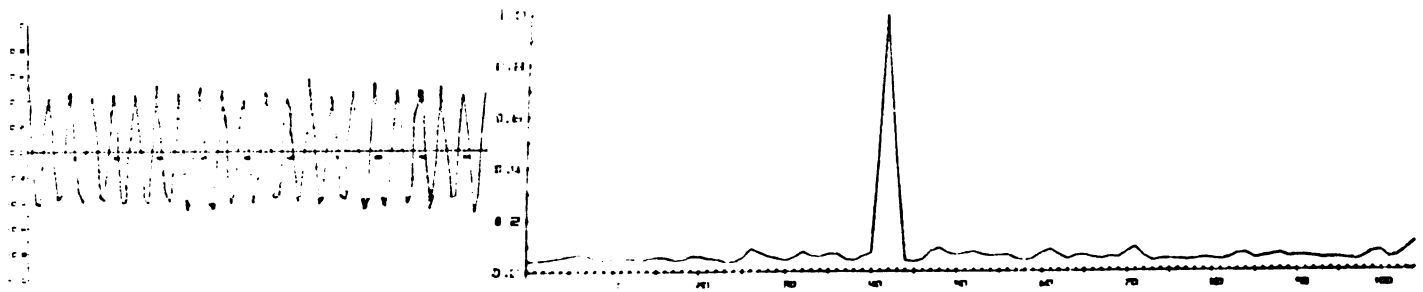

Figure A.30. $\sigma_s^* = .3$, $\sigma_p^* = 0$ and $S^* = 14.3$.

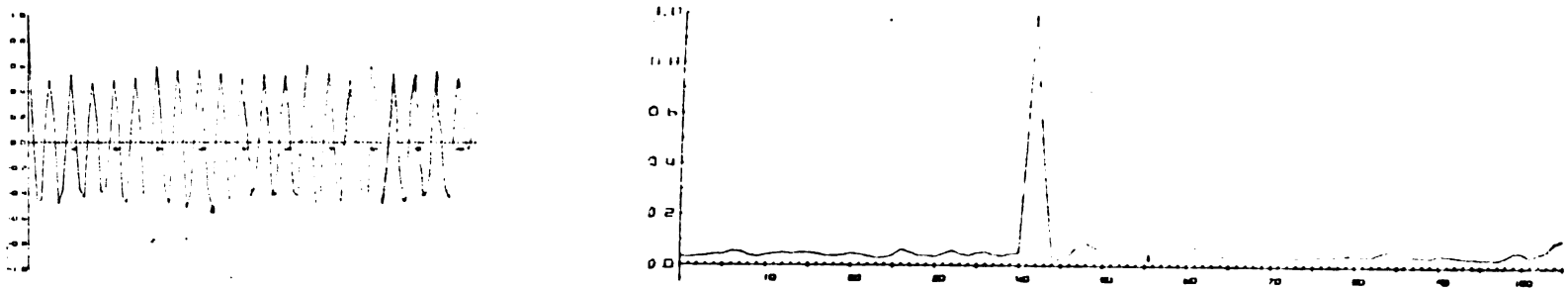

Figure A.31. $\sigma_s^* = .3$, $\sigma_p^* = 0$ and $S^* = 17.9$.

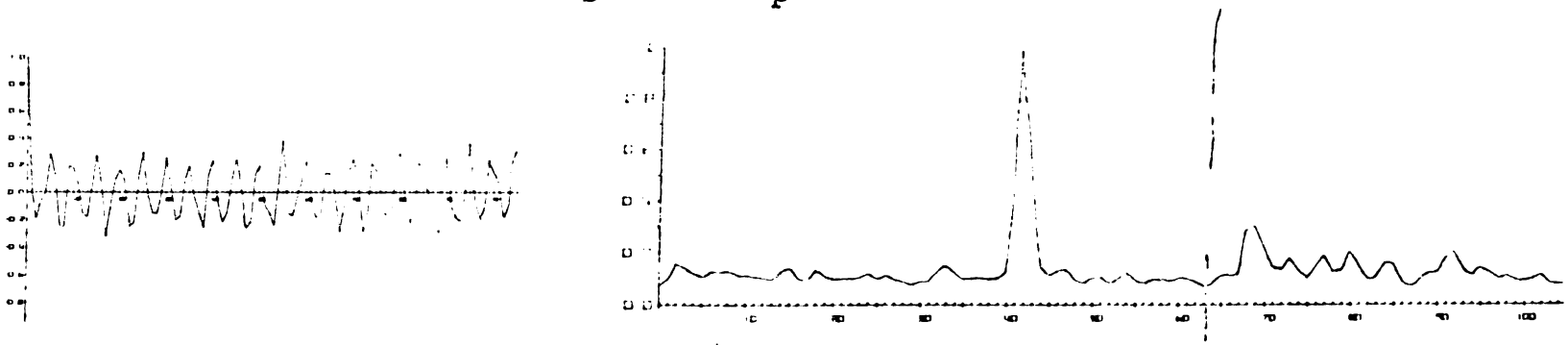

Figure A.32. $\sigma_s^* = .34$, $\sigma_p^* = 0$ and $S^* = 17.9$.

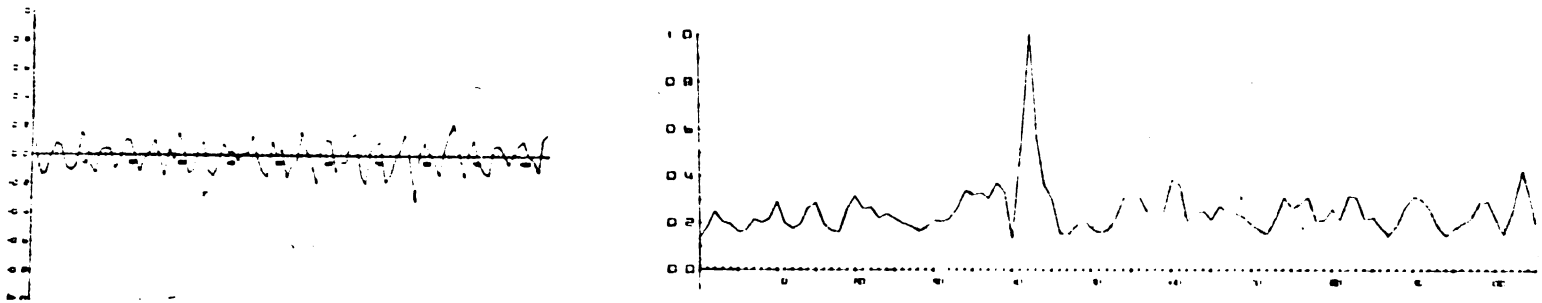

Figure A.33. $\sigma_s^* = .38$, $\sigma_p^* = 0$ and $S^* = 17.9$.

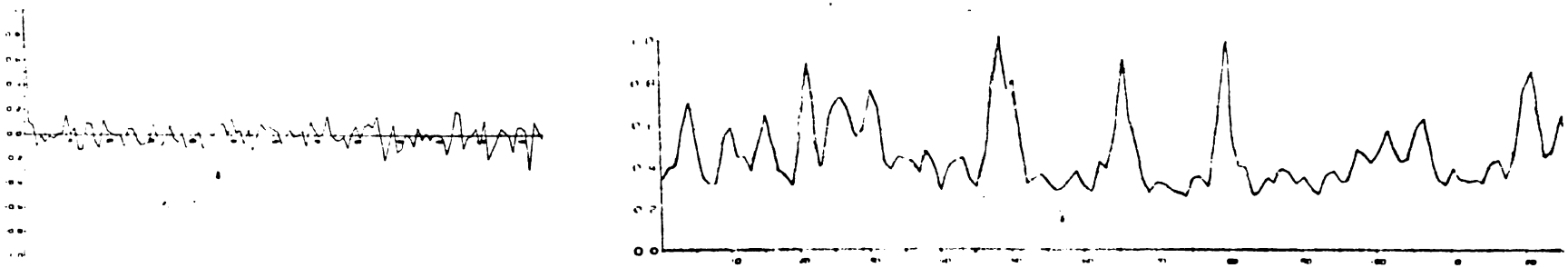

Figure A.34. $\sigma_s^* = .4$, $\sigma_p^* = .04$ and $S^* = 17.9$.

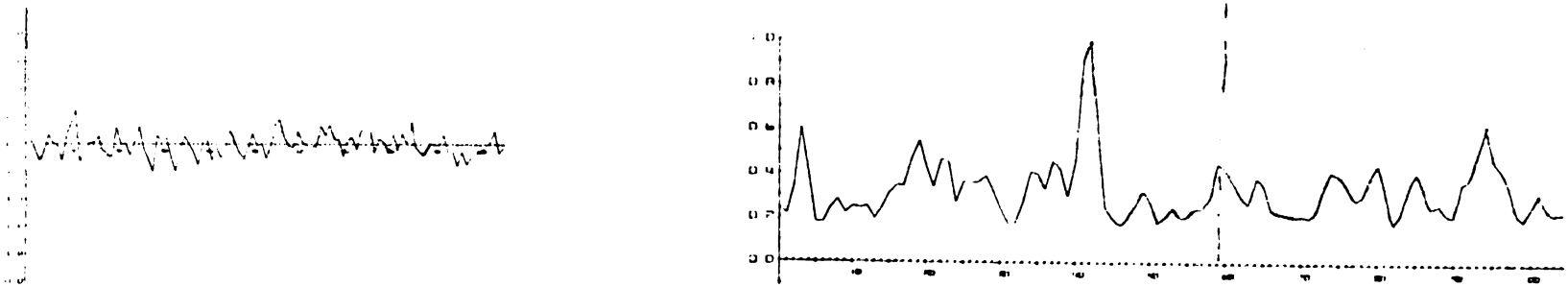

Figure A.35. $\sigma_s^* = .42$, $\sigma_p^* = 0$ and $S^* = 17.9$.

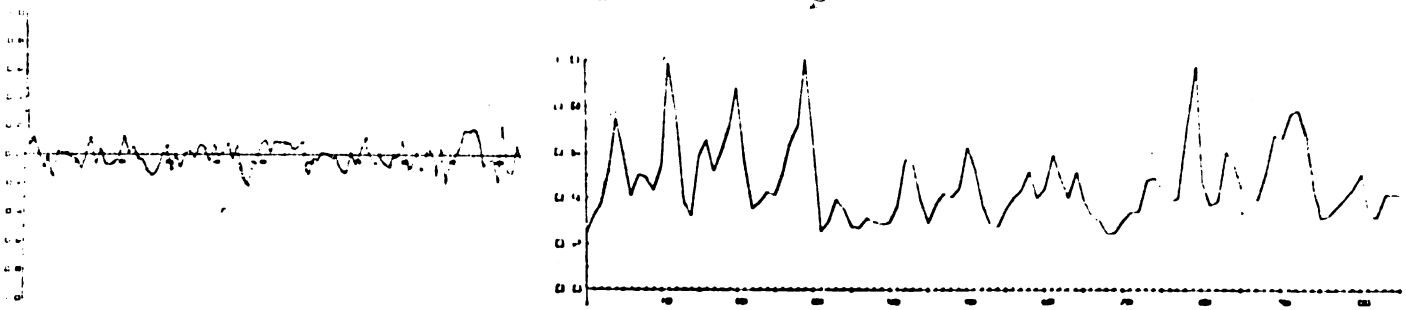

Figure A.36. $\sigma_s^* = .46$, $\sigma_p^* = 0$ and $S^* = 17.9$.

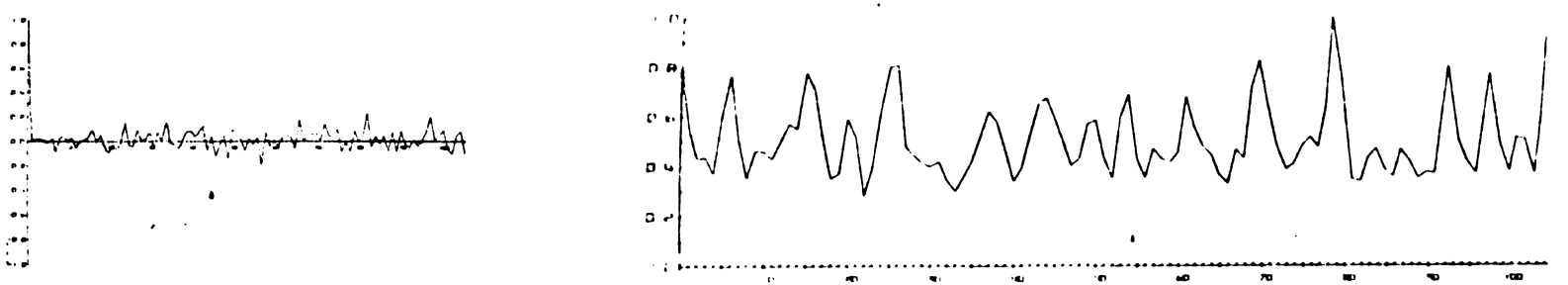

Figure A.37. $\sigma_s^* = .5$, $\sigma_p^* = 0$ and $S^* = 14.3$.

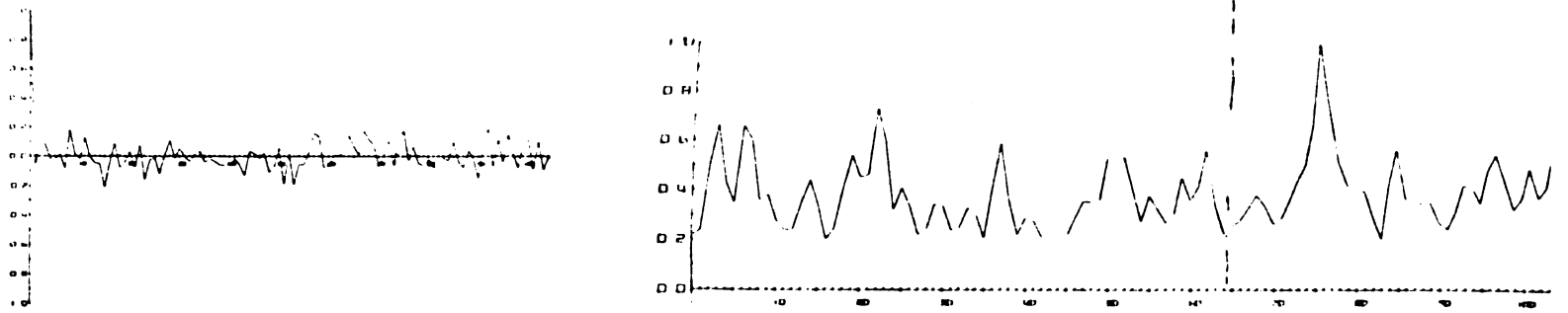

Figure A.38. $\sigma_s^* = .5$, $\sigma_p^* = 0$ and $S^* = 10.8$.

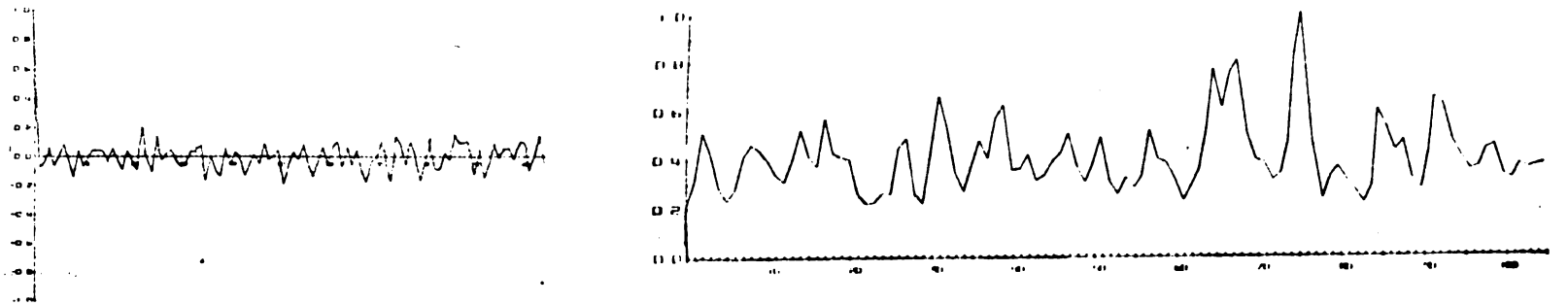

Figure A.39. $\sigma_s^* = .52$, $\sigma_p^* = 0$ and $S^* = 10.8$.

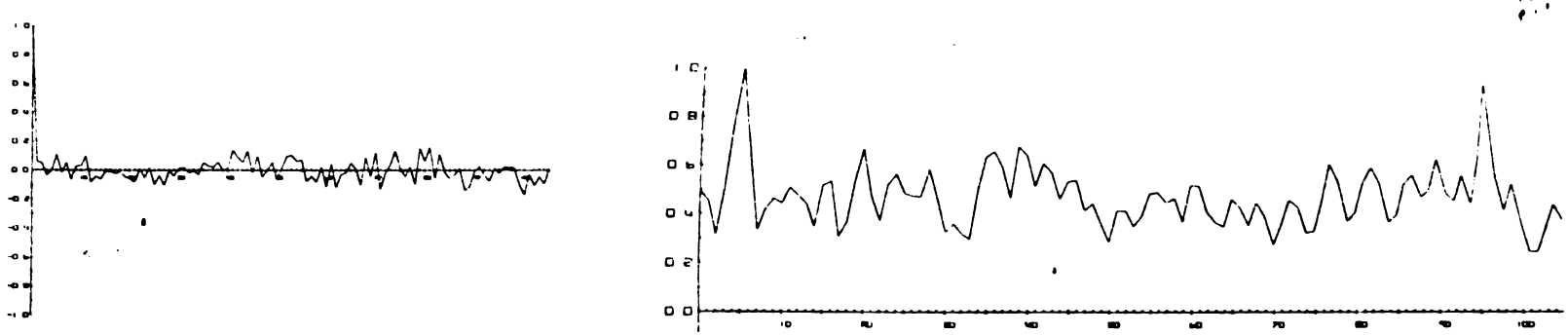

Figure A.40. $\sigma_s^* = .52$, $\sigma_p^* = 0$ and $S^* = 10.8$.

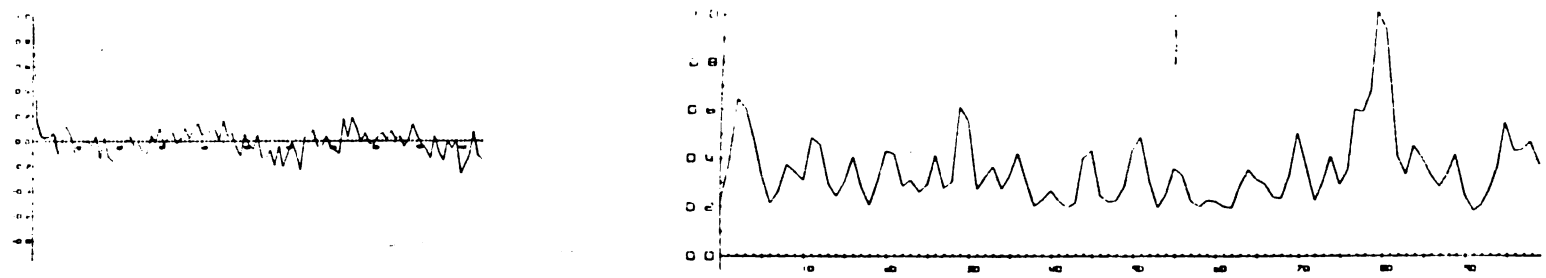

Figure A.41. $\sigma_s^* = .56$, $\sigma_p^* = 0$ and $S^* = 10.8$.

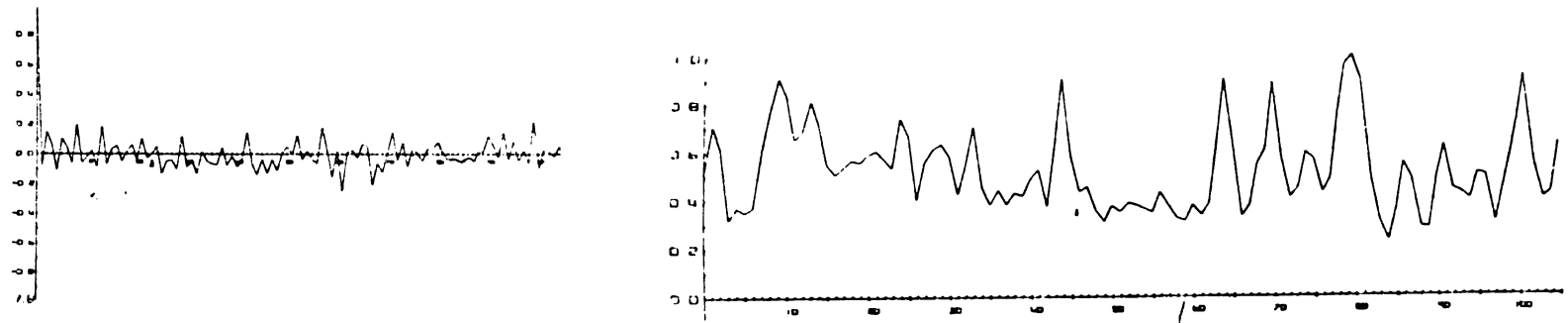

Figure A.42. $\sigma_s^* = .6$, $\sigma_p^* = 0$ and $S^* = 10.8$.

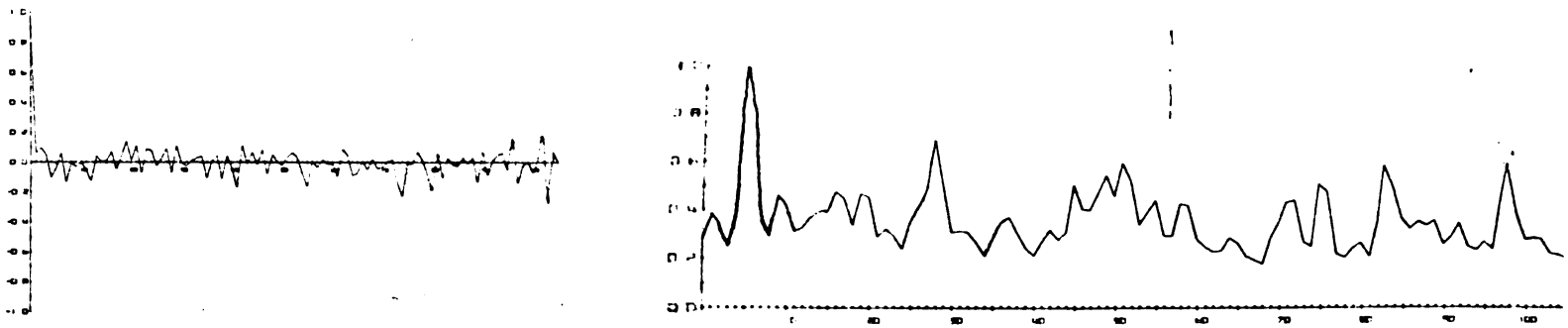

Figure A.43. $\sigma_s^* = .7$, $\sigma_p^* = 0$ and $S^* = 14.3$.

APPENDIX B

APPENDIX B

Each figure in this appendix is a set of power spectral estimates and their autocorrelations for a single histogram generated during Experiment B-3. The parameter values used but not indicated in the figures are t = 10 msec., t_p = msec., t_s = 400 msec., m^* = m'^* = .5 and S^* = 17.9.

Note that power spectral estimates are the upper row of graphs in a figure, their autocorrelations are the second row and a power spectral estimate is the rightmost of the two graphs in the bottom row.

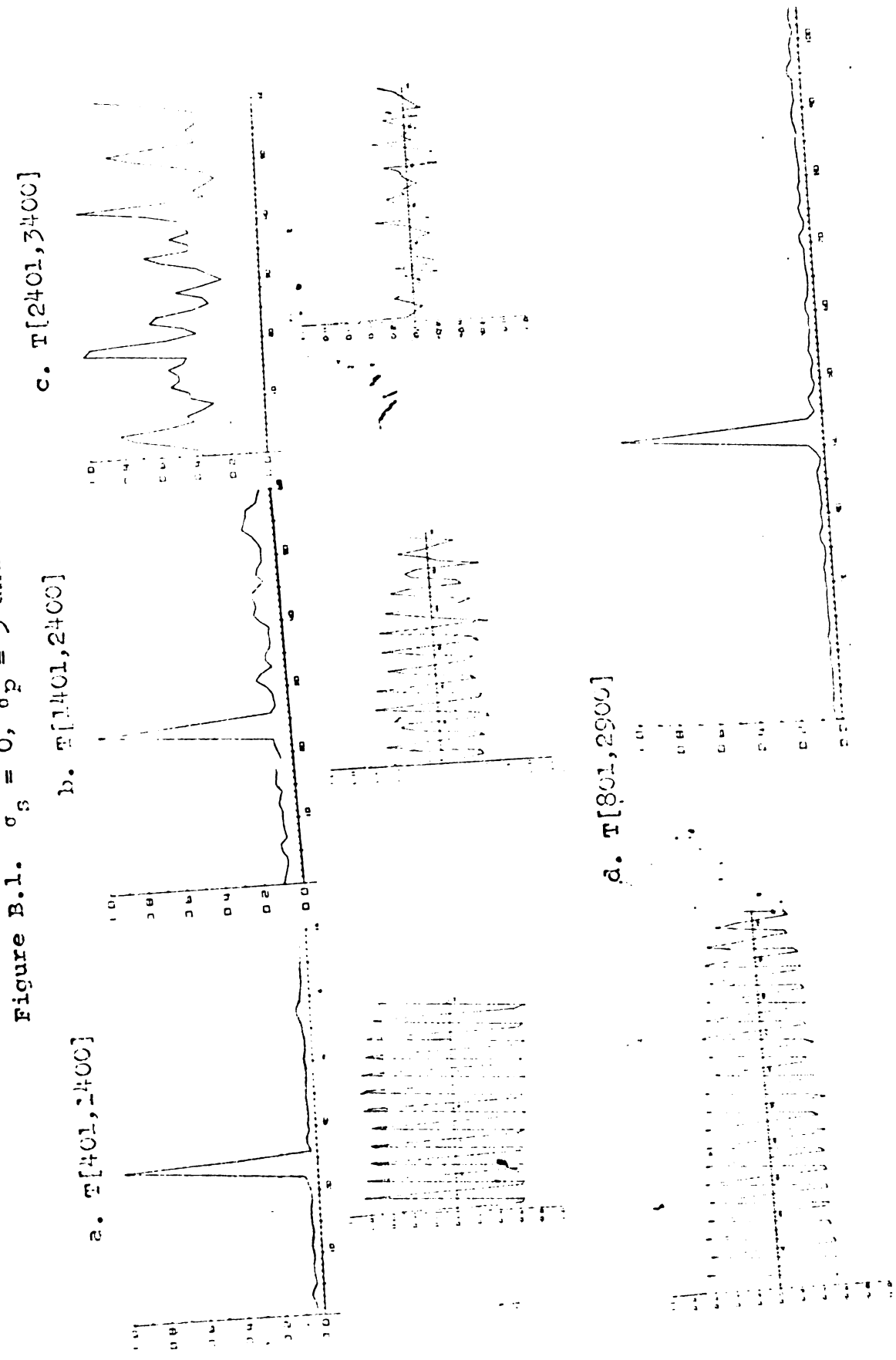

Figure B.1. $\sigma_s = 0$, $\sigma_p = 3$ and

Figure B.2. $\sigma_s = 0$, $\sigma_p = 4$ and

a. T[401,1400]

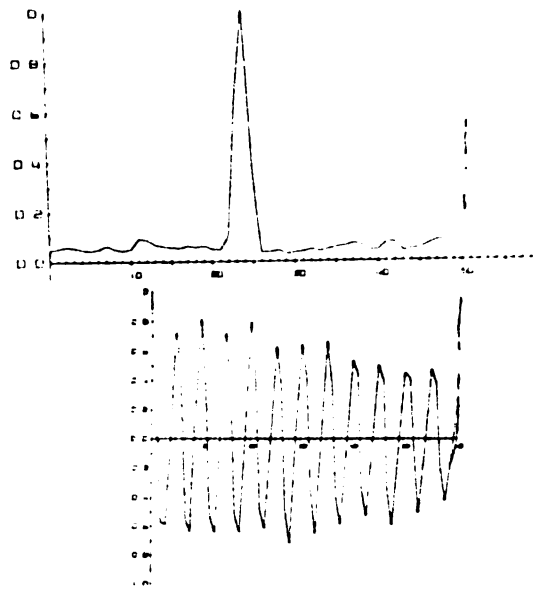

b. T[1401,2400]

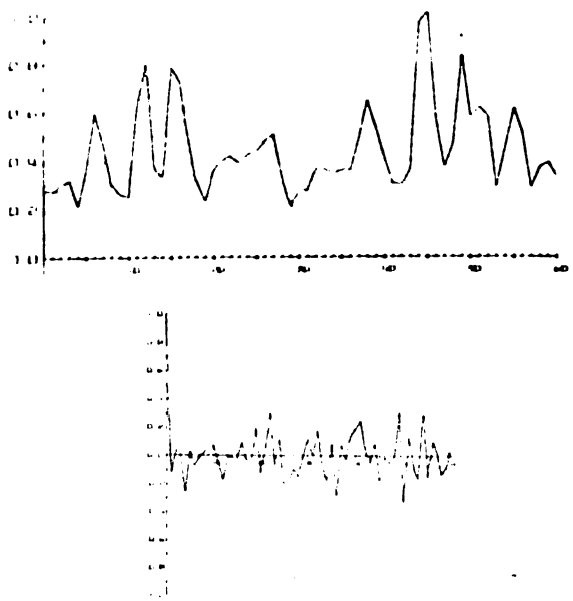

c. T[2401,3400]

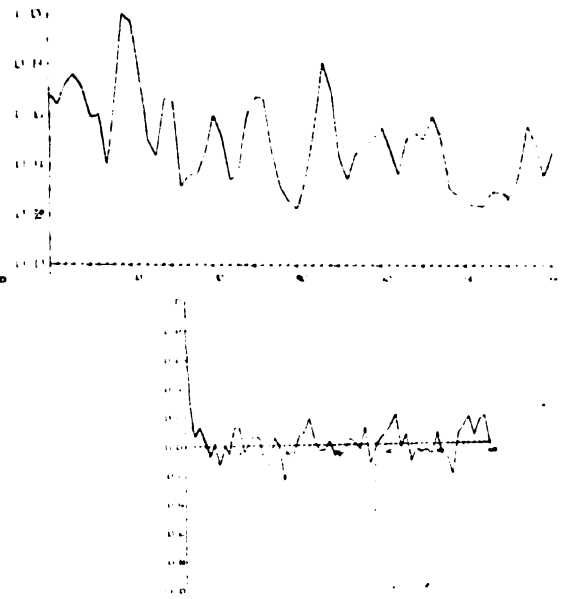

d. T[801,2900]

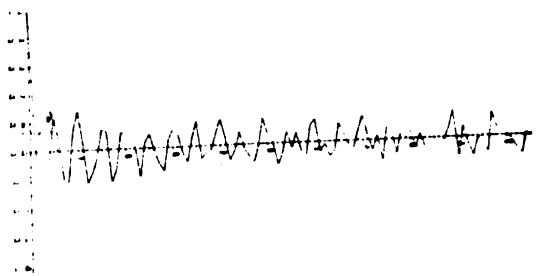

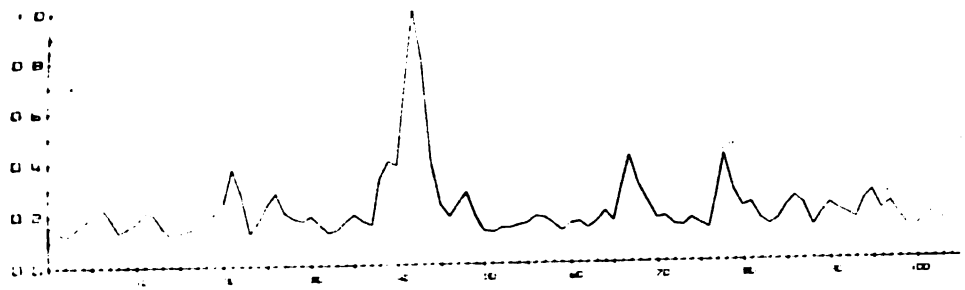

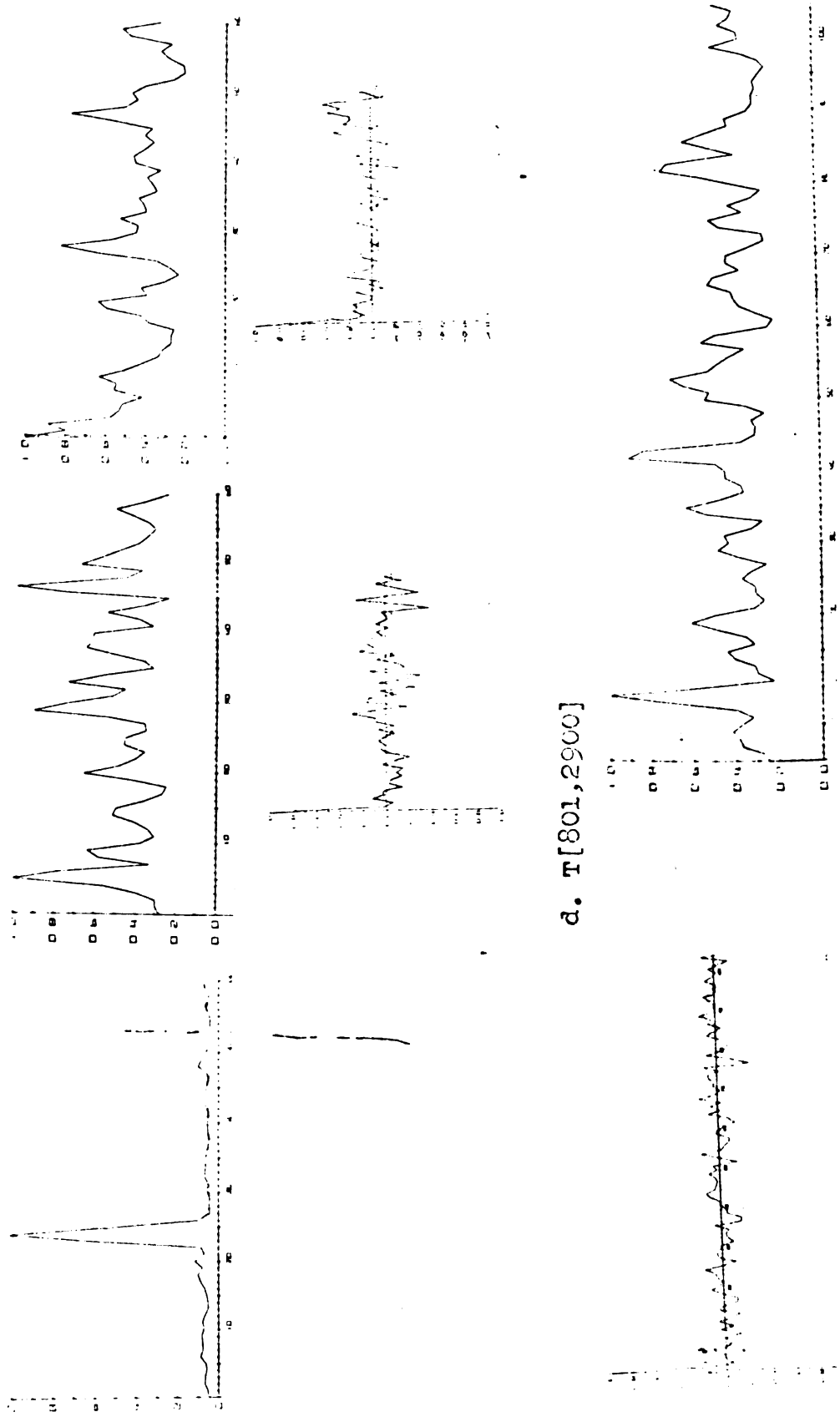

Figure B.3. $\sigma_s = 0$, $\sigma_p = 5$ and

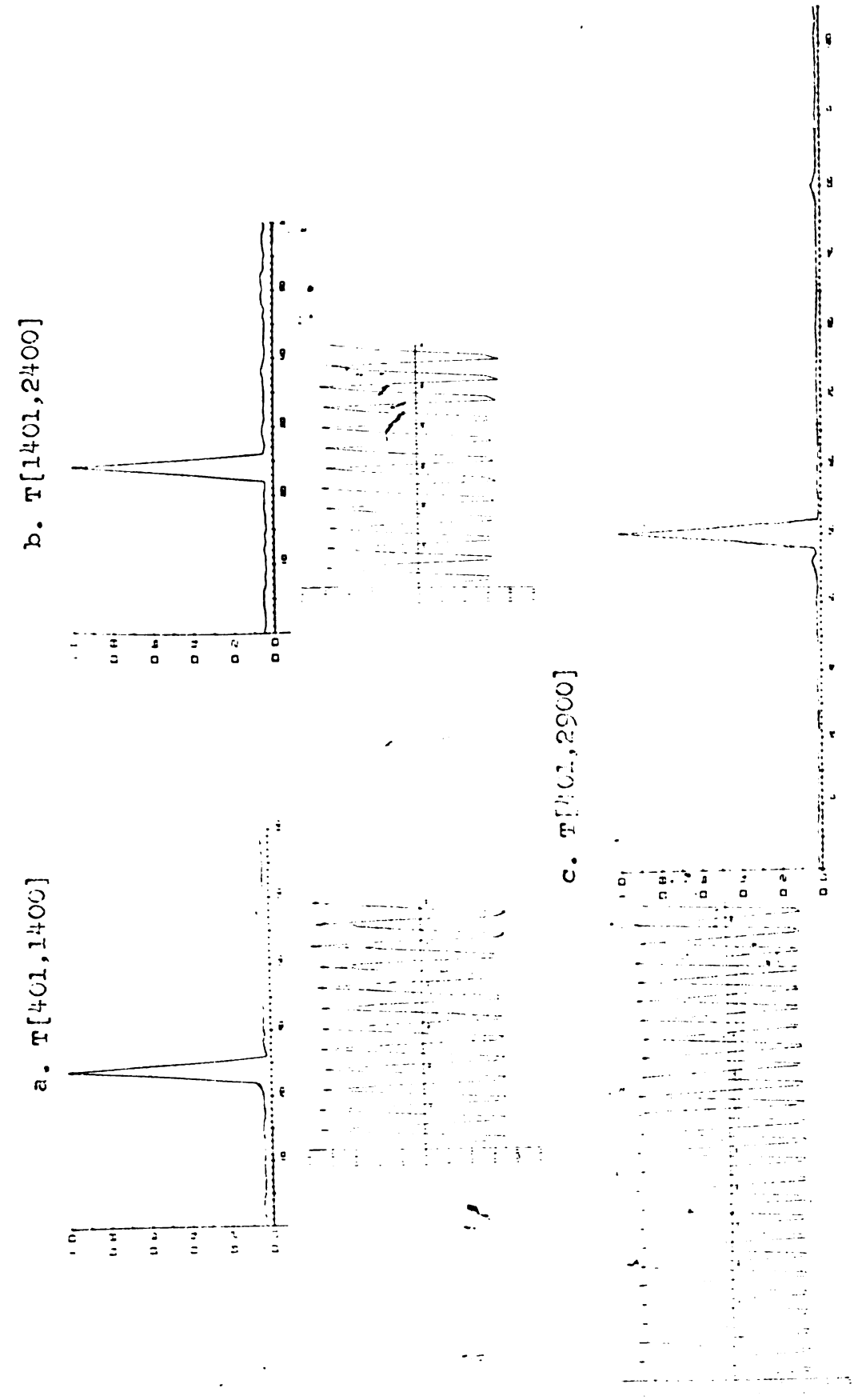

Figure B.4. $\sigma_s = 5$, $\sigma_p = 2$ and

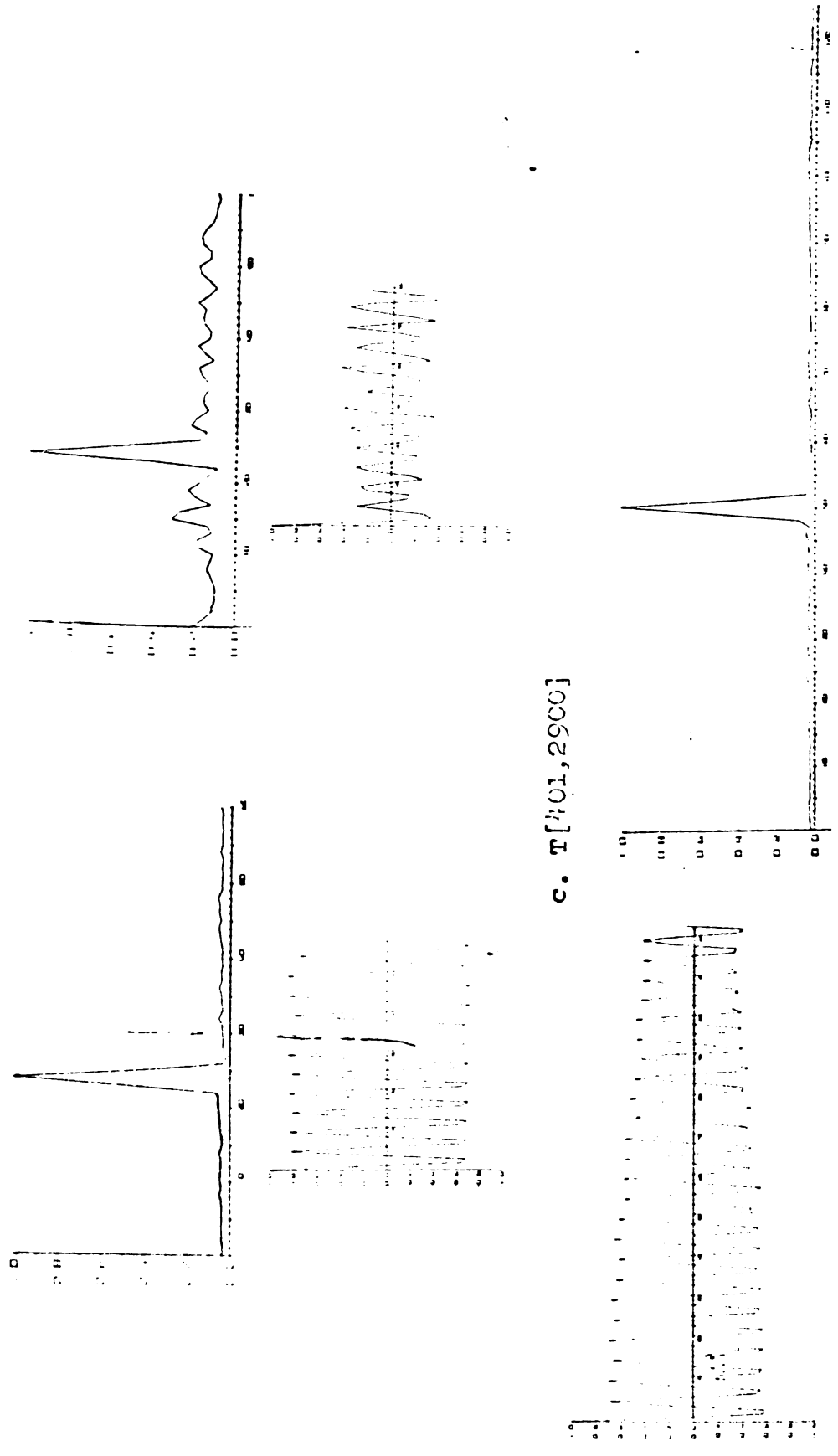

Figure B.5. $\sigma_s = 5$, $\sigma_p = 3$ and

a. T[401,1400]

b. T[1401,2400]

c. T[2401,2900]

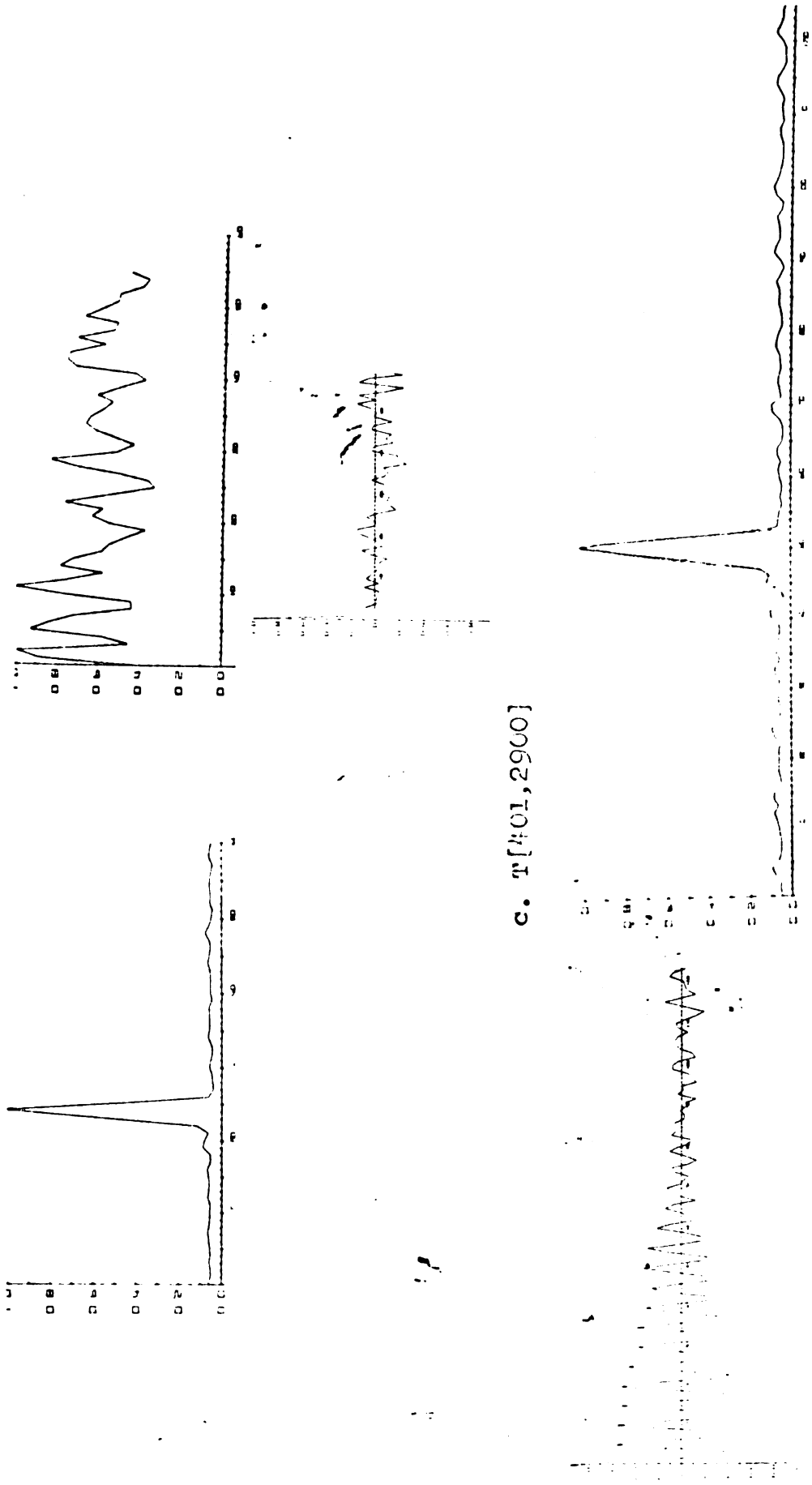

Figure B.6. $\sigma_s = 5$, $\sigma_p = 4$ and

a. T[401,1400]

b. T[1401,2400]

c. T[401,2900]

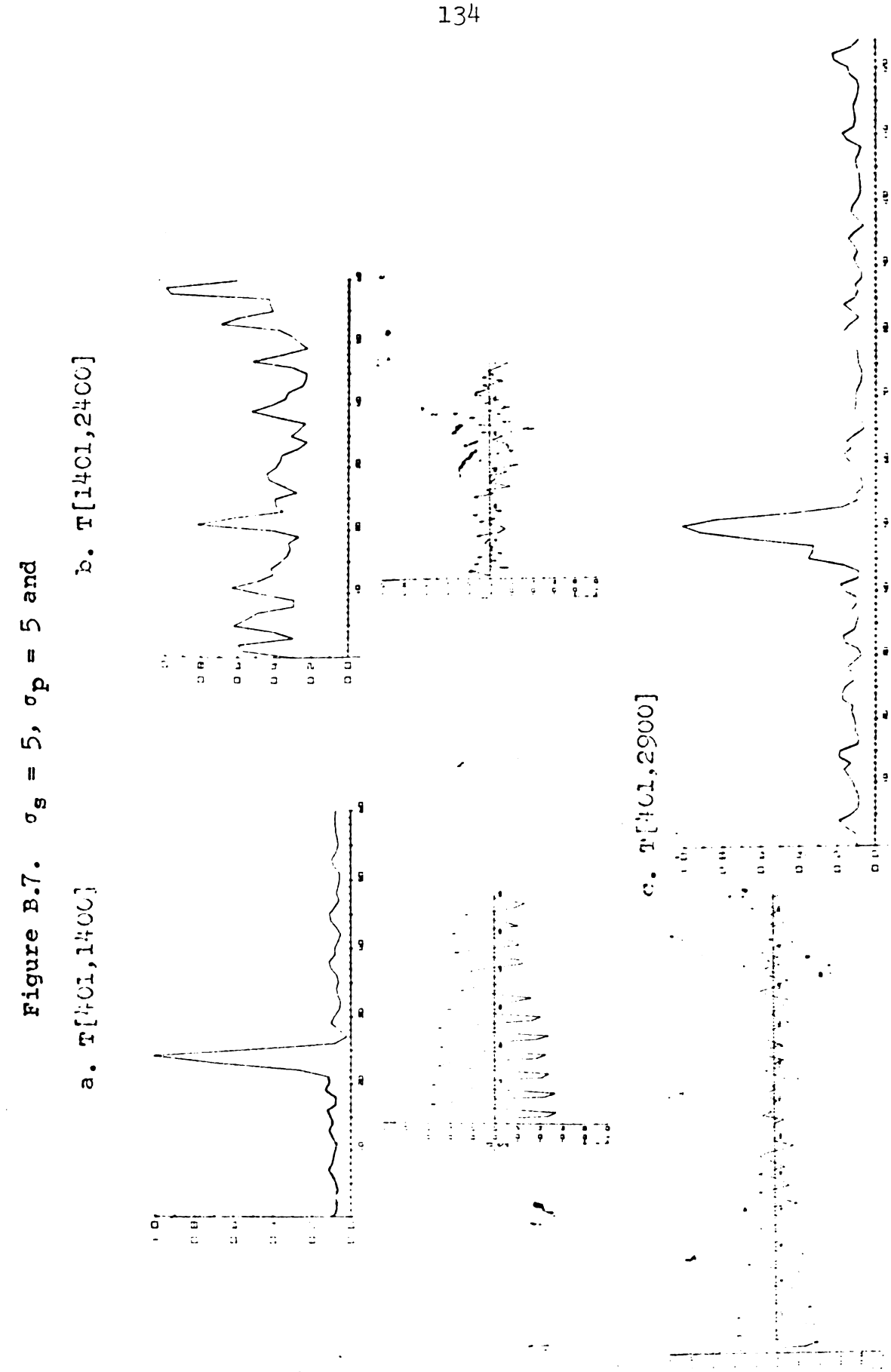

Figure B.7. $\sigma_s = 5$, $\sigma_p = 5$ and

a. T[401,1400]

b. T[1401,2400]

c. T[401,2900]

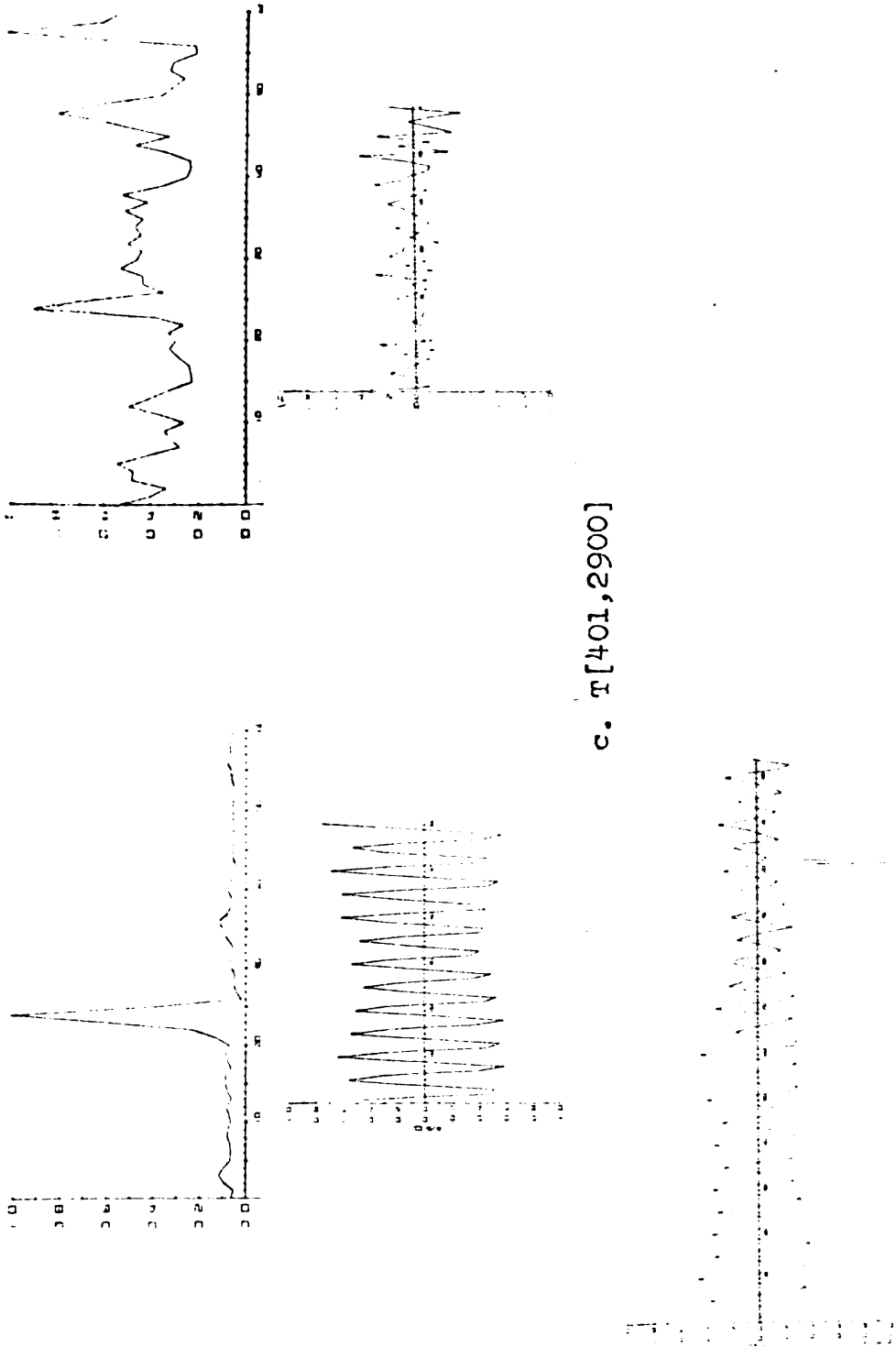

Figure B.8. $\sigma_s = 10$, $\sigma_p = 3$ and

a. T[401,1400]

b. T[1401,2400]

c. T[401,2900]

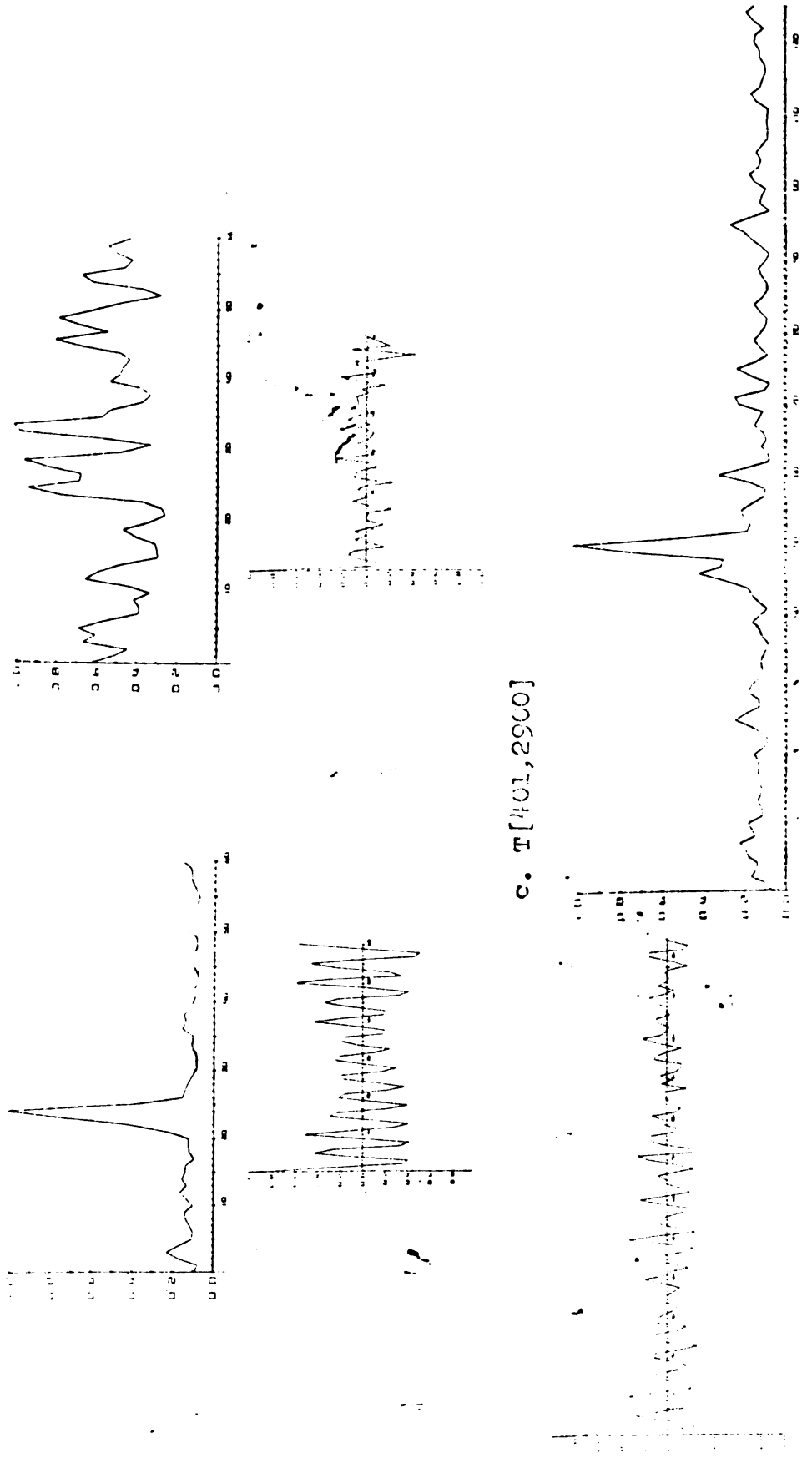

Figure B.9 $\sigma_s = 10$, $\sigma_p = 4$ and

a. T[401,1400]

b. T[1401,2400]

c. T[401,2900]

Figure B.10. $\sigma_s = 10$, $\sigma_p = 5$ and

a. T[401,1400]

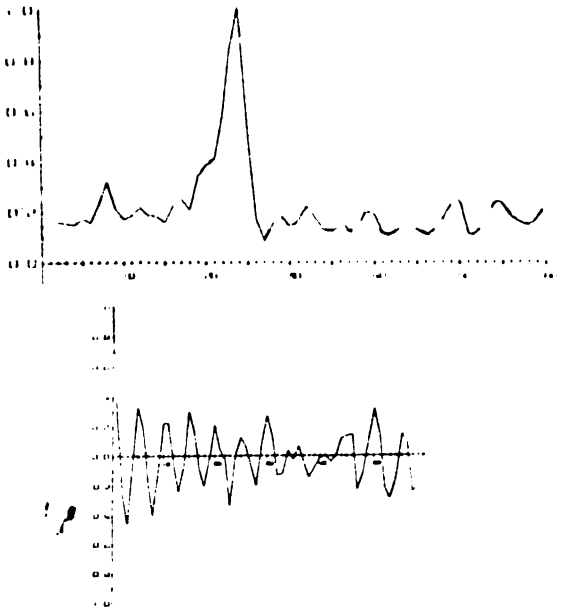

b. T[1401,2400]

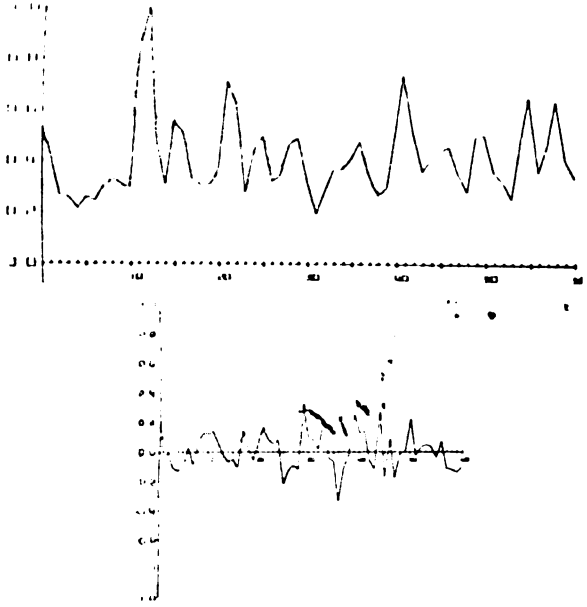

c. T[401,2900]

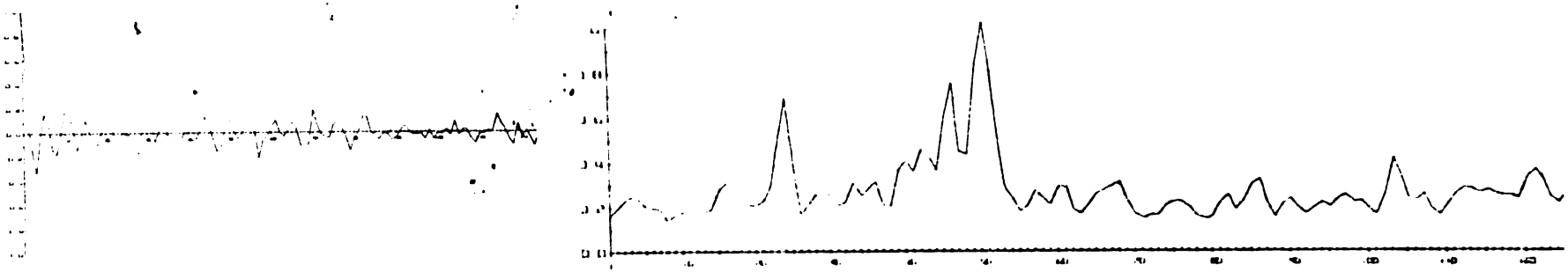

Figure B.11. $\sigma_s = 15$, $\sigma_p = 2$ and

a. T[401,1400]

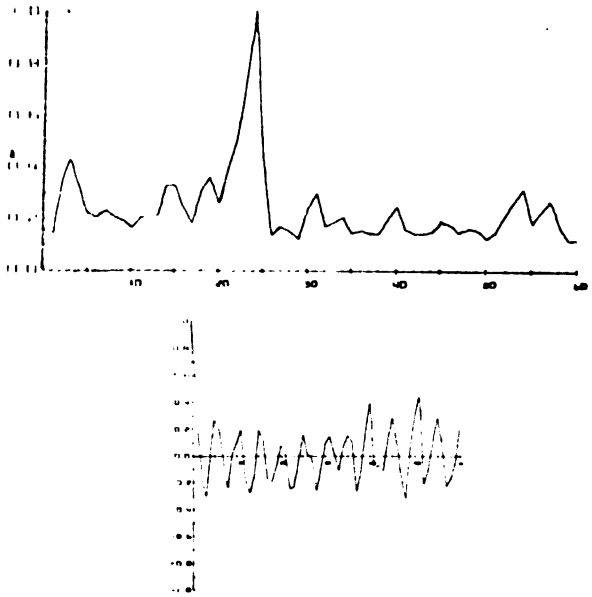

b. T[1401,2400]

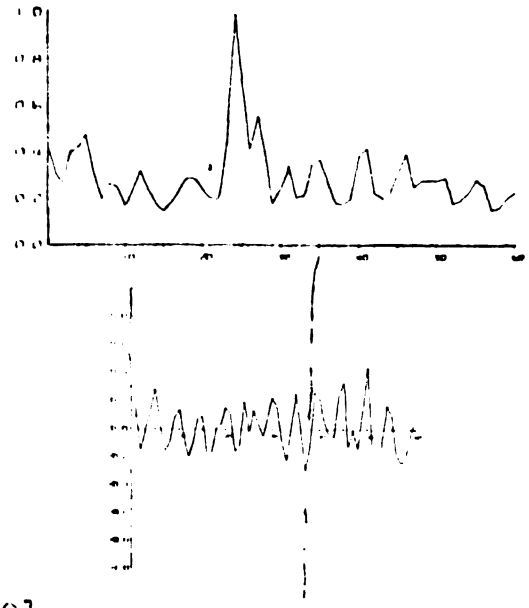

c. T[401,2900]

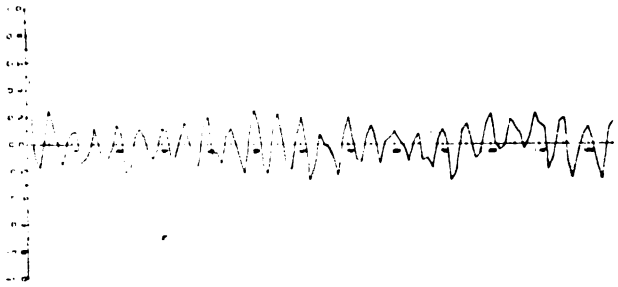

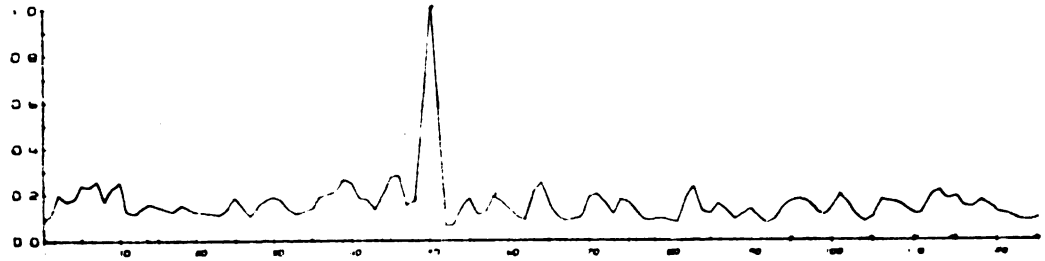

Figure B.12. $\sigma_s = 15$, $\sigma_p = 3$ and

a. T[401,1400]

b. T[1401,2400]

c. T[1401,2900]

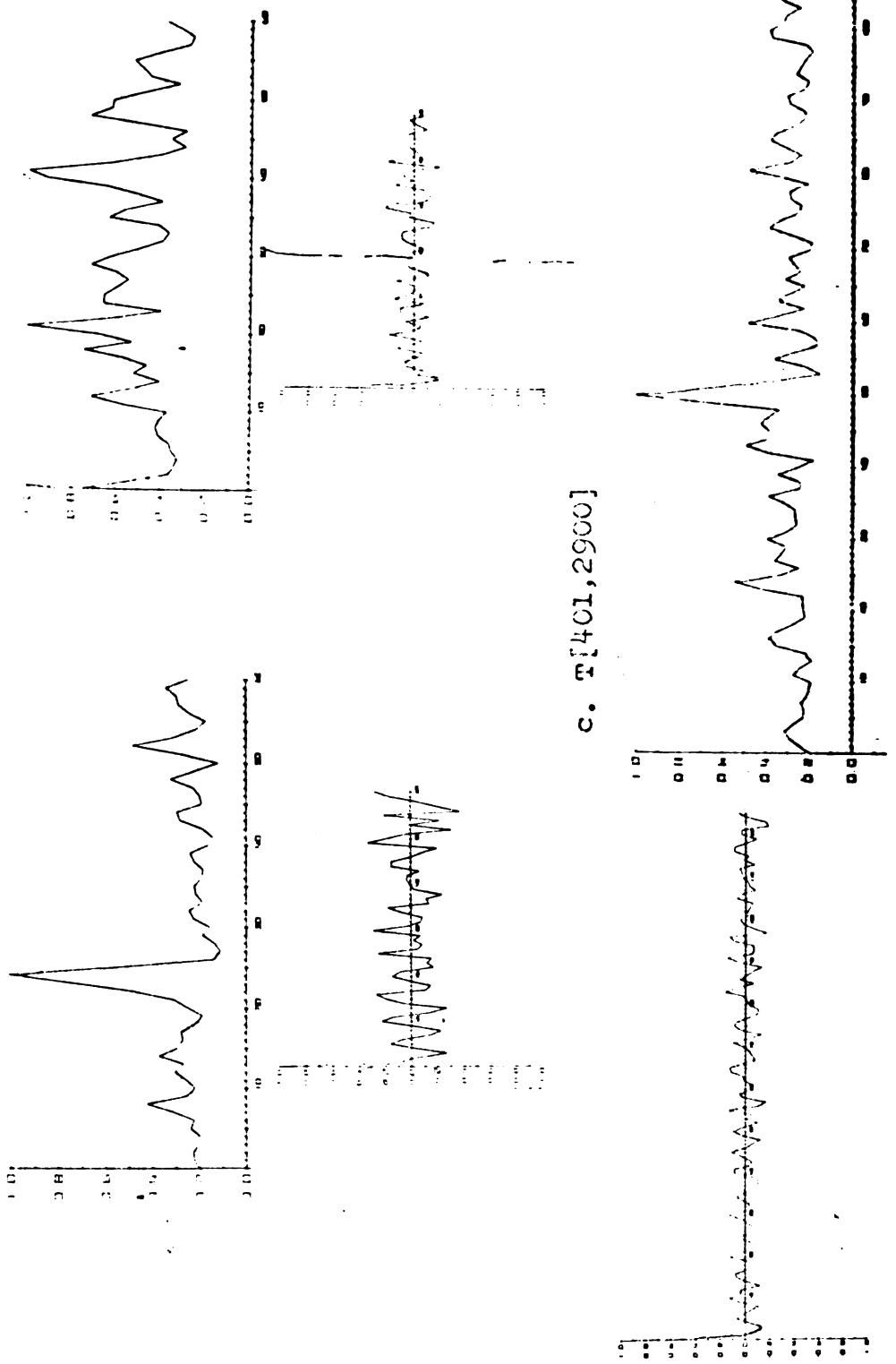

Figure B.13. $\sigma_s = 15$, $\sigma_p = 4$ and

a. T[401,1400]

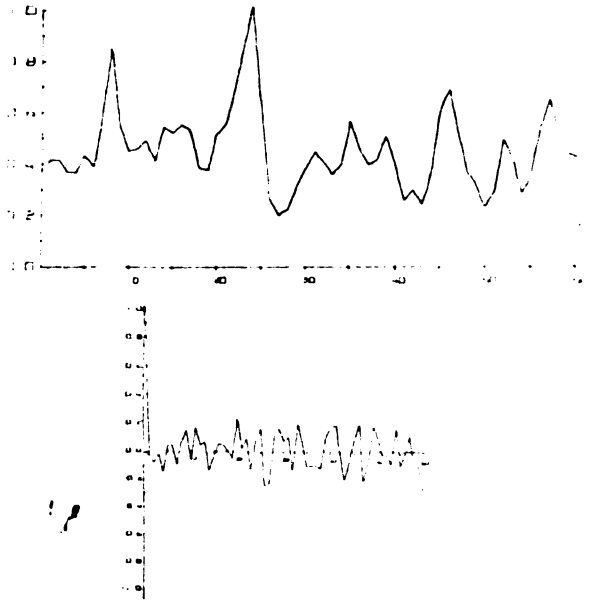

b. T[1401,2400]

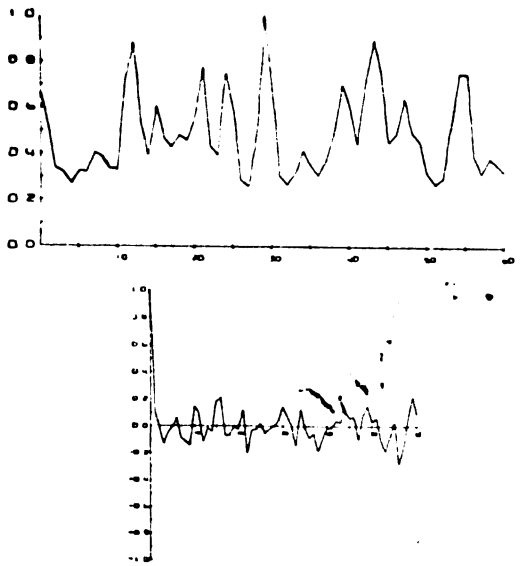

c. T[401,2900]

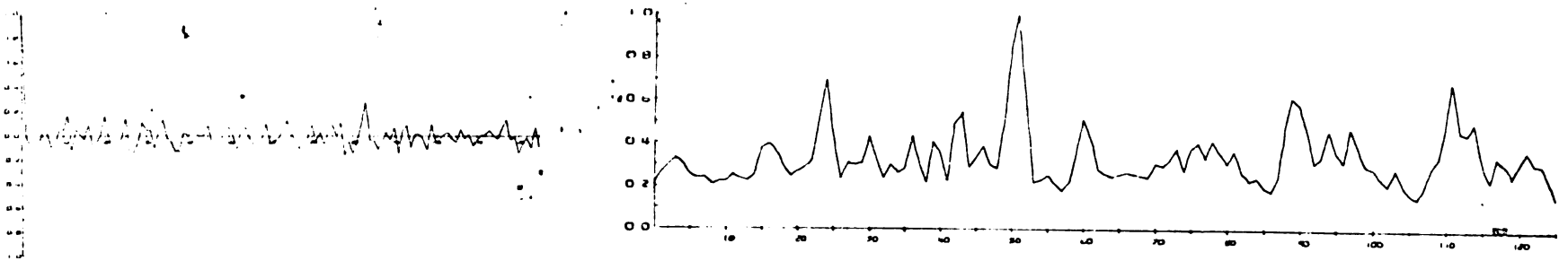

Figure B.14. $\sigma_s = 15$, $\sigma_p = 5$ and

a. T[401,1400]

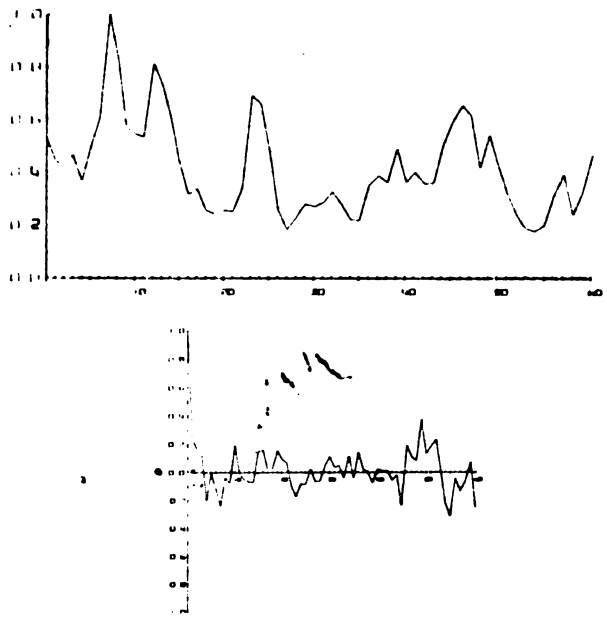

b. T[1401,2400]

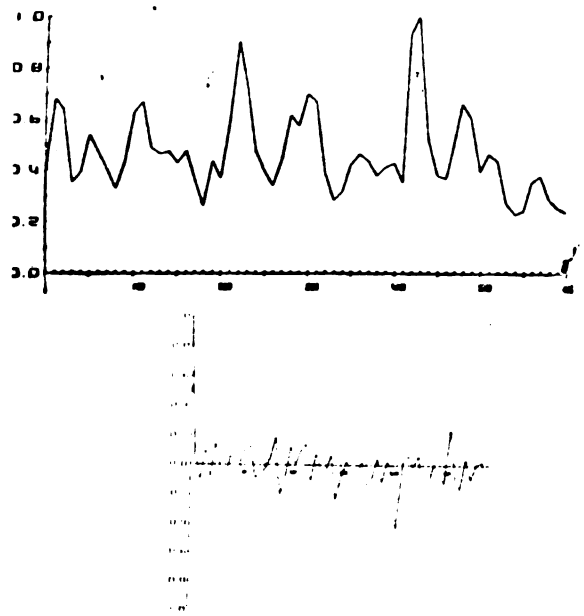

c. T[401,2900]

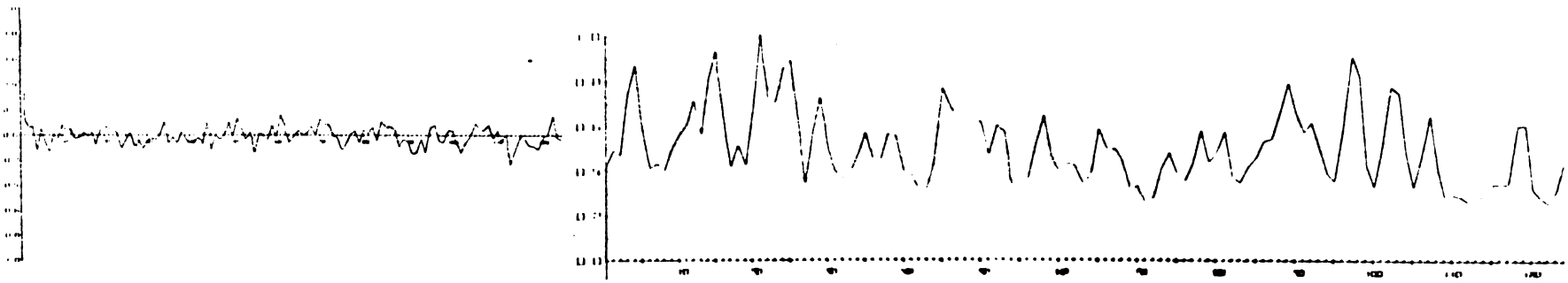

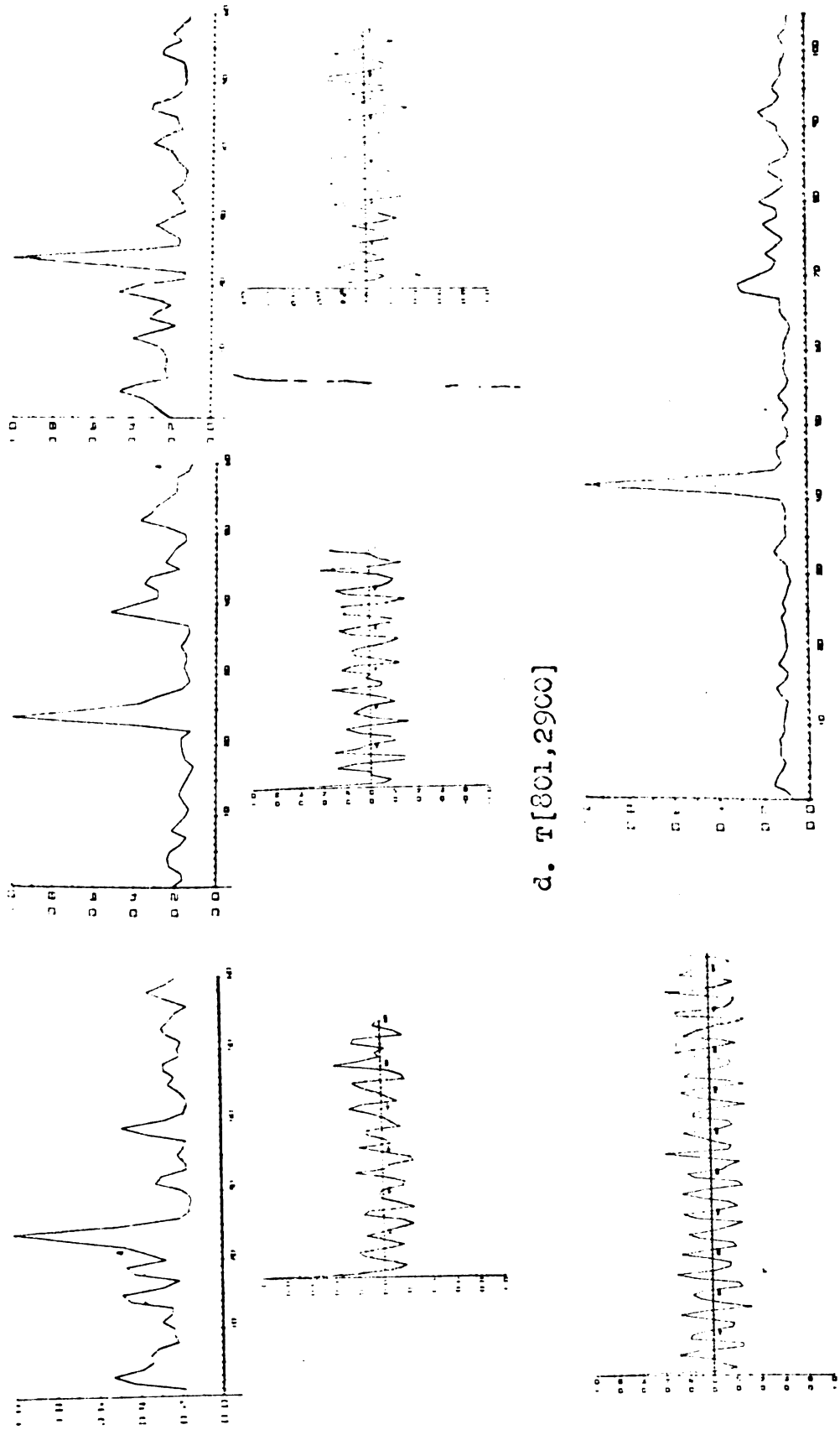

Figure B.15. $\sigma_s = 17$, $\sigma_p = 0$ and

Figure B.16. $\sigma_s = 20$, $\sigma_p = 2$ and

a. T[401,1400]

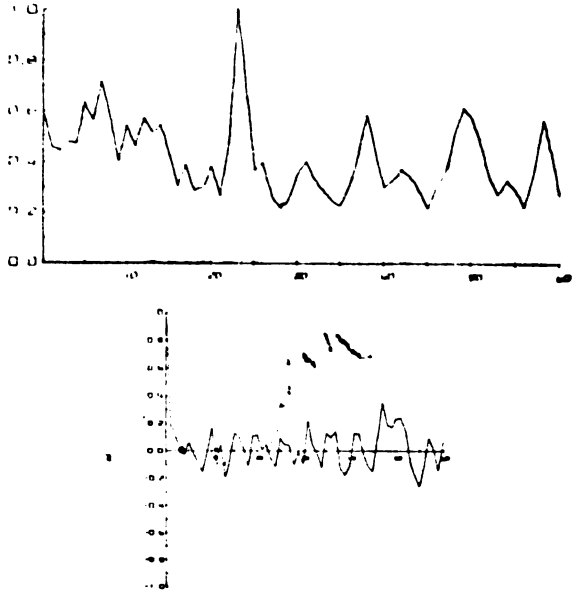

b. T[1401,2400]

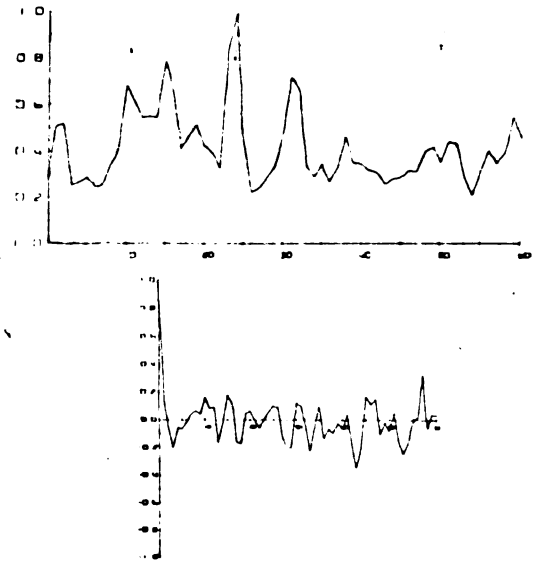

c. T[401,2900]

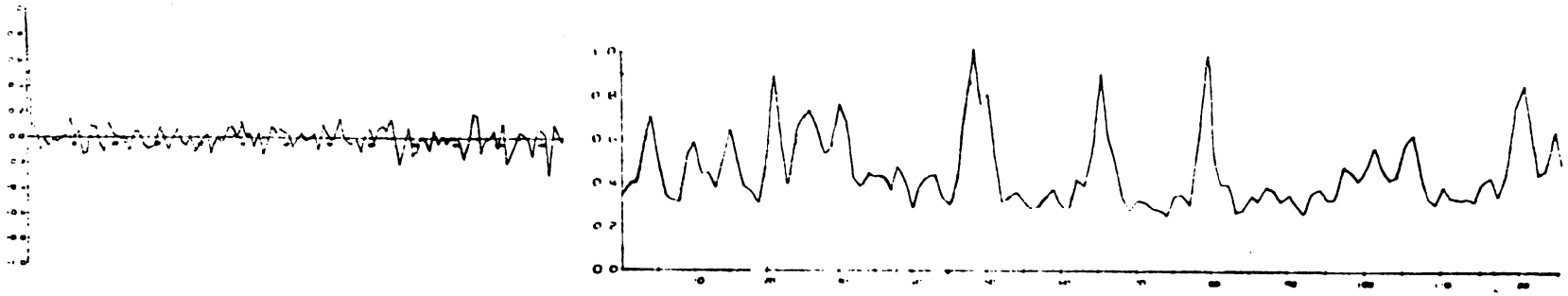

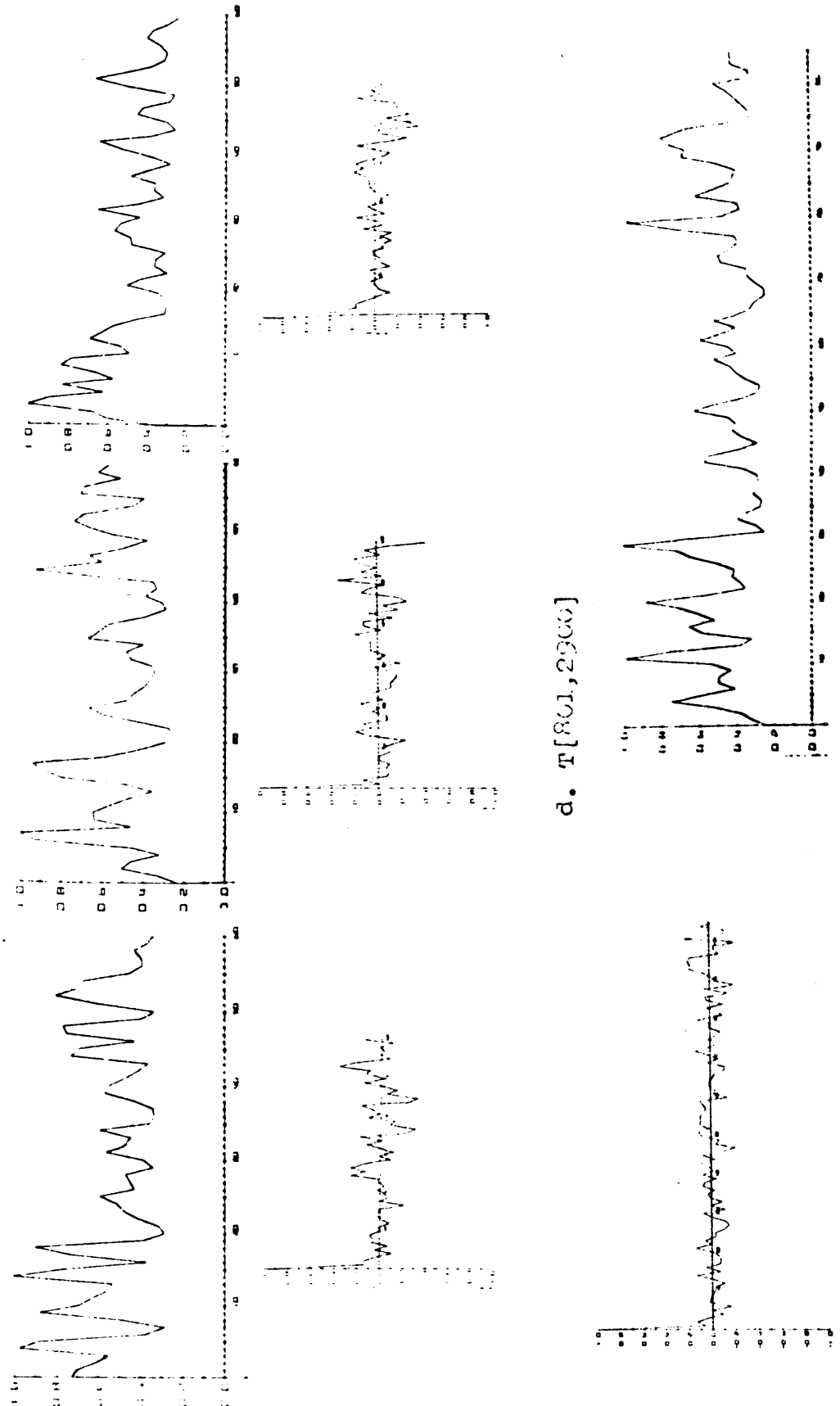

Figure B.17. $\sigma_s = 23$, $\sigma_p = 0$ and

a. T[401,1400]

b. T[1401,2400]

c. T[2401,3400]

d. T[801,2000]

APPENDIX C

APPENDIX C

Miscellaneous Notes on PSE Behavior

During Experiment B-3 a number of properties relating parameter values to power spectral and histogram behavior were noted. Some of these are discussed in this appendix.

C.10. The Effect of Different Values of t_p on the PSE Shape

The effect of different values of t_p on the PSE shape was found to be intimately related to the value of the parameter Δt. To see this, note that at least two points of a sinusoid are required per period in order to determine the frequency of the sinusoid. Applying this to a histogram with intervals of width Δt, the highest frequency which can be detected without error by any method is

Eqn C.1. $$f_c = 1/2\Delta t.$$

Therefore, the shortest period which can be detected is $2\Delta t$. Experimentally, it was found that when the value of t_p was less than $2\Delta t$, the PSE's had a shape which would have placed them in group B (defined in Sec. V.30). This is fortunate because it says that if the value of t_p is less than $2\Delta t$, the PSE will not be mistaken for one that indicates t_p correctly (i.e., the maximum power density is at f_p).

It was also noted that when f_p was set equal to odd values (e.g., 21.4 cps) either the maximum power density occurred at that frequency (if f_p was one of the discrete values on the abscissa) or the maximum power density was shared between the two frequencies on the abscissa closest to f_p.

C.20. The Effect of Different Values of Δt on the PSE Shape

The effect of the value of the parameter Δt on the shape of the PSE's was tested by generating PSE's from histograms where Δt = 3 msec. The results indicated that the background of these PSE's tended to be more irregular and were of lower average background than the PSE's generated for the histograms with Δt = 10 msec.

C.30. The Effect of Different Values of T[a,b] on PSE Shape

Several of the histograms which were generated for the PSE's of Figure V.10 were used to test the effect of different values of T[a,b] on PSE shape. Values of T[401,1400], T[1401,2400] and in some cases T[2401,3400] were used, with all other values remaining the same as those used for the PSE's calculated from the entire histogram. The shape of the PSE's generated from the intervals T[401,1400] and T[1401,2400] have been summarized in Figures V.20 and V.30. By comparing these Figures with each other

and Figure V.10 it is apparent that the first third of the histogram has PSE's classified in group A over a much wider range of σ_s^* and σ_p^* values than does any other portion of the histogram tested.

The source of this property is demonstrated by Figure C.1. The Figure contains some of the histograms generated in conjunction with Experiment B-3. Note that as σ_p increases, the histograms become more uniform. The uniformity is present only at the far right of the histograms generated from small σ_p and drifts to the left as σ_p increases. The first third of the histogram is the last section to succumb to this tendency. Therefore, if the experimental histograms exhibit this property, the first third of the histogram should be used for PSE analysis.

C.40. A Note on the Averaging of Power Spectral Estimates

Recall that a major step in Augenstein's analytical procedure was to average several of the model PSE's. He had, however, given no indication that this procedure was valid. This procedure was tested using the PSE's of Appendix A (those which were done in duplicate). The results suggest that averaging does increase the resolution of the PSE.

The reason for this is clear from the following argument. Consider all histograms generated from a single

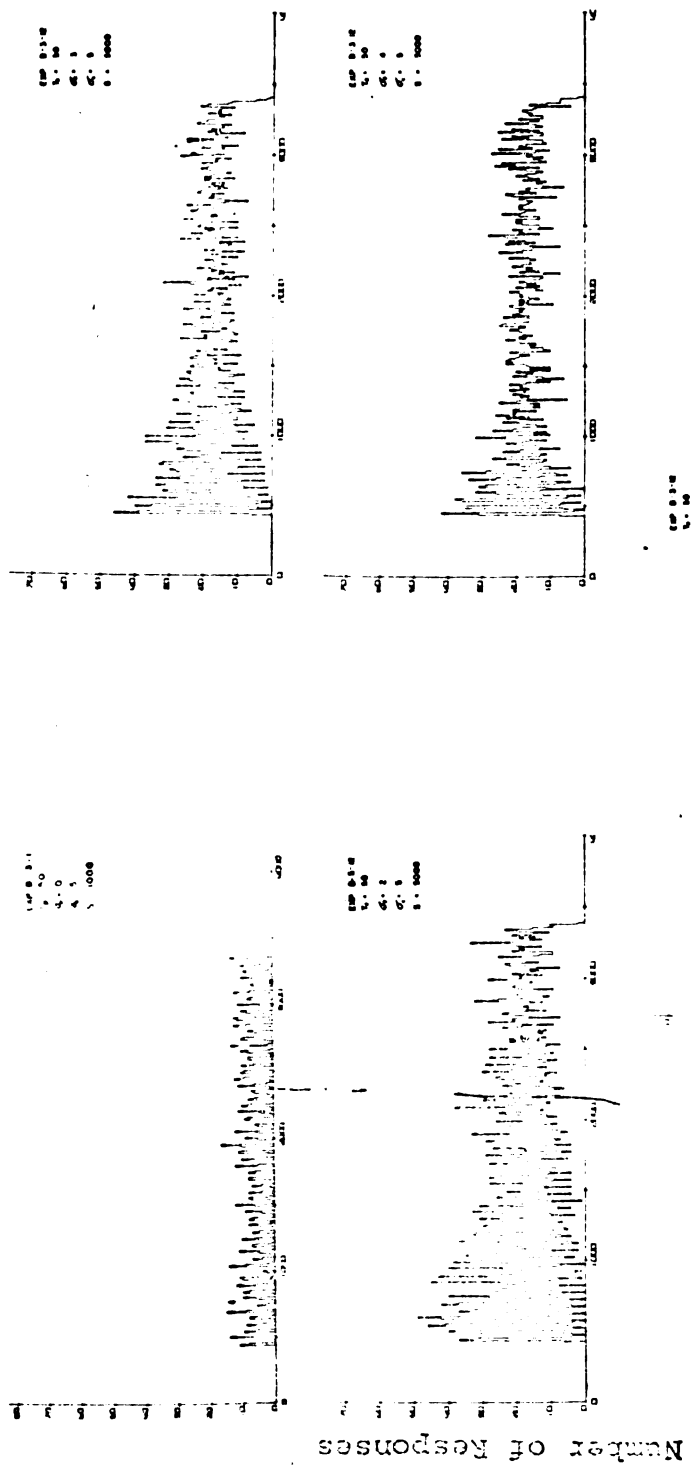

Figure C.1. Examples of 10 msec. interval histograms generated from the density function of Eqn. III.20.20. The component density functions are Eqns. V.10.1-V.10.3.

density function. It would be expected that averaging the histograms would give a better estimate of the density function which generated them. If the parameter values to be specified in order to calculate a PSE are kept constant, then for each histogram there is one PSE. Therefore, averaging the PSE's should give a better estimate of the power spectrum of the density function. As a matter of fact, the PSE's should converge faster than the histograms because the PSE's do not contain phase information.

BIBLIOGRAPHY

BIBLIOGRAPHY

1. Augenstein, L. G. "Human Performance in Information Transmission, Part VI: Evidence of Periodicity," Control Systems Laboratory, Urbana, Illinois, Report Number R-75 (1957).

2. Augenstein, L. G. "Sampling Distribution of the Autocorrelation and Power Spectrum Functions," Control Systems Laboratory, Urbana, Illinois, Report R-78 (1958).

3. Augenstein, L. G. in Information Theory in Psychology, Free Press, Glencoe, Illinois. Quastler (editor), pp. 208-226 (1955).

4. Bendat, J. S. Measurements and Analysis of Random Data, McGraw Hill (1967).

5. Blackman, R. B. and Tukey, J. W. The Measurement of Power Spectra, Dover Publications, Inc., New York (1958).

6. Dubes, R. Class notes. Summer, 1967.

7. Enochson, L. D. and Otnes, R. K. "Digital Spectral Analysis," National Aeronautic and Space Engineering and Manufacturing Meeting, Los Angeles, Calif., Oct. 4-8, 1967. Society of Automotive Engineers. Inc.

8. Guyton, A.C. Textbook of Medical Physiology, W. B. Saunders Co., Philadelphia, Pa., p. 644 (1966).

9. Lee, Y. W. "Communication Applications of Correlation Analysis," Symposium on Applications of Auto-correlation Analysis to Physical Problems, Woods Hole, Mass, 13-14 June, 1959. ONR Publication NAVEXOS, p. 735.

10. Lee, Y. W. Statistical Theory of Communication, John Wiley (1960).

11. Papoulis, A. Probability, Random Variables and Stochastic Processes, McGraw Hill, New York (1965).

12. Richards, P. I. "Computing Reliable Power Spectra," I.E.E.E. Spectrum, Jan., 1967, pp. 83-90.

13. Seiwell, H. R. Reviews of Sci-Instruments, 21: 481-484 (1950).

14. Stroud, J. M. "The Fine Structure of Psychological Time," Information Theory in Psychology, Free Press, Glencoe, Illinois, Quastler (editor), pp. 174-205 (1955).

15. Tukey, J. W. "The Sampling Theory of Power Spectrum Estimates," Symposium on Applications of Autocorrelation Analysis to Physical Problems, Woods Hole, Mass., 13-14 June, 1959. ONR Publication NAVEXOS, p. 735.

16. MSFC Vibration Committee. Vibration Manual, George C. Marshall Space Flight Center, Huntsville, Ala.

17. Wallis and Moore, J. Am. Statist. Assoc., 36, 401-408 (1951).

18. Graham, C. H. Vision and Visual Perception Wiley (1965).

19. Dubes, R. Class Project, Summer, 1967.

20. Von Bekesy, G. Sensory Inhibition, Princeton Univ. Press (1967).